Guidelines for the Hydraulic Design of Bypass Water Control Structures

By

M. M. Wilsnack, P.E.

Principal Engineer

Acknowledgements

Revision Chart

Revision	Description	Date	Prepared By	Reviewed By	Approved By
----	Original Issue	9/4/2013	M. Wilsnack	L. Cadavid, E. Damisse, S. Yue, R. Musalem, H. Gao, J. Zeng	L. Cadavid, S. Sylvester
001	Corrected the first design example in Appendix F, applying the 5/3 correction factor to $V^2/2g$ instead of V and updated all subsequent calculations, corrected steps M - P of Example 1, and corrected steps M – O of Example 2. Corrected the equation for E in step 9 of the design example in Appendix B on page B12, updated all subsequent calculations, and corrected typos on pages B12 and F15.	10/25/2018	M. Wilsnack	S. Dawadi	
002	Corrected a typographical error on page H6 so Equation H9 is specified instead of Equation H6; corrected the two design examples in Appendix H so that D_{50} is increased by 50% as specified in Section IIE.	1/9/2020	M. Wilsnack		

Table of Contents

List of Figures

List of Tables

Introduction and Purpose

The water management infrastructure within the SFWMD contains many water control structures that are aging or no longer capable of providing their intended level of service due to deterioration as well as the increasing demands imposed on them over the years. As a result, it is expected that there will be an increasing number of incidents where a major water control structure will require repairs, maintenance or upgrades, necessitating their temporary deactivation. In such an instance, if no alterative operational scheme that can completely compensate for the inactive structure is possible, the construction of a temporary bypass structure that is capable of diverting flows will be required. The capacity of a bypass structure must be commensurate with the magnitudes of historical flows through the primary structure, the percentages of these flows that can be diverted elsewhere, the level of failure risk that can be tolerated, the amount of funds for construction and maintenance, and the allowable time window for construction activities.

Given the recent declines in public revenues that are available for civil works projects, the shift in flood policy discussed by Meyer (2007) that traverses from the old concept of "flood protection" to the newer concept of "flood risk management" appears to be advantageous to formulating a comprehensive approach to developing bypass structure designs. Such designs must both be economically justified and address the specific hydrologic risks associated with the project at hand. This type of approach can help to avoid solutions that are either over or under designed. Therefore, it is this design philosophy that partially sets the framework for the design guidelines proposed here.

On the other hand, it is acknowledged that the level of effort required to achieve this objective may not always be justified. For example, when designing a bypass structure situated in a remote or otherwise low-risk setting, the conventional approach of using of a single, pre-established storm event as a basis for design may suffice. Moreover, the design of a bypass structure that is needed to address a hydrologic emergency may also be restricted to a more abbreviated approach.

Currently, no set of guidelines exist for the hydraulic design of bypass structures. The purpose of this document is to present a generalized, comprehensive procedure that can be used to plan and design hydraulic structures whose function is to divert flows past a permanent, deactivated structure that is undergoing repairs, maintenance or upgrades. Such a procedure should address

- establishing the accepted level of risk (i.e. probability of flooding at an unacceptable level) during the time frame when the permanent structure is deactivated;

- identifying all of the constraints and requirements that will limit the design alternatives;

- conducting a hydrologic frequency analysis of historical stages and flows;

- developing a set of alternative designs;

- estimating, for each alternative design, the relationship between total expected cost (TEC) and return period for which the alternative is designed (i.e. level of service);

- identifying the most cost effective design alternative and level of service

While these phases of the analysis are intended to cover all of the steps that may be needed to develop the most economical design alternative for a bypass water control structure, it should be recognized that not all of these aspects of the design process may be necessary or even meaningful in every project. The necessity of any given step will essentially be dictated by the drainage area of and current level of service provided by the permanent structure, the spectrum of possible design alternatives, the anticipated duration of primary structure deactivation, the project budget and the availability of alternative water management plans that can supplement the bypass structure. In other words, these guidelines can be perceived as conservative in that they identify all of the facets of the hydraulic design process for a temporary bypass structure (see below) that should be *considered*. Ultimately, it is the responsibility of the project engineer to determine which steps or phases can be omitted, or if special procedures not addressed here are needed.

Organization of the Guidelines

These guidelines are organized into a main body along with various appendices. Presented first in the main body are the types of possible constraints that should be considered when planning and designing a bypass structure. This is followed by a discussion of the recommended procedure for conducting the hydrologic frequency analyses needed to determine the design stages and discharges. The actual recurrence frequency used for the basis of design will vary depending on whether it is based on a single designated storm event or a comprehensive risk analysis that considers a spectrum of storm event frequencies. Hence, the section of the report that follows provides a hydraulic design methodology that is based on a comprehensive risk analysis. It can be used to estimate the total annual costs associated with a given structure design, identify an economically optimal design, and compare the economic feasibilities and hydrologic risks associated with different designs. The final section of the report provides guidance on developing a hydraulic design that is based on a single, predetermined storm event.

Included also in these guidelines are appendices that provide detailed hydraulic design procedures for various types of bypass structures, including culverts, channels, weirs and pump stations. These proposed procedures are based on a comprehensive review of design standards and procedures developed by various organizations over the years as well as a review of the literature on research that has been carried out to develop new and improved hydraulic design techniques.

Identification of Design Constraints

The number, types and characteristics of suitable design alternatives will always be limited by various constraints. The types of design constraints that will be commonly encountered are identified and discussed below. It should be noted that this set is not all-inclusive. The project engineer should be aware of other limitations that may influence the design process.

Functionality of the Existing Water Management Infrastructure

The current functionality of those components of the water management system that interact with the deactivated structure may influence the design of the bypass structure. For example, a downstream structure that has historically passed the peak discharges of the deactivated structure may not be fully functional during the planned construction period. In this case, the design discharge for the bypass structure may have to be compromised while alternative water management plans are included with the design. Similarly, the deactivated structure may itself have recently become a key component of a modified water management plan that was devised to compensate for deficiencies in another structure. In this case, the design of the proposed bypass structure will have to consider the historical flows that occurred within another part of the water management system.

Capacities of Downstream Discharge Channels

The design peak discharge of the bypass structure, as determined from historical flows and other considerations, may be greater than the *current* capacity of the channel located immediately downstream from the proposed location of the bypass structure. The capacity of this channel should be evaluated, if necessary, during the design process.

Site Limitations

Certain features of the proposed bypass structure location may pose restrictions on the structure's design. For instance, historical landmarks, archeological sites and endangered species habitats may pose restrictions on the maximum allowable water level. Subsurface conditions and surrounding infrastructure may prohibit excavation below a certain elevation. Site access may impede construction equipment. It is imperative that these types of limitations be identified and documented prior to initiating any later steps in the design process.

Regulatory Constraints

Design alternatives requiring the placement of fill within a federally protected water body will normally require an individual Section 404 permit unless the proposed activities are covered under an existing general permit. This may be time prohibitive and could render such alternatives as unfeasible.

Alternatives that encroach on private lands may be subject to the eminent domain process. In such an instance, the amount of time required for litigation will most likely be prohibitive. Any encroachment on private lands should therefore be avoided to the extent possible.

Any proposed design that involves modifications to USACE facilities may be subject to the regulatory requirements established by 33 USC 408. For hydraulic design purposes, relevant alterations include, but are not limited to, changes to inflows, water surface elevations, flow distributions and amounts of sediment transport (Skipwith, 2009). As is the case for Section 404 permitting, the approval process imposed by 33 USC 408 can be time prohibitive. Hence, alternatives that involve any hydraulic, hydrologic, structural or geotechnical changes to USACE water control facilities should be avoided to the extent possible.

Water Supply and Environmental Constraints

During non-storm conditions, the deactivated structure may have to pass certain amounts of flow needed for downstream water supply and environmental purposes. The capacity of each alternative design under the expected dry season conditions should be adequate to pass these flows while maintaining any required stages.

Operational Criteria

The bypass structure should be designed so that it can perform adequately within the operational framework of the surrounding water management system. While a temporary bypass structure should not be expected to have all of the same operational capabilities as the associated primary structure, it should not be an impediment to the operation of any other portion of the water management system. In addition, restrictions on stages, downstream velocities and discharge rate increases that were imposed on the deactivated structure should be considered in the design process for the proposed bypass structure.

Hydrologic Data Compilation and Analysis

The intent of the hydraulic design process is to produce a bypass structure that can pass the peak flow associated with a designated return period while keeping possible flood damages at or below an acceptable level. An analysis of historical hydrologic data is therefore needed to determine the design discharge. For reasons discussed in a later section, the hydrologic data and frequency analysis tasks presented below should normally be carried out on a seasonal basis (i.e. hydrologic data will be limited to either the wet season or dry season).

Compile Seasonal Maximum Structure Discharges

As a first step, the appropriate period of record containing the maximum seasonal discharges should be identified. During this time window, land use and water management objectives within the drainage area of the structure should be consistent over time and representative of current conditions within the watershed. Significant changes in land use, water management system components or operational plans during the life of the structure can limit the period of record that

can be selected. Once the appropriate time frame is established, breakpoint flow data should be acquired for the structure that will be deactivated. For each annual wet season (May 15 – October 15) or dry season (October 15 – May 15) within the period of record, the maximum flow rate should be identified and recorded.

Frequency Analysis of Seasonal Maximum Breakpoint Flows

The next step is to conduct a frequency analysis of seasonal maximum flows. The frequency analysis should be based on the log Pearson Type 3 distribution (see, for example, Haan, 2002 or USACE, 1993) and used to determine the distribution parameters associated with the seasonal peak flows. These parameter sets should be used to plot peak flow versus exceedence frequency. The plot should show the fitted parameter distribution along with the measured data. From this plot, estimate the seasonal peak discharges for the desired return period(s). The statistical analysis software HEC-SSP developed by USACE-HEC (2010) can be used to carry out the required computations. For additional information, see Bulletin 17B of the USGS (1982) entitled, "Guidelines for Determining Flood Flow Frequency". It should be noted that significant revisions to Bulletin 17B are expected to be completed by the end of 2013. An updated bulletin should be issued sometime in 2014.

Depending on the operational protocol of the permanent structure along with the hydrologic characteristics of its drainage area, it's possible that the log Pearson Type 3 distribution (or any analytical distribution) may not fit the plotting positions of the peak flow data. The more strictly regulated the peak discharges are, the more likely it is that an analytic frequency distribution will not accurately represent the exceedance frequencies of the measured data. Under these conditions, a graphical frequency analysis would be more appropriate (USACE-HEC, 2010) for estimating the peak annual discharges associated with various return frequencies. A graphical frequency analysis essentially allows the engineer to manually fit an exceedance frequency curve to the plotted positions of the data. Guidance on carrying out this type of frequency analysis is provided by USACE-HEC (2010) and USACE (1993).

Design Head and Tail Water Stages

The purpose of determining peak discharges with various return periods is to later consider each one as a design discharge. When designing a hydraulic structure to pass a specified design discharge, design head and tail water stages are also needed. Unfortunately, within the District's water management system, a structure discharge with a given recurrence frequency is not necessarily associated with head and tail water stages of the same recurrence frequency. This is partially due to the fact that canal stages at a structure are influenced by not only the flow rate through the structure but possibly also by conditions upstream and downstream from the structure. Furthermore, for a given operation setting (i.e. gate opening or pump speed) and flow regime, structure discharge is essentially a function of the static head across the structure. Hence, a discharge with a specified return period can sometimes be induced by many combinations of head and tail water stages of different frequencies. Consequently, the head and tail water stages that correspond to the design discharge are not readily apparent.

A rational basis for specifying design head and tail water stages is nonetheless needed. For design purposes, the design head water stage associated with the design flow can be specified as the maximum allowable stage upstream of the bypass structure location. In determining this stage, site conditions, regulatory constraints, land surface elevations and channel freeboard requirements should all be considered. In some cases, water surface profiles corresponding to the design discharge may need to be computed upstream of the structure to verify the choice of design head water stage. The back water computations can be carried out using HEC-RAS, MIKE 11 or other similar software.

In contrast, determining a design tail water stage is less straight forward. The most direct (and preferred) approach to establishing the design tail water stage is to determine, at the design discharge, the water surface profile between the bypass structure site and the next structure (or other boundary) downstream. Unfortunately, such an effort may not be feasible where large unknown inflows into the downstream channel reaches occur. Moreover, if insufficient geometric data are available, back water computations may not be reliable. Under these conditions, the next best alternative is to set the design tail water stage of the bypass structure equal to the corresponding head water stage of the next structure or boundary downstream. This head water stage would naturally pertain to a structure discharge that is of the same recurrence frequency as the design discharge of the bypass structure. It is possible, however, that this head water stage has not been determined and significant effort would be expended in doing so. Hence, a third (and least desirable) approach to establishing the design tail water stage is to determine, at the associated permanent structure, the tail water stage with the same recurrence frequency as the design flow. Although this tail water stage may not have historically coincided with the design discharge, it is reasonable to assume that canal stages and back water effects will likely increase as storm event flows increase since the water management system will be "working harder" to make the required releases. Thus, despite the factors discussed previously, it is reasonable to assume that canal stages will indeed correlate to some extent with discharge return period. *For design purposes*, therefore, it will be assumed in this case that the design discharge and the design tail water stage of the bypass structure are of approximately the same return period.

According to USACE (1993), a frequency analysis of stage data is best carried out using an arithmetic-probability plot. In some cases, a logarithmic or other mathematical transformation of the data can improve the linearity of the plot. Head and tail water stage estimates with the return periods indicated previously can be obtained from this plot. Details on this procedure are provided by USACE (1993).

Hydraulic Design Based on Risk Analysis

Background

Conventional hydraulic design procedures are based on the premise that the structure should pass a discharge with a specified recurrence frequency while maintaining acceptable stages upstream and downstream of the structure. As indicated by the Florida Department of Transportation, the actual level of risk is seldom quantified in the traditional hydraulic design process (FDOT,

2004). Rather, it is implied through the use of pre-established design frequencies which reflect the importance and allowable risk associated with the facility to be designed. FDOT (2004) indicates that the selection of an appropriate design frequency from its standards is a matter of professional judgment due to the risks associated with floods that are less frequent and greater in magnitude than the design flood. In cases where this risk is significant, a risk analysis can be useful in identifying the design that provides the best tradeoff between risk and cost. In particular, FDOT (2004) indicates that a detailed economic analysis of alternative designs should be carried out under such circumstances in order to identify the design with the least total expected cost (LTEC) to the public. This cost should reflect the annual costs associated with building and maintaining the structure as well as the expected annual costs resulting from flood damages. In order to obtain a reasonable estimate of expected annual flood damage costs, it is suggested that they be evaluated for bypass structure discharges with return periods of 2, 5, 10, 25, and 50 years. The largest return period evaluated can, of course, be limited by the maximum capacity of the permanent structure (i.e. its maximum capacity may be associated with a recurrence frequency that is less than 50 years). The various aspects of a risk analysis are discussed in the sections that follow.

In the hydraulic design of bypass structures, it is best that this type of risk analysis be carried out in order to identify the LTEC design. This is the recommended approach for projects where the required data and resources are available. Furthermore, since both storm characteristics and structure operational protocol can vary significantly between the wet and dry seasons, it may be necessary to conduct separate analyses for wet and dry season conditions if the permanent structure has critical roles in both flood control and water supply operations. Under these circumstances the hydrologic data compilation and frequency analysis tasks discussed earlier will need to be carried out separately for the wet and dry seasons. A comparison of the resultant LTEC designs can assist operations and construction managers in selecting the most advantageous time window for deactivation of the primary structure.

Evaluation of Project Risk

Background

The USACE (1996), in EM 1110-2-1619, outlines a comprehensive approach to conducting risk-based analyses for flood damage reduction studies. The procedures contained therein acknowledge the uncertainties associated with the various facets of a flood damage study (stage vs. damage relationships, computed stages, flow vs. exceedance probability, etc.) and provide techniques for evaluating and presenting them. Meyer et al. (2009) discuss a comprehensive approach to flood risk assessment that addresses economic as well as social and environmental losses. In any case, the primary objective of a flood risk assessment is to estimate the relationship between inundation depth and loss. The USACE (1996) emphasizes the importance of quantifying the uncertainties inherent to this relationship and taking them into account during any subsequent decision making process.

The total cost associated with a flood event can be taken to be the sum of economic, social and environmental losses. Traditional approaches to assessing flood damages, however, have only addressed economic losses since they are generally tangible and can be directly related to the physical aspects of surface water inundation. In contrast, the social and environmental consequences of flooding are difficult to quantify. Nonetheless, it is recommended that each type of impact along with any uncertainties inherent to its quantification be considered insofar as is practical and justifiable. The evaluation of each of these types of flood losses is discussed below.

Direct Economic Flood Losses

Direct economic flood losses are comprised primarily of damage to residential and commercial buildings along with their contents. In some situations, damages to transportation facilities need to also be considered. A complete assessment of these types of losses over the entire drainage area of the permanent structure would require a land surface DEM with adequate resolution along with data on the relationship between damage values and inundation attributes (i.e. depth, area and duration). The damage values would have to include the costs of relocation and temporary housing of residents while damage repairs are carried out. If such data exist, they are likely to be maintained by a local government and should be used to quantify the direct economic losses. Unfortunately, these data are seldom readily available and, even if they are, they may not be indicative of current conditions (e.g. property values, stage vs. depth relationship, etc.). Hence, in most projects the quantification of these direct losses will require an economic analysis of the affected area.

For the purpose of designing a temporary bypass structure, such an economic damage assessment will often not be realistic. As an alternative, economic losses can be inferred by tallying the number of residences and businesses flooded at a specified inundation elevation and multiplying these numbers by average real property values for the area. However, it should be recognized that, for large bypass structures situated near urbanized areas, this approach for estimating economic losses may not be reliable. In such an instance, economic losses should be evaluated by an experienced economist with local knowledge of the area.

Indirect Economic Flood Losses

Indirect economic flood losses generally stem from losses of business production, disruption of transportation, and recovery costs. Meyer et al. (2009) discuss the theoretical and practical difficulties associated with quantifying these types of economic losses. It should be noted that the procedure discussed above for estimating direct losses assumes that if a home or business is inundated to any degree for any duration, the damage cost is essentially the replacement cost for the structure and its contents. This is very conservative. Consequently, for the purposes of comparing alternative bypass structure designs, the indirect costs can generally be neglected. In exceptional cases where indirect economic losses need to be considered, they should be evaluated by a qualified economist.

Environmental Losses

Assigning an economic value to environmental degradation due to temporary flooding is a complicated and extensive process. Meyer et al. (2009) describe Contingent Valuation (CV) as a novel method for monetizing environmental changes. CV is a survey-based method that requires a substantial amount of data and appears to be most applicable to widespread environmental changes. In contrast, there does not appear to be a well-suited approach to assessing the economic value of local environmental degradation, other than estimating the cost of restoration. This approach is consistent with the defensive expenditure method discussed by Venkatachalam (undated report).

Stage-damage relationships for environmentally sensitive tracts are best estimated by knowledgeable scientists and economists. If necessary, a conservative estimate of environmental losses can be obtained by assuming that the habitat will have to be recreated if it becomes inundated above a certain elevation. The cost of doing so should be estimated by a District scientist or planner with experience in this discipline. However, given the tolerance of most south Florida landscapes to occasional inundation, it is expected that environmental losses can be neglected in most projects.

Social Effects

The social impacts of flooding are discussed at length by Meyer et al. (2009) and include losses of irreplaceable items, human stress and the loss of life. Methodologies for assessing these impacts are survey based and include the Event Stress Scale (Parker et al, 1987), the Impact of Event Scale (Zilberg, et al, 1982) and the Guttman scale of worry (Parker et al, 1987). As is the case for other intangible flooding impacts, the quantification of social effects is laborious, data intensive and riddled with uncertainties. For the purpose of making relative comparisons of alternative designs, it is recommended that the social impacts of flooding be only qualitatively considered, if necessary, when comparing two candidate final designs that are otherwise of similar merit. In such an instance, assistance from the appropriate District staff should be sought.

Development of the LTEC Design and Total Expected Cost Estimates

Once the hydrologic frequency analysis discussed previously is completed, steps 1 through 12 below should be completed for each alternative design, in the order given.

(1)   Select one of the return periods specified earlier (i.e. 2, 5, 10, 25 and 50 years, limited by the recurrence frequency of the permanent structure's maximum allowable discharge) and denote the associated peak discharge as the design discharge. Determine the design head and tail water stages as discussed previously.

(2)   Design the structure and bypass channel (if needed) so that they will pass the design flow selected in step 1 at the design head and tail water stages. Once the design is complete, note the

actual head water stage at the specified design flow and tail water stage (the actual head water stage should, of course, be less than or equal to the design head water stage).

Hydraulic design procedures for various structure types that can serve as a bypass facility are provided in appendices A – I (see the list below). Factors of safety should be incorporated into the design process where appropriate.

- *Appendix A : Culverts with Risers*
- *Appendix B : Bypass Channels*
- *Appendix C : Sharp-Crested Weirs*
- *Appendix D: Labyrinth Weirs*
- *Appendix E: Sheet Pile Weirs*
- *Appendix F: Broad-Crested Weirs*
- *Appendix G : Temporary Pump Stations*
- *Appendix H: Channel Stabilization*
- *Appendix I : Channel Transitions*

(3)   For each discharge and associated tail water stage corresponding to a return period <u>not</u> selected in step 1, compute the resultant head water stage for the design produced by step 2 (refer to the appropriate appendix for the necessary procedure).

(4)   Use the results of steps 2 and 3 to construct a head water stage versus return period curve for the proposed design. Construct also the corresponding curve depicting head water versus frequency.

(5)   For each head water stage identified in step 4, determine the total area inundated upstream of the bypass structure along with the average inundation depth within each distinct sub-basin. Strictly speaking, this will require the development and application of a detailed hydraulic / hydrologic model of the watershed drained by the bypass structure. Such an effort, though, will often be infeasible and any guidance in carrying it out is beyond the scope of these guidelines. As a compromise, each head water stage can be used to estimate the inundation and damage within the sub-basins that are drained directly by the bypass structure. If the land uses and land elevations within these basins are representative of the entire watershed affected by the bypass structure, the resultant inundation versus damage relationship can be used to perform meaningful comparisons between bypass structures with varying design frequencies (see below). Otherwise, hydrologic and hydraulic modeling will be required.

(6)   Using the results of steps 4 and 5, construct the damage-frequency curve (Figure 1) pertaining to the proposed design (see Volker, 2007).
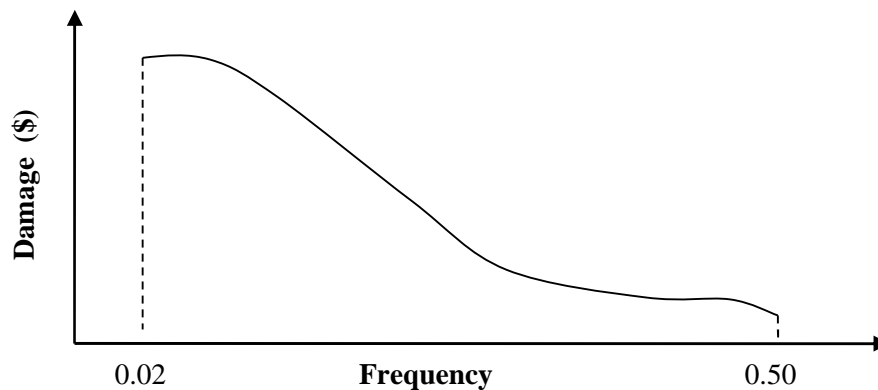
Figure 1. Example of a damage versus frequency curve

(7)   Estimate the expected annual damages associated with the implementation of the proposed design by determining the area under the damage versus frequency curve.

(8)   Estimate the capital cost and life span of the proposed design along with the amortized annual cost (note: the design may remain in place for a specified time while not in use). An illustrative example of the steps involved is provided by FDOT (2004).

(9)   Estimate the annual O & M costs of the design during its life.

(10)   Add the results of steps 8 and 9 to obtain the annual structure cost.

(11)   Add the results of steps 7 and 10 to determine the annual total expected cost (TEC) of the structure.

(12)   Repeat steps 1 – 11 for the next design storm in the list indicated previously.

Once the proposed alternative has been designed to accommodate each design storm as indicated in steps 1 - 12 above, construct the families of curves shown in Figure 2 that relate annual structure cost, expected annual damage cost, TEC, head water stage and total damage cost with the return period (see USDOT, 1981). Identify the design with the minimum annual TEC. It should be noted in Figure 2 that the curves with the shorter recurrence intervals pertain to higher stages and damages since they represent structures with smaller capacities.

(13)   Repeat steps 1 – 13 for the next alternative design (i.e. a different structure type).
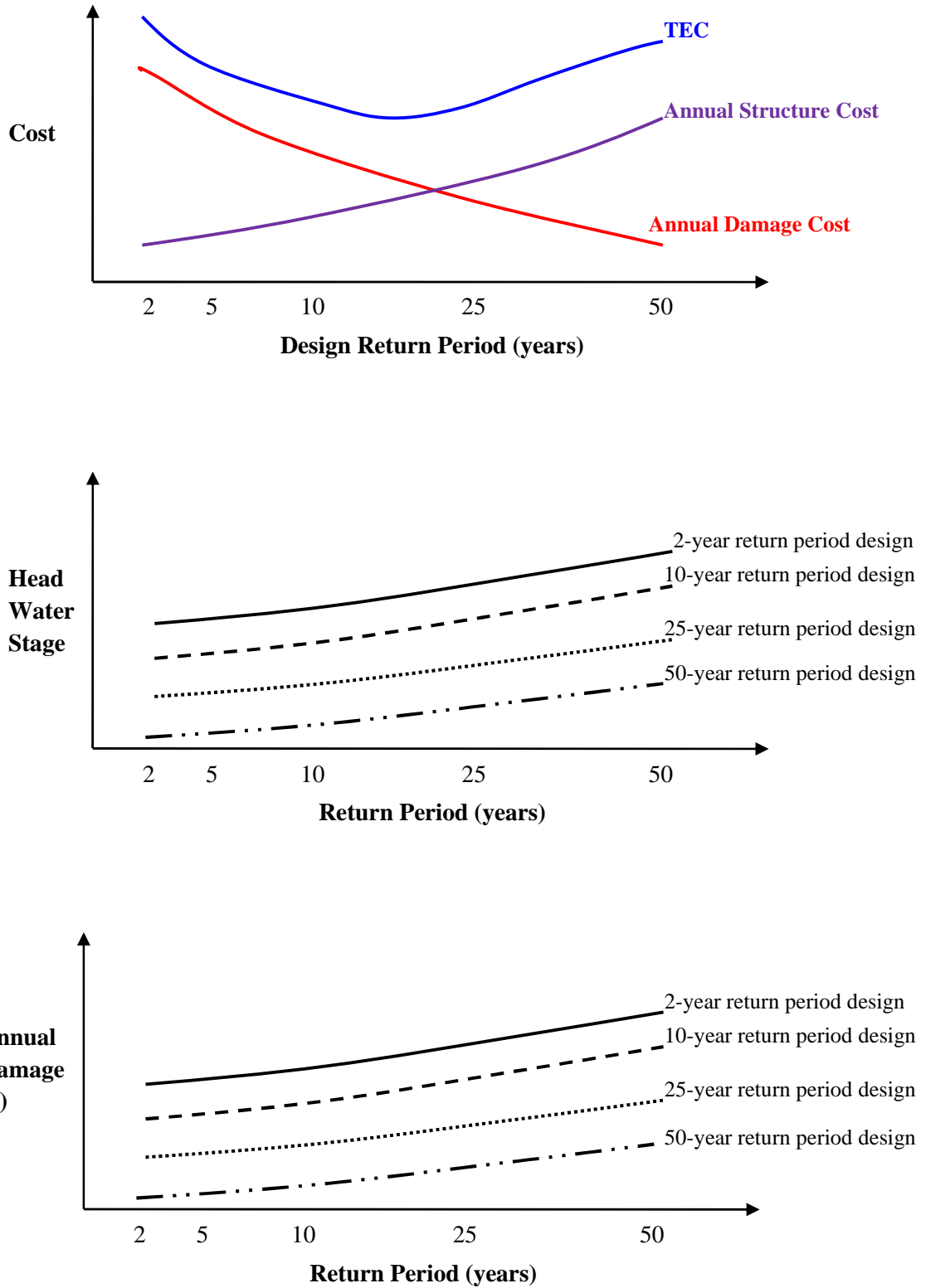
Figure 2. Families of curves depicting cost, head water stage and annual damage versus return period

(14)   Examine the set of curves shown in Figure 2 for each alternative design. Select the design and return period that is most feasible in regards to economics and other intangible factors. Verify that the selected return period for the bypass structure is not be greater than the design return period for the permanent structure unless the capacity of the permanent structure is considered to be inadequate for current conditions.

(15)   Figure 3 summarizes the steps in the cost evaluation process for each alternative.

Conventional Hydraulic Design Procedure

As discussed previously, designing a bypass structure using the procedure presented in the previous section may sometimes be unwarranted. For example, it should be acceptable to employ traditional methods to design a small bypass structure located in a remote area with minimal flood risks. Similarly, a bypass structure posing moderate flood risks may only be in service for a few months. In this case a less elaborate design procedure may be acceptable.

As mentioned previously, for a design discharge with a specified recurrence interval, the hydraulic design process for a specified structure type is as presented in the appendices. What needs to be determined is the recurrence frequency that should be used as a basis for design.

Unfortunately, the various organizations that have produced hydraulic design criteria and procedures over the years offer little advice on this subject. According to FDOT (2013), the design frequencies shown in Table 1 represent an engineering consensus on reasonable return periods for temporary culverts and bridges that are implemented during highway maintenance and repair projects. In addition, it is stipulated that a temporary structure should not cause more than (i) a one-foot increase in the design storm frequency flood elevation immediately upstream of it, and (ii) a 0.1 foot increase in the design storm frequency flood elevation 500 feet upstream of the structure.

Table 1. Design recurrence intervals for temporary drainage facilities (FDOT, 2013)

Duration of Temporary Facility (months)	*Design Recurrence Interval (years)*
Less than 13	2
13 - 40	5
40-85	10
Greater than 85	Use criteria for permanent facilities
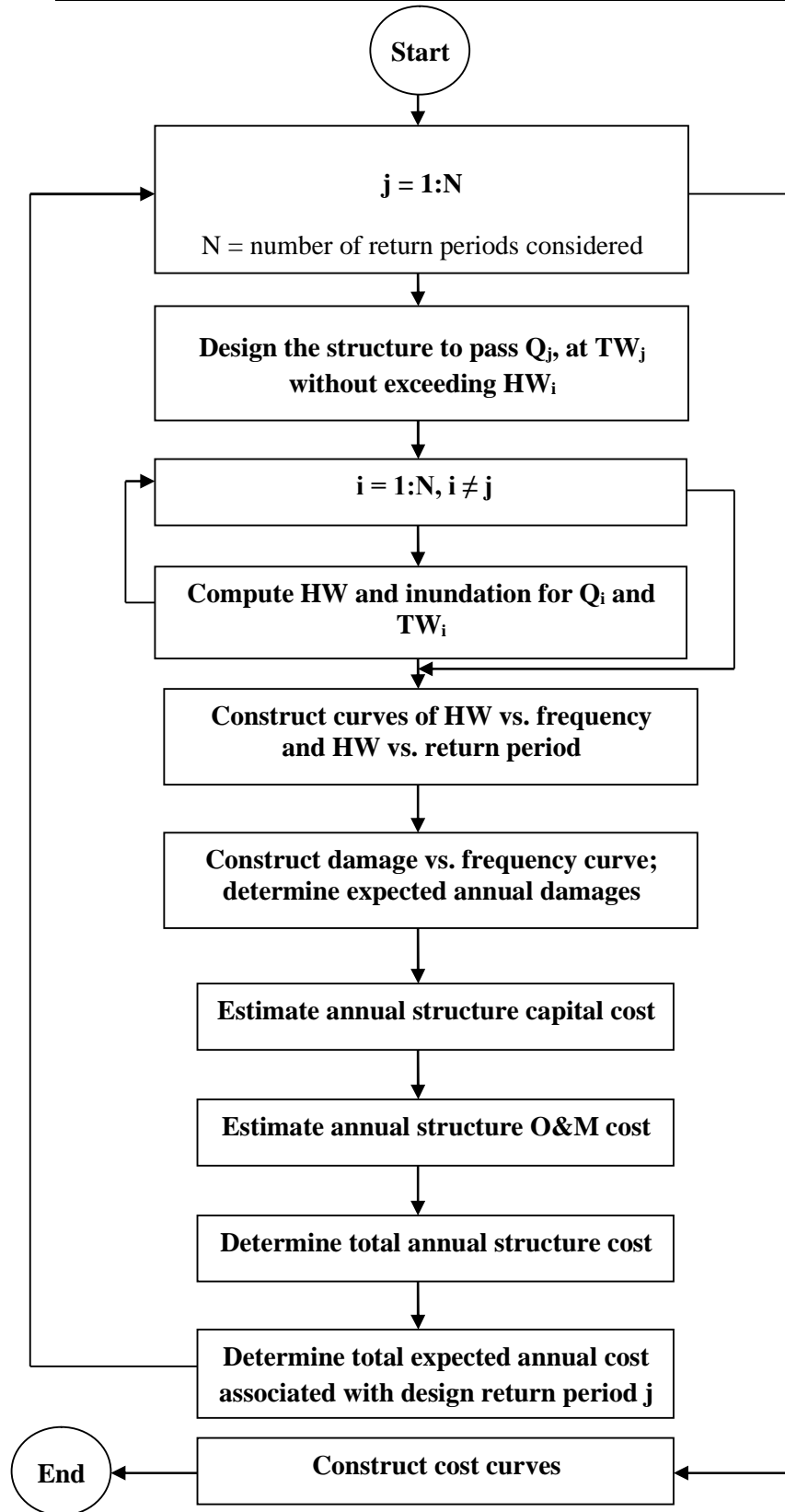
Figure 3. Cost evaluation process for a bypass structure design

The consequences of a temporary highway drainage structure failure resulting from the exceedance of its design capacity are typically limited to road damages and closures. In contrast, the failure of a bypass structure can cause significant damages to surrounding infrastructure and upstream areas. Consequently, the criteria presented in Table 1 should generally not be considered adequate when establishing design discharge criteria for District bypass structures that must provide flood protection to upstream areas. For example, consider a temporary bypass structure that is to be in service for one year (i.e. one dry season and one wet season). Table 1 indicates that its design discharge should have a recurrence interval of 2 years. This implies that there will be a 50% probability of its design capacity being exceeded during that year. In most applications this risk is too high. A similar argument can be made for each of the other criteria in Table 1. More stringent criteria are therefore needed.

The criteria presented in Table 2 were developed in consultation with SFWMD water managers and are based on their prior experiences with the design and operation of temporary bypass facilities. In each of the indicated time windows when the permanent structure is out of service, it is assumed that the bypass structure begins its service period at the beginning of the dry season. The exception is the time window spanning November 15 – February 15. This 90-day period is generally considered by operations staff to be the most favorable for deactivating a permanent structure.

Table 2. Minimum design recurrence intervals for SFWMD bypass structures

Service Period of Bypass Structure	Minimum Design Discharge Recurrence Interval (years)
November 15 – February 15	2
1 Dry Season (approx. 6 months)	5
1 Dry Season + 1 Wet Season (approx. 1 year)	5
2 Dry Seasons + 1 Wet Season (approx. 1.5 years)	5
2 or more years	10

If the proposed service period is one dry season, it is recommended that a bypass structure design for wet season conditions also be prepared prior to the end of the dry season. This is to ensure a timely upgrade to the bypass structure in the event that the permanent structure is not ready to be placed back in service before the beginning of the wet season.

On a final note, it should be pointed out that the criteria presented in Table 2 are intended for most SFWMD bypass structures. In cases where the permanent structure under repair is rarely operated or the project engineer identifies other extenuating circumstances, alternative recurrence interval criteria could be considered after consultation with the SFWMD water managers.

References

FDOT. 2004. Drainage Handbook – Culvert Design. Office of Design, Drainage Section, Florida Department of Transportation, Tallahassee, Florida, 74 pp.

FDOT. 2013. Drainage Manual. Office of Design, Drainage Section, Florida Department of Transportation, Tallahassee, Florida, 83 pp.

Haan, C. T. 2002. *Statistical Methods in Hydrology*. Iowa State Press, Ames, Iowa.

Meyer, Volker. 2007. Flood Risk Assessment. *Proceedings of the Conference on Risk Assessment in European River Basins – State of the Art and Future Challenges,* November 12 – 14, 2007, Leipzig, Germany, pp. 1-4.

Meyer, V., F. Messner, E. Penning-Rowsell, C. Green, S. Tunstall and A. van der Veen. 2009. Evaluating flood damages: guidance and recommendations on principles and methods. Report Number T09-07-03 (Rv. 2_2_P01), FLOODsite, 16 pp.

Parker, D.J., C. H. Green and P. M. Thompson. 1987. Urban flood protection benefits: a project appraisal guide (The Red Manual), Aldershot, UK: Gower Technical Press.

Skipwith, Walter. 2009. Section 408 Review and Approval. A Presentation to the Dallas Council of Engineering Companies, Dallas, TX, 8 pp.

USACE. 1993. Hydrologic Frequency Analysis. EM 1110-2-1415, U.S. Army Corps of Engineers, Washington, D.C.

USACE. 1996. Risk-Based Analysis for Flood Damage Reduction Studies. EM 1110-2-1619, U.S. Army Corps of Engineers, Washington, D.C.

USDOT. 1981. The Design of Encroachments on Flood Plains Using Risk Analysis. FHWA Publication Number EPD-86-112, U.S. Department of Transportation, Washington, D.C.

USGS. 1982. Guidelines for Determining Flood Flow Frequency – Bulletin 17B. Interagency Advisory Committee on Water Data, U.S. Geological Survey, Washington, D.C.

Venkatachalam, L. undated. Economic Valuation of Watershed Services of Commons: Marginal Opportunity Cost Approach within the Environmental Accounting Framework. Institute for Social and Economic Change, Nagarbhavi, Bangalore – 560 072, India, 14 pp.

Zilberg, N. J., D. S. Weiss and M. J. Horowitz. 1982. "Impact of Event Scale: A Cross-Validation Study and Some Empirical Evidence Supporting a Conceptual Model of Stress Response Syndrome", Journal of Consulting and Clinical Psychology 50(3), 407-414.

Appendix A. Hydraulic Design Procedure for Culvert Structures

I.   Identify Site Constraints

There are several site features that may induce constraints on the number and sizes of the culvert barrels that will comprise the design of the temporary bypass facility. These include the dimensions of the discharge channel, the embankment width and the maximum allowable discharge velocity. Throughout the design process, the engineer should remain aware of any constraints imposed by these factors.

II.   Conceptualize the Culvert Structure

While culvert structures can be of a variety of designs, it is assumed in these guidelines that a temporary water control structure will be comprised of horizontal barrels with conventional, semicircular-shaped flashboard risers installed, if desired, at their upstream ends. Typically, both the barrels and the risers will be made of corrugated metal while the weir situated at the upstream face of the riser will consist of removable boards or metal plates. A cross section of this type of design is depicted in Figure A1. The values of HW_D and TW_D are specified as indicated below.
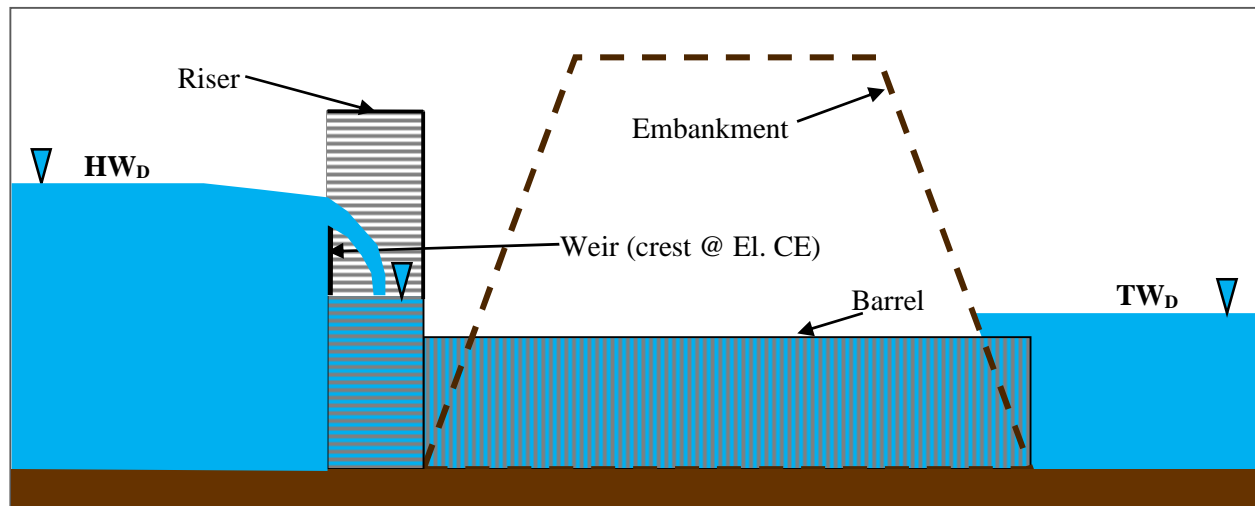
Figure A1. Conceptual design of a culvert structure

III.   Perform Hydraulic Design Tasks

The tasks listed below should be performed in the order given. It is left to the engineer's discretion as to which barrel materials, shapes and sizes are considered. Pricing, availability and manufacturer reliability will usually determine the range of choices. While the procedure presented here is directly intended for circular or square box cross sections, a similar approach can be followed for rectangular box cross sections. Additionally, the procedure outlined below is based on the assumption that the proposed culvert structure is of a passive nature, where the weir

crests of risers installed at the upstream ends of the culvert barrels are set at a fixed control elevation. Also assumed is that all barrel inverts are installed at the same elevation.

A. Determine the required barrel length and maximum allowable size based on the results of phase I above. Also determine the minimum allowable barrel size that is stipulated by existing engineering standards. The potential for clogging by debris, local maintenance practices and access requirements should also be taken into account.

B. Specify the design flow (Q_D), the maximum allowable head water stage (HW_D) and the design tail water stage (TW_D). Each of these quantities was determined through the procedures discussed in the main body of the report.

C. Select the barrel material and shape (circular or box).

D. Determine the desired seasonal control elevation upstream of the structure (CE). If this control elevation is to be maintained by risers installed at the upstream ends of the culvert barrels, set the weir crest of the upstream control riser at this elevation and then proceed to step F while skipping step E. Alternatively, if risers are not to be used in this design, the barrel inverts must be set at CE. In this case, proceed to step E and skip step F.

E. Using the outcomes of steps A - D, determine the number of barrels of minimum dimension needed to pass the design flow at the specified head water and tail water stages. The data and procedures provided in FHWA HDS5 (Schall et al., 2012) can be used to complete this task. Freeware such as HY-8 and HEC-RAS may also be useful. Alternatively, the SFWMD Atlas of Flow Computations (Wilsnack et al., 2010) contains flow rating equations for culvert structures throughout the District. These equations may be useful if the intended design resembles an existing culvert structure. The culvert barrels should pass the design flow in outlet control.

F. For the design tail water stage and minimum barrel dimension, plot the relationship between discharge per barrel (Q_B) and the water stage within the riser (H_R). The data and procedures provided in FHWA HDS5 can be used to complete this task. The resultant barrel rating curve is illustrated conceptually in Figure A2 for the case where $CE > TW_D$. On the same set of axes, plot the relationship between discharge and riser stage for a riser of specified width (D) and the design head water stage. For weir flow, use the appropriate equations given in Appendix C to compute flows over the riser crest. For orifice flow, the discharge can be computed from the standard orifice equation which, in this case, can be expressed as

$$Q_o \ = \ \tfrac{1}{8}\,\pi\,C_o\,D^2\,[HW_D - \max(CE,H_R)]^{1/2} \tag{A1}$$

where $C_o \approx 0.6$ is the orifice coefficient (see, for example, Brater and King, 1976). If CE $>$ TW$_D$ and the riser stage is less than CE, the riser opening will act as either an unsubmerged weir or an unsubmerged orifice. Note that under these circumstances, the discharge will remain constant for a specified head water stage until the riser stage exceeds the riser crest elevation. When this occurs, the riser opening will then be acting as either a submerged weir or a submerged orifice, depending on which of the two riser rating curves shown in Figure A2 provides the lower discharge for the riser stage in question. On the other hand, if CE $\leq$ TW$_D$, TW$_D$ would remain at the origin and the horizontal portions of the riser rating curves would not exist
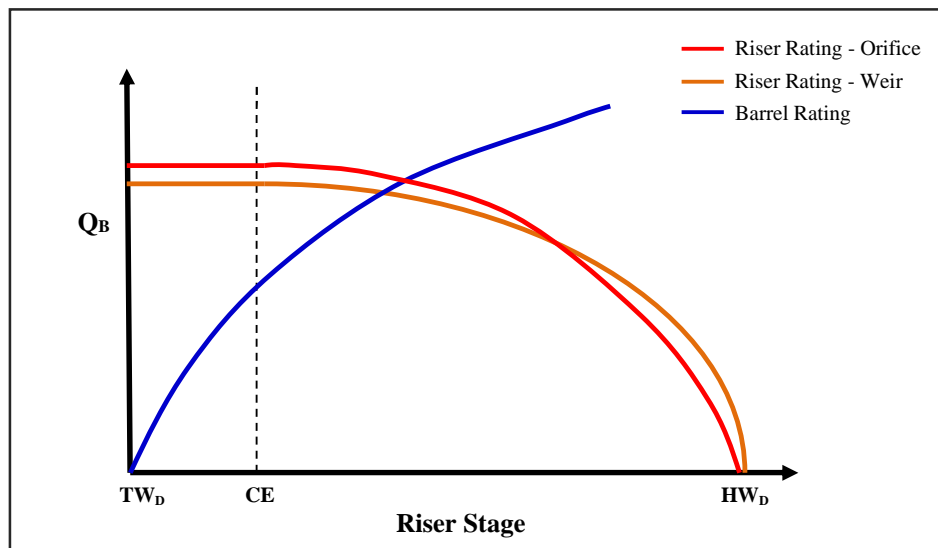
Figure A2. Conceptual barrel and riser rating curves with fixed head and tail water stages

The coordinates of the point where the barrel rating curve intersects a riser rating curve provide the discharge per barrel and the riser stage that will result if that barrel and riser combination is installed under the boundary conditions given by HW$_D$ and TW$_D$. If the intersection of the barrel rating curve with the riser orifice rating curve for a specified size occurs at a lower discharge than the intersection of the barrel rating curve with the corresponding riser weir rating curve, this indicates that the riser will function as an orifice. This implies that the riser diameter is too small and needs to be increased so as to allow the riser to function as a weir (which is generally how risers are intended to pass flow). The riser diameter will be limited by availability, the culvert barrel spacing or other site conditions. This limiting riser size will maximize the discharge per barrel, but not necessarily minimize the required number of barrels. By constructing a family of riser rating curves and determining their intersections with the barrel rating curve, one can determine through trial and error the smallest riser size that minimizes the required number of barrels while adhering to any constraints. In any case, the barrels should flow full in the final design to enhance the accuracy of computed discharges and facilitate flow measurement in the field.

As an example, suppose that a culvert/riser structure is needed to pass a design discharge rate of 100 cfs at specified head and tail water stages. If the weir flow rating curve for a 5-feet diameter riser is controlling at its intersection with the barrel rating curve (for some assumed barrel size – refer to Figure A2) where Q_B = 30 cfs, then 3.33 → 4 riser/barrel installations would be required to pass the flow. If, however, the corresponding Q_B value for a 4.5-feet riser is 25 cfs, 4 riser/barrel installations are still required. Furthermore, a riser diameter smaller than 4.5 feet would necessitate the installation of more than 4 barrels since Q_B would be less than 25 cfs. Suppose also that the 5-feet diameter riser was the largest that could be installed due to the required culvert barrel spacing. Under these circumstances, the 4.5-feet riser would be the optimal choice for the given barrel size.

Under seasonal conditions, the riser stage will typically be at a distance of $CE - TW_D$ below the upstream head water stage. The antifloatation anchor for the riser should be designed accordingly and based on any existing standards and guidelines. In the absence of any such guidelines, the riser should be extended below the channel bottom a distance (d_{af}) that, when filled with concrete, will counter the buoyant force acting on the riser. More specifically,

$$\gamma_c \, d_{af} \geq \gamma_w \, (CE - TW_D) \tag{A2}$$

where $\gamma_c \approx 155$ lb/ft^3 is the specific weight of concrete and $\gamma_w = 62.4$ lb/ft^3 is the specific weight of water.

G. Estimate the cost of acquiring and installing the number of barrels (with risers, if required) determined in step E or F. If necessary, assistance should be sought from engineers who are experienced in construction and cost estimating.

H. Increment the barrel dimension by one nominal size and repeat steps E or F, and G. Continue this process until the maximum allowable (or available) barrel dimension is reached.

I. Determine and plot the obtained relationship between total structure cost and barrel size. Identify the most economical barrel size that should be used in the design.

J. If desired, repeat steps C – I for a different barrel material or geometry.

K. If step J was performed, then a family of cost versus barrel size curves can be constructed based on the various barrel materials and geometries examined. From these curves, the most economical barrel design should be evident. The actual head water stage that was computed for this design at the specified Q and tail water stage should be noted.

The hydraulic design procedure for a bypass culvert structure is summarized in Figure A3 and illustrated in the example that follows.

```
                           ┌─────────┐
                           │  Start  │
                           └─────────┘
                                │
       ┌────────────────────────────────────────────────┐
       │  Determine required barrel length, constraints on sizes  │
       └────────────────────────────────────────────────┘
                                │
       ┌────────────────────────────────────────────────┐
       │           Specify Q_D, HW_D, TW_D              │
       └────────────────────────────────────────────────┘
                                │
       ┌────────────────────────────────────────────────┐
       │          Select barrel material and shape       │
       └────────────────────────────────────────────────┘
                                │
       ┌────────────────────────────────────────────────┐
       │  Determine CE; set weir crest or barrel invert elevation  │
       └────────────────────────────────────────────────┘
```

Specify Q_D, HW_D, TW_D

i : 1, # barrel sizes considered

Determine required number of barrels and riser sizes (if needed)

Design antifloatation measures (if needed)

Estimate cost

Plot cost vs. barrel size

Consider other barrel types?

yes

no

Select optimal design

End
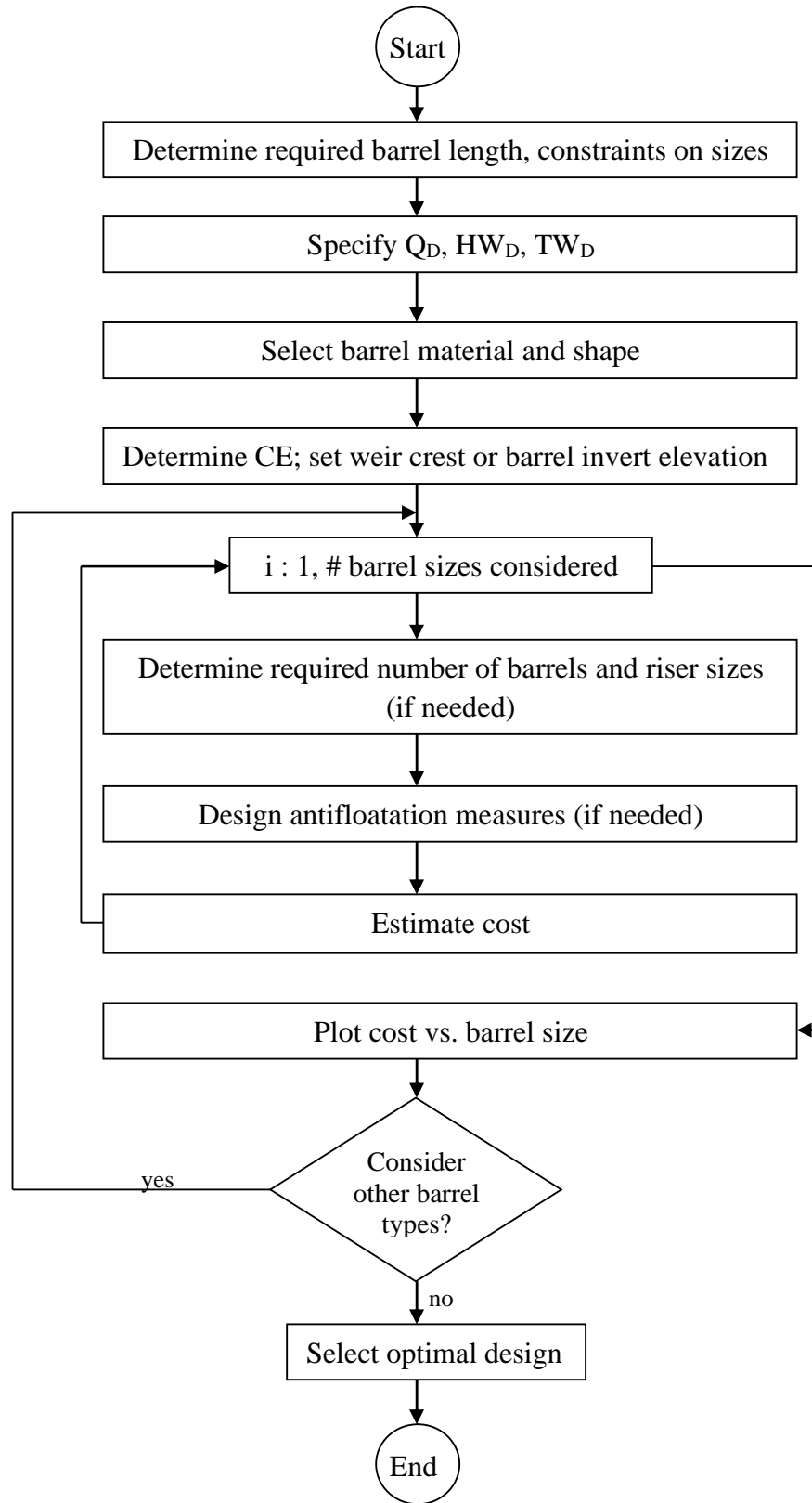
Figure A3. Hydraulic design procedure for bypass culvert structures

IV. Design Example

A bypass channel with a bottom width of 20 feet, a bottom elevation of 0 feet, a top-of-bank elevation of 15 feet and 2:1 side slopes carries a design discharge of 500 cfs. The design head water and tail water stages for the proposed structure location are 13 and 9 feet, respectively. Design a temporary culvert structure with risers that will pass the design flow at the design head and tail water stages while providing a seasonal control elevation of 11 feet. The culverts are to be installed with their inverts along the channel bottom, where the required barrel length will be 70 feet.

Each step of the design process is carried out below.

Step A.

As stated in the design requirements, the required barrel length is 70 feet. Assume that the maximum barrel size available for most pipe materials from suppliers in the region is 96 inches. Assume also that maintenance considerations necessitate a minimum barrel size of 36 inches.

Step B.

The design requirements indicate that Q_D, HWD and TWD are 500 cfs, 13 feet and 9 feet, respectively.

Step C.

Assume that circular aluminum CMP is a practical choice and that it should be considered for use in this design.

Step D.

The requested control elevation is 11 feet. In this design, each riser will be comprised of one half of a CMP barrel with stop logs installed in channels that are welded to the vertical edges of the semicircular barrel wall. The top edge of the flat side of the riser will serve as the weir crest and will be set at elevation 11. The remaining portion of the riser wall comprised of CMP will be extended to the top of bank. This type of design will allow stop logs to be added or removed if changes to the control elevation are needed.

Step E.

Not applicable – omit.

Step F.

A cross section of the proposed design is illustrated conceptually in Figure A4.
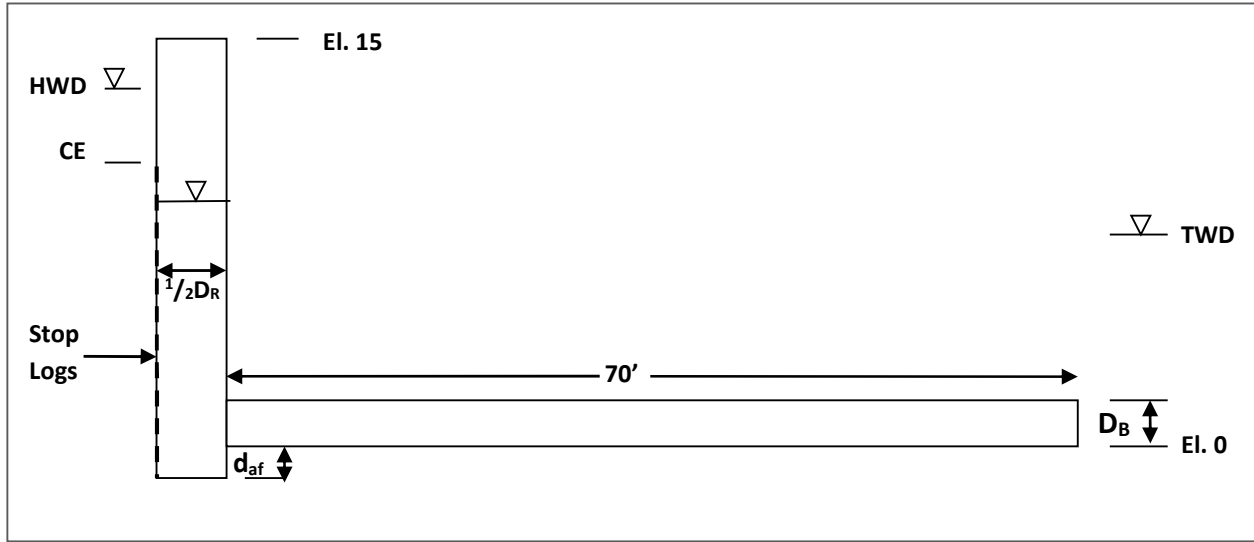
Figure A4. Conceptual design of a riser and barrel for the example problem

The head inside the riser as depicted in Figure A4 is the upstream head for the barrel and the downstream head for the weir. Designating this head as H_R, it is obvious that TWD $< H_R <$ HWD. Writing an energy equation between the water level within the riser and the tail water yields, for full-barreled, outlet-controlled flow,

$$H_R + V_R^2/2g = TWD + h_{fR} + h_{fB} + (1+K_e)V_B^2/2g \tag{A3}$$

where K_e is the entrance head loss coefficient for the barrel; V_R and V_B are the flow velocities within the riser and barrel, respectively; h_{fR} is the friction head loss within the riser; and h_{fB} is the friction head loss within the barrel. At the barrel entrance, $K_e \approx 0.7$ according to the District's Flow Program.

While friction losses within the riser are often neglected in design, they can sometimes comprise a significant percentage of the total head loss; hence, they are included here for completeness and illustrative purposes. In a full-flowing culvert barrel of length L and diameter D, the friction head loss h_f is derived from Manning's equation and can be stated as

$$h_f = \frac{n^2 V^2 L}{2.21 R^{4/3}} \tag{A4}$$

where V is the velocity and R = D/4 is the hydraulic radius. Using Equations A3 and A4 along with conservation of mass while neglecting the resistance of the flat side of the riser, it can be shown that the discharge Q_B through the culvert barrel when flowing full is given by

$$Q_B = \pi \sqrt{\frac{g}{8}(H_R - TWD)\left[\frac{1+K_e}{D_B^4} + \frac{4}{D_R^4} + 184.9n^2\left(\frac{L_B}{D_B^{16/3}} + \frac{4L_R}{D_R^{16/3}}\right)\right]^{-1}} \tag{A5}$$

In Equation (A5), the subscripts B and R denote barrel and riser, respectively. When applying this formula, conventional English units must be used for each term with dimensions.

Figure A4 depicts conditions that are common for many culvert structures in southern Florida, where the barrel is relatively long and horizontal while its outlet is submerged. Under these conditions, the barrel will not operate in inlet control. Consequently, the possible discharge under inlet control will not be checked here. Under different conditions, it may be advisable to compute the corresponding discharge under inlet control using the methods provided in FHWA HDS5.

Using Equations A1, A5, C1, C2, C4 and C7, the performance curves depicted in Figure A2 were constructed for four singe riser/barrel combinations of the following sizes: $D_R = 5$ and $D_B = 3$, $D_R = 6$ and $D_B = 4$, $D_R = 7$ and $D_B = 4$, and $D_R = 8$ and $D_B = 4$. These performance curves are shown in Figures A5 and A6 for the first two designs. For $D_R = 5$ and $D_B = 3$, the riser is flooded above the weir crest, with a head inside the riser of approximately 11.45 feet. In this case, the riser crest is acting as a submerged weir and the resultant discharge rate is about 45 cfs. In contrast, with $D_R = 6$ and $D_B = 4$, the riser crest is acting as an unsubmerged weir and is controlling the discharge rate at approximately 57 cfs.
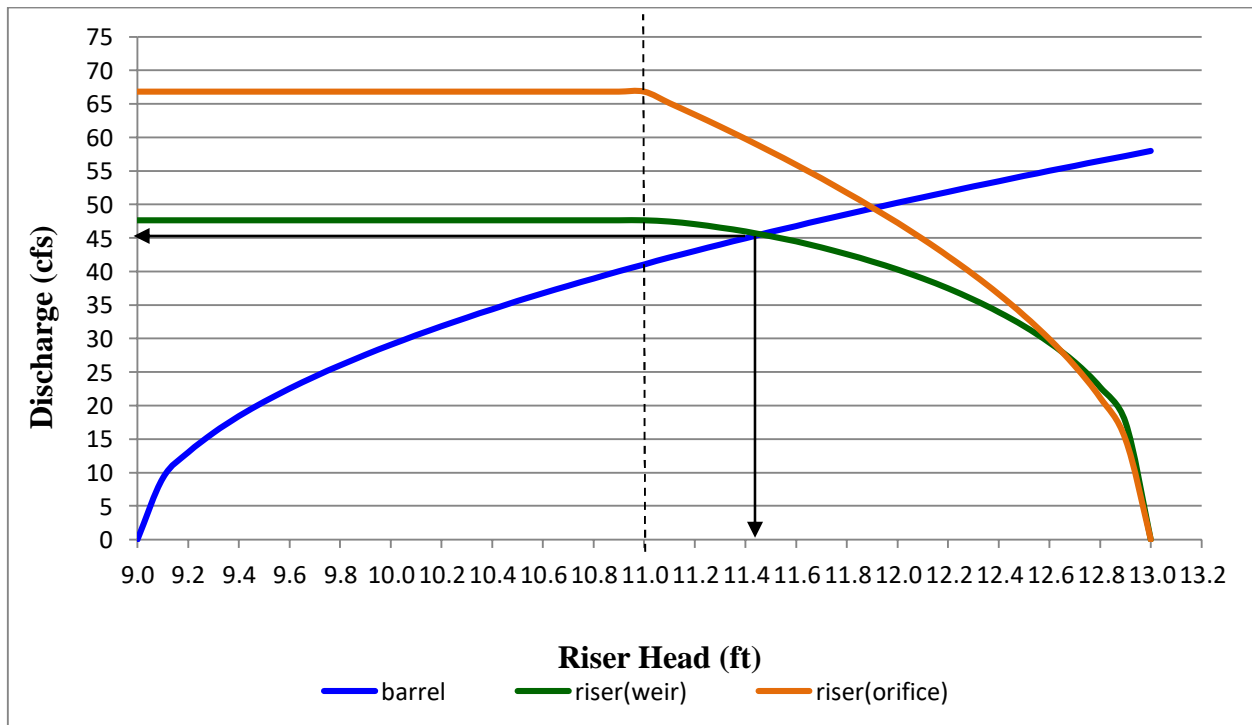
Figure A5. Unit structure rating curves for DR = 5, DB = 3
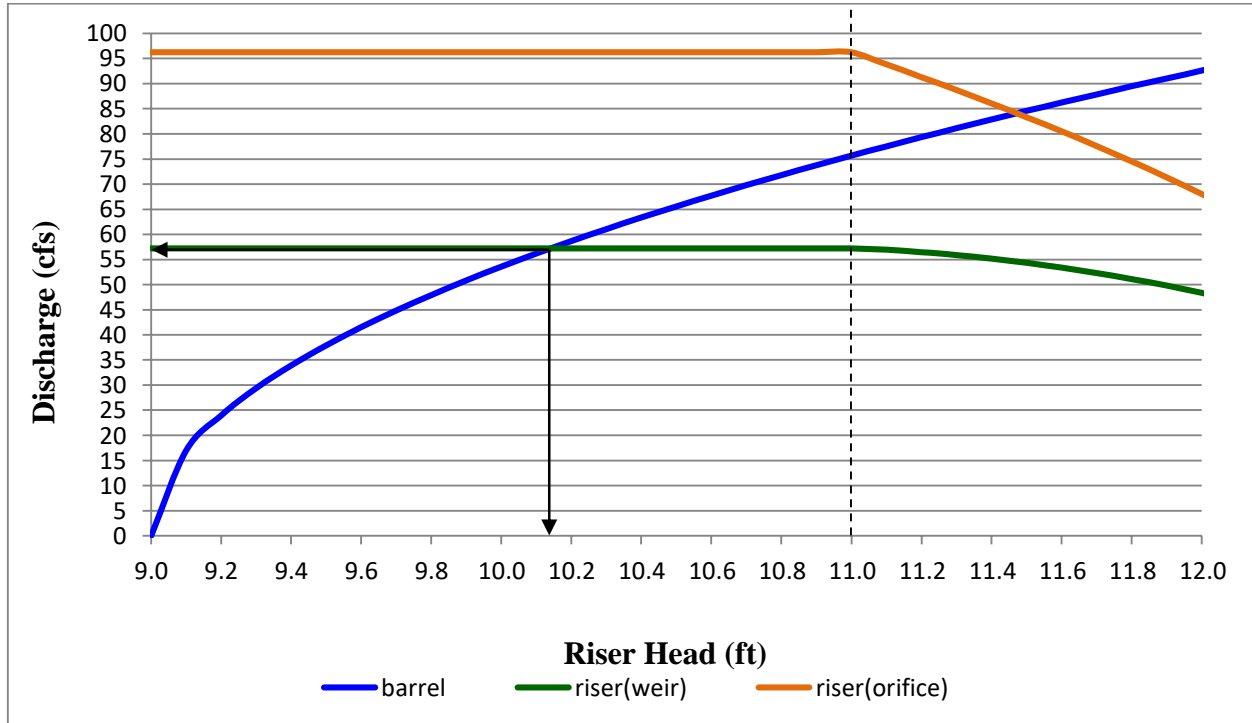
Figure A6. Unit structure rating curves for DR = 6, DB = 4

For the first design, since Q_B = 45 cfs, Q_D/Q_B = 500/44 = 11.36, implying that 12 barrels and risers will be needed. Similarly, in the second case, Q_B = 57 cfs and Q_D/Q_B = 500/57 = 8.77, indicating that 9 risers and barrels are needed to pass the design flow at the design head water and tail water. Performance curves similar to those shown in Figure 5b were constructed for the third and fourth cases where D_R = 7, D_B = 4 and D_R = 8, D_B = 4, respectively (not shown). The resultant unit discharges obtained were approximately 67 and 76 cfs, respectively.

From Equation A2, it is easily determined that d_{af} = 0.8 ≈ 1 foot. Hence, for anti-buoyancy purposes, each installed riser must be extended one foot below its nominal invert at elevation 0 and filled with concrete.

Steps G - K.

For illustrative purposes, the unit cost data ($ per foot installed) given in Table A1 were used for estimating the costs of the example designs. These costs include appurtenances. Neglected were the costs of the concrete and stop logs. Table A2 contains the computed cost estimate for each design. Shown also in Table A2 is the number of barrels and risers needed for each design along with the required channel bottom width at the structure location. Since only four designs are examined in this example, no plots are needed.

From Table A2, it is evident that designs 1 and 4 (numbered from left to right) are nearly equal in cost and required channel width. However, design 4 is preferable since the barrels do not

Table A1. Unit cost data for barrels and risers

Diameter (ft)	Unit Cost ($/ft installed)	
	Barrel	*Riser*
3	150	----
4	225	----
5	325	400
6	450	500
7	600	650
8	800	825

restrict the flow and the required channel width is slightly less. Transitions between the culvert structure and the main channel should be designed according to the procedures given in Appendix I.

In practice, additional barrel materials and shapes should be considered and included in the preceding analysis. Culvert barrels with smooth interiors and corrugated exteriors may lead to more economical designs.

Table A2. Design features and costs

Quantity	Design			
	$D_R = 5, D_B = 3$	$D_R = 6, D_B = 4$	$D_R = 7, D_B = 4$	$D_R = 8, D_B = 4$
# Barrels & Risers	12	9	8	7
Total Cost ($)	202,800	213,750	209,200	202,650
Channel Width (ft)	60	54	56	56

V.   References

Brater, E. F. and H. W. King. 1976. *Handbook of Hydraulics*. McGraw-Hill, New York, NY.

Schall, J. D., P. L. Thompson, S. M. Zerges, R. T. Kilgore and J. L. Morris. 2012. Hydraulic Design of Highway Culverts (3rd ed.). Report No. FHWA-HIF-12-026 (HDS 5), Federal Highway Administration, Washington, DC.

Wilsnack, M. M., J. Zeng and L. Zhang. 2010. Atlas of Flow Computations at Hydraulic Structures in the South Florida Water Management District. SHDM Report # 2009-005, Hydro Data Management Division, South Florida Water Management District, West Palm Beach, Florida, 157 pp.

Appendix B. Hydraulic Design Procedure for Bypass Channels

I.   Introduction

The primary objectives that should drive the hydraulic design process of a bypass channel for a primary water control structure include:

- Minimizing the costs of land acquisition, channel excavation and land clearing
- Minimizing impacts to existing buildings, utilities and other infrastructure
- Minimizing regulatory and permitting requirements
- Minimizing environmental impacts
- Maximizing channel stability while satisfying conveyance requirements

While these objectives are typically considered in the planning and design of permanent channels, they should also be addressed during the planning and design of temporary channels. It is assumed that in most cases it is the use and operation of the channel that is temporary as opposed to its existence. In other words, it is expected that, in the absence of compelling reasons to the contrary, a temporary bypass channel will not be filled in after the associated primary structure resumes normal operations. Rather, it would be maintained and remain dormant until the primary structure is taken out of service again.

The necessity of a temporary bypass channel is not only short-lived or intermittent but also generally more urgent with respect to time since repairs or enhancements to the primary structure cannot commence until the bypass channel is constructed and operational. These factors will generally render the first three objectives listed above more critical than they would otherwise be for a permanent facility. Consequently, they should be given more weight when planning and designing a temporary facility. In contrast, environmental impacts will most likely be a lesser concern for a temporary canal while strict adherence to engineering standards for channel stability and conveyance may not always be economically feasible.

The planning and design procedures presented below are consistent with published standards and criteria for the hydraulic design of flood control channels, without regard to the intended service life. This is conservative in that the proposed procedures will help to ensure that all relevant design issues and hydraulic engineering considerations are at least recognized and considered before any compromises are made. No guidance on how or when to deviate from these procedures, however, is provided here. Such deviations are always project specific and must ultimately be left to the discretion of the design engineer.

A number of publications containing hydraulic design procedures developed by federal agencies were reviewed prior to developing these guidelines. These included USDA-SCS (1977), USACE (1994), Schall et al (2001) and Kilgore and Cotton (2005). Also consulted were numerous reputable hydraulic engineering references, including Chow (1959), French (1985), Chadwick and Morfett (1985), and Zipparro and Hasen (1993).

II.   Initial Field Survey and Plan Layout

The first major task in designing a new channel is to identify the possible corridors and select the most feasible one based on economic, engineering and social considerations. Each of these subtasks is explained below.

Preliminary Survey and Corridor Analysis

The first step is to identify several potential corridors for the new channel and compile the relevant data for each one. The tasks listed below should be performed for each candidate route.

1. Using ArcGIS, locate on high-resolution aerial photos the approximate centerline location of each possible canal route. Demark the vertex locations in state plane coordinates. Overlay onto this map any feature class showing land parcel boundaries, right-of-ways, utilities and associated easements, archeological sites, political jurisdictions, wetland boundaries, soil classifications and surficial geologic units. If any of these feature classes are nonexistent, they should be created by qualified personnel.

2. Using LIDAR or other topographic data, estimate the ground surface profile along each corridor.

3. Identify along each candidate route any obstructions such as trees, buildings, roads and above-ground utilities.

4. Construct a profile drawing of each alternate corridor centerline. The data shown on this drawing should include land surface elevation, soil layers along with their classifications, and geologic units. This profile should be depicted to as low of an elevation as the data will allow. The locations of any data gaps should also be indicated.

5. At this point the design engineer should conservatively estimate the required depth and top width of the proposed channel.

Preferred Corridor Selection

Using the outcomes of the previous step, the preferred canal route should be selected. The factors guiding the decision will normally include, but not be limited to, the following:

1. Total corridor length
2. Land acquisition issues
3. Regulatory / permitting requirements
4. Expected engineering characteristics of the subsurface materials.
5. Expected difficulties with excavation
6. Estimated volume of excavation

Once the most favorable route has been identified, its planned location should be evaluated in the field by a team of qualified professionals. Included on this reconnaissance team should be the project engineer, the design engineer, a geotechnical engineer, a survey party chief, a real property manager and an environmental analyst trained in wetland delineation. As a final outcome, the centerline of the proposed corridor should be established and staked with a GPS.

III. Geotechnical Data Acquisition

The purpose of this task is to acquire the geotechnical data needed to design a stable channel cross section. The subtasks listed below should be carried out in the order indicated after completion of the previous task. Where applicable, all AASHO, ASTM and ASCE standards and test procedures should be adhered to. USACE (1970) also provides useful information on conducting laboratory soils testing for engineering design purposes. Furthermore, depending on subsurface conditions, data and test results not listed below may be required while some of those listed may not be useful. Additional guidance for conducting geotechnical investigations can be found in USACE (2001) and ASTM D420-98.

1. Determine the locations along the channel corridor where stratigraphic borings are to be extracted. This determination should be made by an experienced geotechnical engineer and a geologist. These locations should be staked in the field.

2. Extract each boring with the appropriate equipment and secure so as to minimize any disturbance during transport to the testing facility. If complex or unfamiliar subsurface conditions are encountered, geophysical logging is recommended. Test pits may also be constructed at the discretion of the geotechnical engineer.

3. Within each boring, determine the USCS soil types and obtain, for each distinct layer,

   - D_{50}, D_{65}, D_{75}
   - angle of repose
   - plasticity index, plastic limit, liquid limit
   - permeability
   - particles smaller than the #4 sieve
   - particles larger than the #4 sieve
   - natural dry unit weight and moisture content
   - the results of a drained, direct shear test
   - the results of a unconfined compression test

4. All data and test results should be summarized in a geotechnical evaluation report.

IV. Determination of Channel Side Slopes

The maximum allowable channel side slopes can be determined through slope stability analysis. In general, a slope stability analysis can be carried out using either conventional methodologies or numerical analysis techniques. Conventional techniques, also known as *limit equilibrium* analyses, are based on the premise that the soil mass comprising the channel banks tends to slide down along a critical slip surface due to the influence of gravity. The factor of safety, defined as the ratio of the forces resisting sliding to those opposing it, is at a minimum when the bottom of the soil mass prone to sliding is situated along this critical surface. Factors of safety could conceivably be determined in such a manner for a number of channel side slopes, where the side slope that results in the minimum acceptable factor of safety is the steepest side slope that can be used in the design. Limit equilibrium analyses constitute the slope stability analysis technique with the most wide-spread use in the design of civil works.

Numerical methods based on the concept of continuum modeling can also be used to analyze slope stability. Such techniques are generally used to solve the governing differential equations that represent the physical processes of sliding and failure. Like the conventional techniques, inherent to the numerical methods are simplifying assumptions that will limit their application. Unless the availability of data and the complexity of the project necessitate the use of numerical methods, conventional techniques should be used instead. In cases where numerical analyses are implemented, it is recommended that the engineer verify the results obtained from them using an alternate method.

Guidelines and comprehensive discussions on conducting slope stability analyses are provided by USACE (2003) and USDA-SCS (1977). A determination of the maximum allowable channel side slope with an appropriate factor of safety, based on these and other applicable guidelines, should be made by an experienced geotechnical engineer.

V. Determination of Channel Depth and Width

Once the design side slopes have been determined, the determination of the design depth and bottom width should follow. The channel should be large enough to carry the design discharge without exceeding the maximum allowable tractive shear stress along the wetted perimeter. The maximum permissible tractive stress that the channel bottom or side walls can be exposed to depends on the engineering properties of the earth materials located along the wetted perimeter. The most important properties include the soil grain size, represented by D_{75}, and the cohesiveness of the soil matrix, assessed through the Plasticity Index (PI).

Permissible Values for Tractive Shear Stress

According to the Federal Highway Administration (Kilgore and Cotton, 2005), the maximum tractive shear stress imposed on a channel bottom comprised of a fine-grained, non-cohesive soil (PI < 10) with $D_{75} < 0.05$ inches is 0.02 psf. For coarse-grained, non-cohesive soils where 0.05 inches $< D_{75} < 2$ inches, the maximum allowable shear stress τ_p (psf) is given by

$$\tau_p = 0.4 \, D_{75} \tag{B1a}$$

where D_{75} is in inches.

Kilgore and Cotton (2005) indicate that cohesive soils are primarily fine-grained and have a maximum allowable shear stress that depends on cohesive strength and soil density. The former property is related to the PI while the latter is a function of the void ratio (e). For these soils the permissible tractive shear stress on the channel bottom is given by

$$\tau_p = (c_1 \, PI^2 + c_2 \, PI + c_3)(c_4 + c_5 e)^2 \, c_6 \tag{B1b}$$

where c_1, c_2, c_3, c_4, c_5 and c_6 are empirical coefficients provided in Table B1.

Table B1. Coefficients for allowable soil shear stress (from USDOT, 2005)

USCS Designation	Applicable Range	c_1	c_2	c_3	c_4	c_5	c_6 (psf)
GM	$10 \le PI \le 20$	1.07	14.3	47.7	1.42	-0.61	0.0001
	$PI > 20$	-	-	0.076	1.42	-0.61	1.0
GC	$10 \le PI \le 20$	0.0477	2.86	42.9	1.42	-0.61	0.001
	$PI > 20$	-	-	0.119	1.42	-0.61	1.0
SM	$10 \le PI \le 20$	1.07	7.15	11.9	1.42	-0.61	0.0001
	$PI > 20$	-	-	0.058	1.42	-0.61	1.0
SC	$10 \le PI \le 20$	1.07	14.3	47.7	1.42	-0.61	0.0001
	$PI > 20$	-	-	0.076	1.42	-0.61	1.0
ML	$10 \le PI \le 20$	1.07	7.15	11.9	1.48	-0.57	0.0001
	$PI > 20$	-	-	0.058	1.48	-0.57	1.0
CL	$10 \le PI \le 20$	1.07	14.3	47.7	1.48	-0.57	0.0001
	$PI > 20$	-	-	0.076	1.48	-0.57	1.0
MH	$10 \le PI \le 20$	0.0477	1.43	10.7	1.38	-0.373	0.001
	$PI > 20$	-	-	0.058	1.38	-0.373	1.0
CH	$PI > 20$	-	-	0.097	1.38	-0.373	1.0

The maximum allowable tractive shear stress on the channel sides, τ_{ps}, is less than that for the channel bottom since, on the sloping sides, gravitational forces are working alongside the tractive forces to dislodge soil particles (Chow, 1959). Chow (1959) demonstrated that the relationship between τ_{ps} and τ_p is

$$\tau_{ps} = K\tau_p \tag{B2}$$

where

$$K = [1 - \sin^2(\theta) \, csc^2(\varphi_R)]^{1/2} \tag{B3}$$

$$\theta = \arctan(1/z) \tag{B4}$$

In Equations B2 – B4, z = the channel side slope determined through slope stability analysis, φ_R = the angle of repose for the soil comprising the channel side walls, and τ_p is computed by either Equation B1a or B1b.

Design Values for Tractive Shear Stress

The actual tractive shear stress imposed on a channel perimeter under field conditions depends on the channel slope (S_o), the specific weight of the water (γ) and the flow depth (y). According to Kilgore and Cotton (2005), the tractive stress τ_o acting on the channel bottom can, for design purposes, be computed by

$$\tau_o = \gamma\, y\, S_o \tag{B5}$$

under uniform flow conditions. Theoretically, Equation B5 is directly applicable to a channel with a bottom width to depth ratio (B/y) that is greater than 4. For B/y ratios less than 4, Equation B5 is conservative in that it over-estimates τ_o. A discussion of the degree of over-estimation is provided by Kilgore and Cotton (2005).

In south Florida, uniform flow conditions usually cannot be assumed for design purposes and, in fact, many canals have a horizontal bottom slope. It is assumed here that bypass channels will generally be designed with a horizontal bottom in order to minimize construction costs. In such a case, the friction slope S_f should be used in place of S_o. In the general case, then,

$$\tau_o = \gamma\, y\, S_f \tag{B6}$$

From the preceding discussions on permissive values of tractive stress, it follows that the design value for the tractive shear stress acting on the channel side walls, τ_{os}, can be computed from

$$\tau_{os} = K\tau_o \tag{B7}$$

where K is determined from Equations B3 and B4.

Estimating S_f

It is readily apparent that neither Equation B6 nor Equation B7 can be evaluated without a value of S_f that reflects design conditions. Chow (1959) demonstrates that, for a horizontal channel with the distance from its upstream end denoted by x, the slope of the water surface can be determined analytically from

$$\frac{dy}{dx} = S_c\, \frac{p^{M-N}}{1-p^M} \tag{B8a}$$

where

$$p = y/y_c \tag{B8b}$$

and y_c = the critical depth at the design discharge, S_c = the channel bottom slope that would carry the design discharge at a uniform flow depth $y_n = y_c$, M = the hydraulic exponent for critical flow computation and N = the hydraulic exponent for uniform flow computation. For a trapezoidal channel cross section with a bottom width of B, Chow (1959) specifies the following dimensionless parameters:

$$M = \frac{3\left[1+2z\left(\frac{y}{B}\right)\right]^2 - 2z\left(\frac{y}{B}\right)\left[1+z\left(\frac{y}{B}\right)\right]}{\left[1+2z\left(\frac{y}{B}\right)\right]\left[1+z\left(\frac{y}{B}\right)\right]} \tag{B9}$$

$$N = \frac{2}{3}\left\{5\left[\frac{1+2z\left(\frac{y}{B}\right)}{1+z\left(\frac{y}{B}\right)}\right] - 4\left[\frac{\left(\frac{y}{B}\right)\sqrt{1+z^2}}{1+2\left(\frac{y}{B}\right)\sqrt{1+z^2}}\right]\right\} \tag{B10}$$

In a trapezoidal channel carrying a discharge Q, y_c can be computed using the principles of open-channel hydraulics or read from published tables or charts. The use of commercial software or freeware to compute the critical depth is the most efficient approach. Once y_c has been determined, the corresponding value of Sc can be computed with Manning's equation.

In Equations B9 and B10, y should depict the average flow depth within the channel reach and should not vary appreciably. In south Florida canals, hydraulic and energy grade line slopes are generally small at locations not situated near a control structure or major point of withdrawal. Hence, in most canal reaches with a uniform cross section, y will not vary appreciably. Where this is not the case, Chow (1959) indicates that the channel reach should be divided into several sub reaches where y varies minimally within each one.

Where velocities are small (less than 2 ft/s), it can be assumed for design purposes that

$$S_f \approx |dy/dx| \tag{B11}$$

Estimating Flow Depths

Since the bypass channel will often be constructed with a horizontal bottom slope and flow will almost always be characterized as subcritical, the representative steady profile for capacity analysis purposes will be H2. This implies that a flow depth should be known or assumed at or near the downstream end. This depth may be associated with the head water stage of the temporary control structure or with the stage of a receiving water body. Using the notation presented earlier, Chow (1959) demonstrated that the change in flow depth over a horizontal channel reach of length L can be computed from the expression

$$L = \frac{y_c}{S_c}\left[\left(\frac{p_2^{N-M+1}}{N-M+1} - \frac{p_2^{N+1}}{N+1}\right) - \left(\frac{p_1^{N-M+1}}{N-M+1} - \frac{p_1^{N+1}}{N+1}\right)\right] \tag{B12}$$

where the subscripts 1 and 2 denote the upstream and downstream ends, respectively, of the reach. This can be rewritten more conveniently as

$$S_c\left(\frac{x}{y_c}\right) = \left(\frac{y_2}{y_c}\right)^E\left[\left(\frac{y_2}{y_c}\right)^M\left(\frac{\varepsilon^{E+M}-1}{E+M}\right) - \frac{\varepsilon^E-1}{E}\right] \tag{B13}$$

where

$y_1 = \varepsilon y_2$
ε = a factor greater than 1 that is equal to the fractional increase in depth from y_2 to y_1
x = the distance between the locations of y_2 and y_1
$E = N - M + 1$

Freeboard Requirements

According to USDA-SCS (1977), the minimum channel freeboard should be 20% of the design depth, but not less than 1 foot. Florida DOT requirements (FDOT, 2013) also stipulate a minimum freeboard of 1 foot for channels that are hydraulically connected to a storm water management system. Greater values can be specified at the design engineer's discretion.

VI.   Design Procedure

Based on the principles and formulas presented above, the following procedure can be used to determine the design depth of the channel cross section. Complete each step in the order indicated. Before starting this procedure, use the soils engineering data along with Equations B1 – B4 to determine the maximum permissive shear stresses τ_p and τ_{ps}.

1. *Obtain the design side slopes from the stability analysis.*

2. *Specify the bottom width.* Initially, this should be the smallest value that can be constructed given available equipment and subsurface conditions. Typically, this will be about 10 feet, although a range of 5 – 20 feet is possible.

3. *Specify the total depth.* This is the depth below land surface and should take into account subsurface conditions, the outcome of step 1, and any restrictions on the channel top width.

4. *Determine y_2.* Set y_2 = the design head water elevation at the downstream control structure minus the channel bottom elevation determined in step 3.

5. *Estimate the required freeboard.* Use the result of step 4 along with the criteria discussed previously to compute the required freeboard. The available freeboard at the control structure head water is the result of step 3 minus the result of step 4. If the available freeboard is less than what is required, the channel top-of-bank elevation should be increased with appropriate fill material.
6. *Estimate S_f.* Compute S_f at $y = y_2$ using Equations B8 – B11.

7. *Estimate τ_o and τ_{os}.* Using the results of the stability analysis, compute the limiting values of τ_o and τ_{os} with Equations B3, B4, B6 and B7.

8. *Compare τ_o with τ_p and τ_{os} with $\tau_{ps.}$* If the actual tractive stresses exceed the maximum allowable values, increase the depth and/or bottom width and repeat steps 4 – 7.

9. *Check the flow profile and available freeboard.* In order to verify that the design cross section completed so far is adequate for the entire reach, compute the increase in depth between the downstream and upstream ends using Equations B9, B10 and B13 along with the definition E = N – M + 1. If one of the following conditions occurs increase the bottom width and repeat steps 6 and 9:

    - the amount of freeboard at the upstream end is insufficient
    - $\varepsilon > 1.1$

10. *Specify the final design.* The channel depth and bottom width obtained with the last iteration of steps 4 – 9 is the design cross section depth.

At this point, the cross section design is complete. This iterative design procedure is depicted in Figure B1. An example given in the next section further illustrates the process.

VII. Design Example

A bypass channel 1000 feet long is needed to convey a design discharge of 750 cfs along a corridor whose land surface elevation is 15 feet.. The control structure at the downstream end of the channel has a design head water elevation of 12 feet. Geotechnical borings revealed that the soil is non-cohesive down to an elevation of 0 feet, where hard limestone layers were encountered. Additionally, the accompanying geotechnical laboratory tests indicate that $D_{75} = 0.1$ inches while the angle of repose is 30°. A maximum side slope of 2:1 is recommended based on the slope stability analysis.

Each step of the design process is carried out below.

Preliminary

Using the specified geotechnical data, determine the following channel stability parameters:

$\tau_p = 0.4(0.1) = 0.04$ psf   (Equation B1a)
$\theta = \arctan(1/2) = 26.57^O$ (Equation B4)
$K = [1 - \sin^2(26.57^O)\csc^2(30^O)]^{1/2} = 0.45$ (Equation B3)

Start

Obtain USCS designations of subsurface materials along with D_{75}, φ_R

Determine design side slopes through stability analysis

Compute τ_p, τ_{ps}

Specify bottom width

Specify total depth

Compute y_2

Verify freeboard

Compute S_f

Compute τ_o, τ_{os}

$\tau_o < \tau_p$?

No → Increase bottom width and/or total depth

Yes

Compute y_1, ε ← Recompute S_f

$\varepsilon < 1.1$ with sufficient freeboard @ upstream end ?

No → Increase bottom width

Yes

End
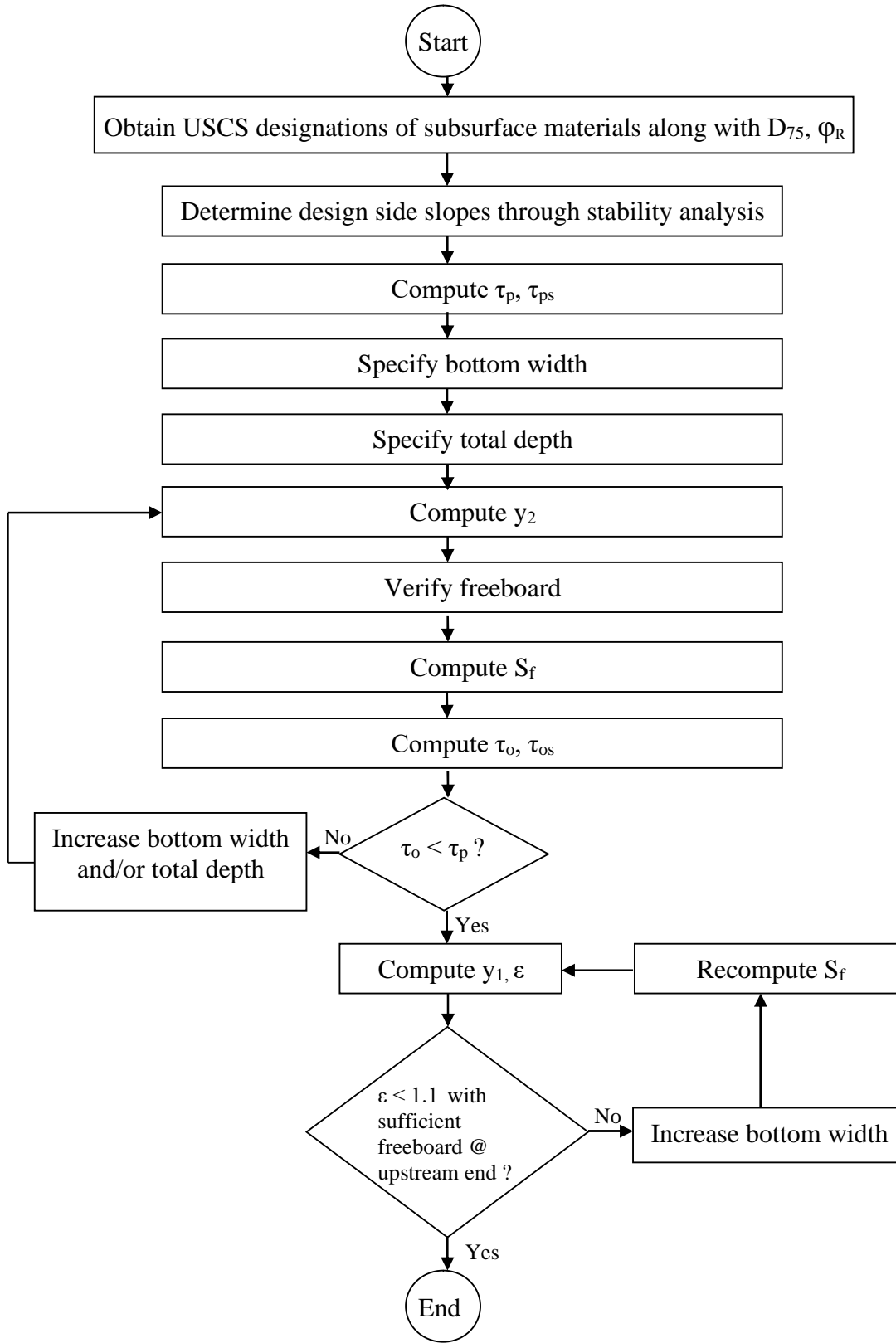
Figure B1. Design process for a canal cross section

$\tau_{ps} = 0.45(0.04) = 0.018$ psf   (Equation B2)

Step 1.

As indicated in the problem statement, the slope stability analysis indicates that the maximum allowable side slope is 2:1.

Step 2.

As an initial estimate, assume B = 15 feet.

Step 3.

Given the subsurface conditions, construction costs will likely be minimized if none of the hard limestone has to be excavated or blasted. Hence, the channel bottom will be set at elevation 0 feet, resulting in a total depth of 15 – 0 = 15 feet.

Step 4.

Given the design head water stage of 12 feet, $y_2 = 12 – 0 = 12$ feet.

Step 5.

Required freeboard = max[(0.2)(12),1] = 2.4 feet. The available freeboard = 15 – 12 = 3 feet > 2.4 feet. Thus, the required freeboard is available.

Step 6.

For $y_2 = 12$ ft, B = 15 ft and z = 2, Equations B9 and B10 yield M = 4.08 and N = 4.34. The section factor Z for critical flow computation (see, for example, Chow, 1959) is given by $Z = Q/g^{1/2} = (750)/(32.17)^{1/2} = 132.23$. this leads to $Z/B^{5/2} = (132.23)/(15)^{5/2} = 0.152$. From Figure 4-1 of Chow(1959), the dimensionless critical depth is $y_c/B = 0.48$, resulting in $y_c = (0.48)(15) = 7.2$ feet.

From Equation B8b, $p = y_2/y_c = 12/7.2 = 1.67$. At a depth of $y_c = 7.2$ ft, $A_c = [15 + 2(7.2)](7.2) = 211.68$ ft^2 and $P_c = 15 + 2(7.2)(5)^{1/2} = 47.2$ ft. For a channel excavated in granular soil, n = 0.035 is realistic. Putting these values of A_c, P_c and n along with Q = 750 cfs into Manning's equation yields a critical friction slope of $S_c = 0.00094$.

According to Equation B8a, $dy/dx = (0.00094)(1.67)^{4.08-4.34} / [1-(1.67)^{4.08}] = -0.00012$. Equation B11 indicates that $S_f \approx 0.00012$.

Step 7.

From Equation B6, $\tau_o = (62.4)(12)(0.00012) = 0.09$ psf $> \tau_p = 0.04$ psf. Likewise, Equation B7 implies that $\tau_{os} = 0.45(0.09) = 0.041$.

Step 8.

It is readily apparent that $\tau_o > \tau_p$ and, consequently, $\tau_{os} > \tau_{ps}$. The trial cross section is therefore too small and needs to be enlarged. Increase the bottom width to 25 feet.

Steps 3 – 5(2nd iteration)

These steps are not affected by an increase in bottom width only, so the results for these steps obtained during the first iteration apply to the second iteration as well.

Step 6 (2nd iteration).

Repeating the same calculations carried out in the first iteration except with B = 25 yields M = 3.81, N = 4.06, $y_c = 2.75$ ft, p = 4.36, $S_c = 0.015$ and $S_f = 0.000038$.

Steps 7 and 8 (2nd iteration).

Applying the updated results of step 7 to the same calculations carried out previously in step 8 gives $\tau_o = 0.028$ psf $< \tau_p = 0.04$ psf and $\tau_{os} = 0.013$ psf $< \tau_{op} = 0.018$ psf. Thus, the current trial cross section is of adequate size in regards to tractive stresses. Proceed now to step 9.

Step 9.

E = N – M + 1 = 1.25. Substituting this result along with the appropriate parameters from the previous iteration into Equation B13 yields $\varepsilon = 1.004 < 1.1$. This implies that the depth y_1 at the upstream end of the channel is $(1.004)(12) = 12.05$ ft. The available freeboard at the upstream end is then $15 - 12.05 = 2.95$ ft. This is greater than the required freeboard of $(0.20)(12.05) = 2.41$ ft. Therefore, no more iterations are required.

Step 10.

Since the last cross section examined satisfies all of the established criteria, it can be used for design. The bottom width is 25 feet, the bottom elevation is 0 feet and the side slopes are 2:1. The total depth is 15 feet based on a land surface elevation of 15 feet.

VIII. Detailed Survey and Corridor Demarcation

With the design cross section established, a detailed survey of the entire channel corridor should be conducted. This task should be conducted by, or under the supervision of, a Professional Land Surveyor. The accuracy of this survey should be adequate for construction and should locate the following:

1. Canal excavation limits, based on the staked centerline established earlier.

2. Right-of-way boundaries.

3. Property lines.

4. The baseline for horizontal measurements.

5. The location and boundaries of the temporary control structure.

6. Land surface elevations along the proposed centerline and excavation limits (i.e. top-of-bank).

A summary of the process for configuring and designing a bypass channel is summarized in Figure B2.
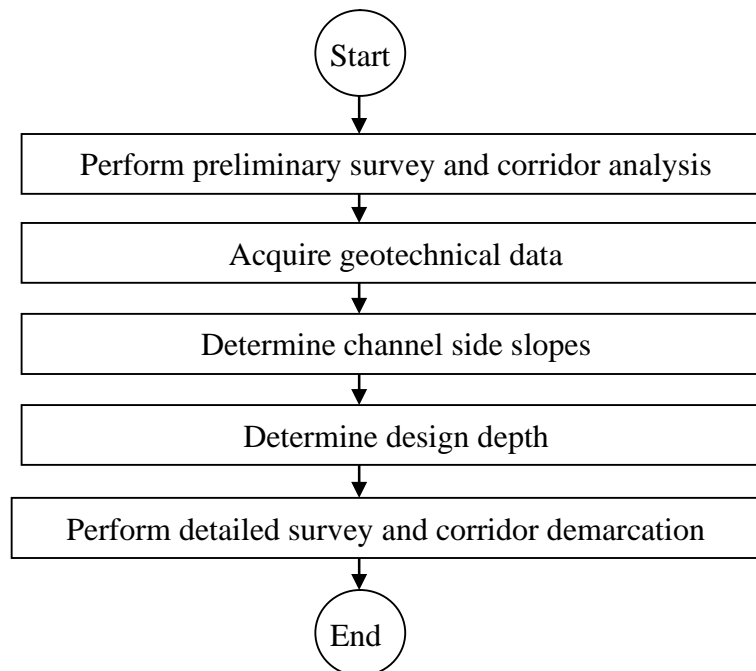
Figure B2. Summary of comprehensive procedure for designing a bypass channel

IX. References

Chadwick, A. J. and J. C. Morfett. 1985. *Hydraulics in Civil Engineering,* Allen & Unwin, London.

Chow, V. T. 1959. *Open-Channel Hydraulics*, McGraw-Hill, New York, NY.

French, R. H. 1985. *Open-Channel Hydraulics*, McGraw-Hill, New York, NY.

Kilgore, R. T. and G. K. Cotton. 2005. Design of Roadside Channels with Flexible Linings. Report No. FHWA-NHI-05-114, U.S. Department of Transportation, Federal Highway Administration, Arlington, VA.

Schall, J. D., E. V. Richardson and J. L. Morris. 2001. Introduction to Highway Hydraulics. Report No. FHWA-NHI-01-019, U.S. Department of Transportation, Federal Highway Administration, Washington, D.C.

USACE. 1970. Laboratory Soils Testing. EM 1110-2-1906, US Army Corps of Engineers, Washington, D.C.

USACE. 1994. Hydraulic Design of Flood Control Channels. EM 1110-2-1601, US Army Corps of Engineers, Washington, D.C.

USACE. 2001. Geotechnical Investigations. EM 1110-1-1804, US Army Corps of Engineers, Washington, D.C.

USACE. 2003. Slope Stability. EM 1110-2-1902, US Army Corps of Engineers, Washington, D.C.

USDA-SCS. 1977. Design of Open Channels. Technical Release No. 25, U.S. Department of Agriculture, Soil Conservation Service, Engineering Division, Washington, D. C.

Zipparro, V. J. and H. Hasen. 1993. *Davis' Handbook of Applied Hydraulics*. McGraw-Hill, New York, NY.

Appendix C. Hydraulic Design Procedure for Sharp-Crested Weirs

I.   Background

A.   Flow Over Sharp-Crested Weirs

Sharp-crested weirs have been used for water control and measurement in a variety of settings for many years since they are relatively simple and economical to construct. Additionally, there are a number of well-established methodologies that can be used to accurately estimate discharge rates over them. A conceptualization of the flow profile over a sharp-crested weir installed in a flat channel is shown in Figure C1. The weir is depicted as having a height P above the channel bottom along with an upstream head H measured from the weir crest. Furthermore, it is assumed to have a linear planform with a crest length of L across the width of the channel.
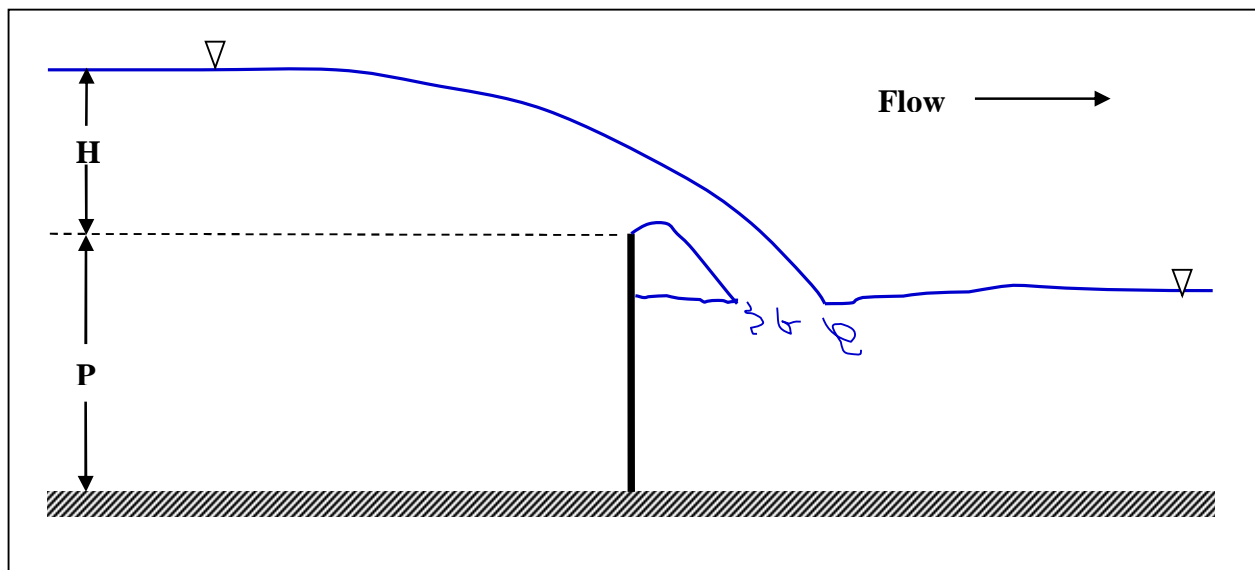
Figure C1. Conceptual flow profile for a sharp-crested weir

The shape of the weir crest along its length can, in practice, be of various forms. These include, but are not limited to, straight (i.e. level), parabolic, circular, triangular and trapezoidal. The characteristics of flow over each of these crest shapes are discussed in detail by Bos (1989). While the crest shapes with variable elevations along their lengths may often be more advantageous for flow measurement and computation purposes (especially at low heads), they are more difficult to construct and are more susceptible to clogging by debris. Minimizing maintenance and construction costs are primary considerations for a temporary bypass structure. Hence, the design procedures presented in this appendix are limited to weirs with straight crests with a constant elevation.

A linear weir behaves as sharp-crested when its crest thickness t is small compared to the upstream head. Swamee (1988) demonstrated that this condition is satisfied when H/t > 1.5.

It is evident in Figure C1 that flow across the weir crest can either be of a free-fall nature (i.e. unsubmerged) or submerged by a tail water whose elevation is above the weir crest. Design techniques for both of these flow conditions are provided in this appendix. Bos (1989) demonstrates that the unsubmerged discharge rate Q_u over a level sharp-crested weir can be computed from

$$Q_u = \frac{2}{3} C_d \, L \, \sqrt{2gH^3} \qquad\qquad (C1)$$

where C_d is a coefficient that accounts for hydrodynamic processes that could not be directly accounted for in the derivation of Equation C1. It should be noted that H denotes the height of the upstream hydraulic grade line above the weir crest as opposed to that of the energy grade line. Falvey (2003) indicates that either entity can be used to formulate weir flow. However, the studies that lead to the development of the expressions presented here for weir flow and the associated discharge coefficient were all based on the upstream hydraulic grade line. Consequently, this convention must be maintained here.

If flow across the weir is submerged by a tail water stage located at a height h above the weir crest (where H > h), the discharge rate Q_s will obviously be less than the corresponding value of Q_u at the same upstream head. Submerged flow over sharp-crested weirs has been studied by a number of investigators over the years. The relationship between Q_u and Q_s has been conventionally stated as (Wu and Rajaratnam, 1996)

$$Q_s = \psi \, Q_u \qquad\qquad (C2)$$

where ψ is a reduction factor that is a function of h/H. A detailed study of submerged weir flow by Wu and Rajaratnam (1996) revealed that the reduction factor can be approximated by

$$\psi = 1.0 + 1.162(h/H) - 1.331\sin^{-1}(h/H) \qquad\qquad (C3)$$

Perhaps the most long-standing and widely used relationship between ψ and h/H was developed by Villemonte (1947). Using both experimentation and an analytic solution based on the principle of superposition, he formulated the submergence reduction factor as

$$\psi = \left[1 - \left(\frac{h}{H}\right)^{\frac{3}{2}}\right]^{0.385} \qquad\qquad (C4)$$

The accuracy and reliability of Equation C4 was rigorously verified by Tullis et al. (2007) through experimentation. Given this along with its wide acceptance and longevity, Equation C4 is preferred for computing ψ in practice.

B.   Determining the Discharge Coefficient

Among the earliest and most comprehensive studies of flow over sharp-crested weirs was that of Rehbock (1929), where the following expression for C_d was proposed (Swamee, 1988):

$$C_d = 0.611 + 0.075\frac{H}{P} + \frac{0.36}{H\sqrt{\frac{\gamma}{\sigma}-1}} \qquad (C5)$$

In Equation C5, γ and σ are the unit weight and surface tension, respectively, of water. The last term in Equation C5 represents the effects of surface tension and can be significant at very low heads. For typical values of $\gamma = 62.4$ lb/ft^3 and $\sigma = 0.005$ lb/ft, this term reduces to

$$\frac{0.36}{111.71H - 1}$$

Under storm conditions, the values of H that are of interest will likely be at least 0.25 foot. This implies that the above term will usually be less than 0.013. Given the uncertainties inherent to the experimental investigations of weir flow and in the quantification of flood stages and discharges, the last term in Equation C5 can generally be neglected.

Experimentation and dimensional analysis of flow over sharp-crested weirs was also carried out by Kindsvater and Carter (1959). They considered a variety weir heads, heights and lengths, and proposed an equation of the form

$$Q = CLH^{3/2}$$

In the above expression, the discharge coefficient C is a function of H/P while the weir length L and head H are adjusted from their actual values so as to account for the effects of viscosity and surface tension. Additional details are provided by Brater and King (1976).

A more recent study of two-dimensional flow over a sharp-crested weir was carried out by Ramamurthy et al. (1987). This effort included both hydraulic experimentation and a hydrodynamic analysis that accounted for the conservation of mass and momentum. They found that the coefficient C_d is related to H/P, the pressure distribution along the upstream side of the weir face, the pressure distribution within the vena contracta, and the thickness of the vena contracta as follows:

$$C_d = \frac{3}{4}\sqrt{\frac{\left(\frac{1+\frac{H}{P}}{\frac{H}{P}}\right)^2(1-K_f)- K_B\left(\frac{Y_B}{H}\right)^2}{\left[\frac{\beta}{\left(\frac{Y_B}{H}\right)}\right]-\left[\frac{\frac{H}{P}}{\left(1+\frac{H}{P}\right)}\right]}} \qquad (C6)$$

In Equation C6, K_f denotes the pressure coefficient (used to correct for non-hydrostatic conditions) for the upstream weir face while K_B, β and Y_B are the pressure coefficient, the momentum correction coefficient and the thickness, respectively, of the vena contracta. A plot of the variation of Cd with H/P (see Figure 6b of Ramamurthy et al., 1987) reveals that, for H/P < 5,

$$C_d \cong 0.61 + 0.085 \left(\frac{H}{P}\right) \tag{C7}$$

The ratio H/P will typically be much less than 5 for most intended applications. Hence, Equation C7 can be used instead of Equation C6. Equation C7 will yield values of C_d close to those computed with Equation C5 with the last term neglected. Equations C1, C2, C4 and C7 are recommended for use in designing linear sharp-crested weirs.

C. Nappe Aeration

Inherent to the equations for C_d presented in the preceding section is the assumption that the air space between the underside of the nappe and the downstream face of the weir (Figure C1) is at atmospheric pressure. From this air pocket, however, air is continually removed by the flow in the nappe (see, for example, Bos, 1989). If unsubmerged flow over the weir crest is in contact with the channel walls, this air space will essentially be isolated from the surrounding atmosphere. This can lead to subatmospheric pressures within the air pocket, resulting in increased curvature of the nappe and values of C_d that are higher than those predicted with the equations presented earlier. Furthermore, in extreme cases the nappe can become unstable and intermittently cling to the downstream face of the weir. This could have undesirable effects, including structural damage. Consequently, under the conditions stated, measures must be taken to ensure that the air pocket is adequately aerated.

Bos (1989) presented a relationship between the unsubmerged weir discharge rate Q_u and the maximum demand of air Q_{air} required for full aeration of the air space below the nappe. This relationship was developed from data acquired by Howe et al. (1955) and is given by

$$Q_{air} = 0.1 \left(\frac{H}{y_p}\right)^{\frac{3}{2}} Q_u \tag{C8}$$

where Q_{air} is in cfs and y_p is the depth of the downstream pool between the weir and the nappe. Under south Florida conditions, y_p will typically be close to the downstream tail water depth. This is because the latter is usually higher than the sequent depth of the hydraulic jump that would occur downstream of the weir in the absence of any tail water. In situations where this is not the case, the value of y_p will depend on the hydraulics of flow within the channel immediately downstream of the weir. For conservative design under these conditions, a small value of y_p (say, 1 - 2 feet) can be assumed.

The air supply determined with Equation 8 is usually provided to the nappe underspace through a conduit that is vented to the atmosphere at its upper end and is perforated along its length under

the nappe. In order to design the conduit needed to deliver the required air flow, the air pressure within the nappe subspace needs to be known. This pressure should be the minimum allowable pressure (or maximum allowable suction). Unfortunately, there is little (if any) guidance in the literature as to what the value of this pressure should be for design purposes, and it may be dependent on site conditions. However, at a minimum, subatmospheric pressures within the nappe subspace should not cause the discharge rate to increase significantly from its design value. A maximum deviation of 1% - 5% is suggested, but should be specified by the project engineer. According to Bos (1989), the percent increase in the discharge that occurs when the gauge pressure within the nappe subspace drops below zero can be estimated from the following expression:

$$X_Q = 20 \left(\frac{-p_{sn}}{H} \right)^{0.92} \qquad\qquad \text{(C9)}$$

where X_Q is the percent increase in flow rate and p_{sn} is the gauge pressure (< 0) within the nappe subspace. If X_Q is set to the maximum allowable deviation and H is the upstream design head, Equation C9 can be solved for the corresponding value of p_{sn} that should be used in designing the air vents. With the gauge pressure at the upper end of the vent equal to zero along with a gauge pressure at the vent outlets equal to p_{sn}, standard techniques used to design conduits transporting compressible fluids can be used to design the vent. If necessary, advice should be sought from a mechanical engineer that specializes in the design of HVAC systems.

II.   Site Constraints

There are a number of site features that can influence both the economic and hydraulic feasibility of a weir installation. These include the dimensions of the discharge channel or outfall, the design discharge rate and downstream backwater effects that may submerge weir discharges. Throughout the design process, the engineer should remain aware of any constraints imposed by these factors.

III.   Hydraulic Design Tasks

Once the design discharge (Q_D), head water stage (HW_D), tail water stage (TW_D) and desired seasonal control elevation (CE) have been established, the tasks listed below should be performed in the order given.

  A. Obtain the approach channel floor elevation (BE), the channel bottom width (BW), the seasonal control elevation of the weir crest (CE), and the design discharge, head water stage and tail water stage.

  B. Compute the following:

   P = CE – BE (the weir height measured from the upstream channel floor)

   H = HW_D - CE

$h = TW_D - CE$

C. Estimate the anticipated thickness of the weir crest (t) based on structural design considerations and established construction practices.

D. Compute H/P and H/t. If H/t < 1.5, do not use this design procedure since the weir is not acting as a sharp-crested weir. Refer to the appropriate section of these guidelines for the recommended design procedure.

E. If H/P < 5, compute C_d using Equation C7. If H/P > 5, Equation C7 will not apply. In this case, refer to Ramamurthy et al. (1987).

F. If h > 0, proceed to step G. Otherwise, compute

$$L = \frac{3Q_D}{C_d\sqrt{8gH^3}}$$

A transition may be needed to modify the channel width to L at elevation CE. Additionally, design, if necessary, the aeration devices needed to provide the required ventilation under the nappe. Refer to the appropriate section of these guidelines.

Proceed next to step H.

G. Compute the submergence reduction factor using Equation C4. Compute

$$L = \frac{3Q_D}{\psi C_d\sqrt{8gH^3}}$$

A transition may be needed to modify the channel width to L at elevation CE.

H. Design any vents or other aeration equipment needed to provide the required ventilation beneath the nappe.

I. Design the apron, the upstream and downstream transitions (if required), and any other structural improvements to the channel that are needed.

J. Complete a cost estimate and note any anticipated maintenance problems.

The procedure for designing a sharp-crested weir is summarized in Figure C2 and is demonstrated by example in the following section.
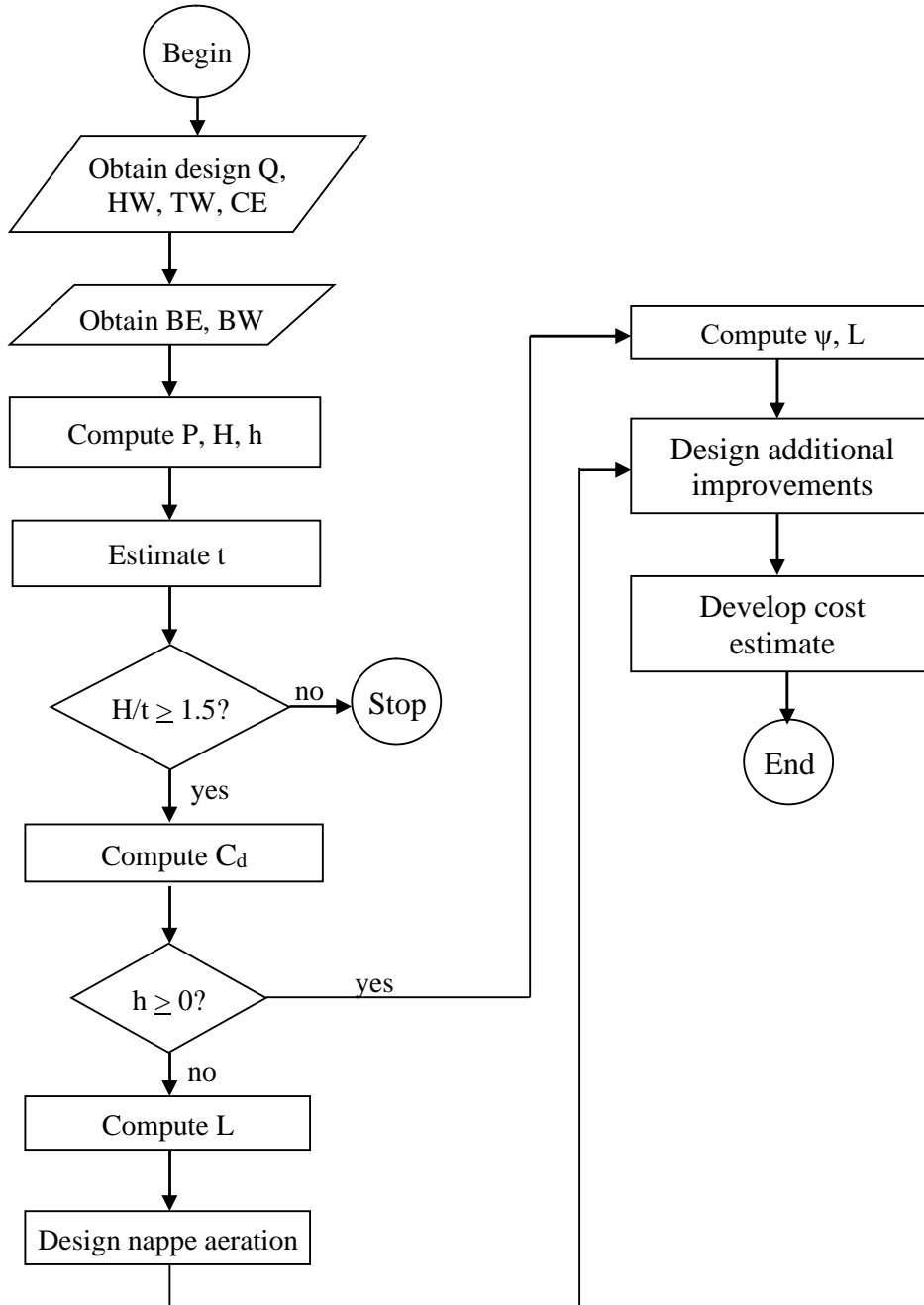
Figure C2. Sharp-crested weir design process

IV. Design Example.

A. Example 1

Design a sharp-crested weir for the same bypass channel and design conditions specified for the design example given in Appendix A. For convenience, these conditions are repeated here:

A bypass channel with a bottom width of 20 feet, a bottom elevation of 0 feet, a top-of-bank elevation of 15 feet and 2:1 side slopes carries a design discharge of 500 cfs. The design head water and tail water stages for the proposed structure location are 13 and 9 feet, respectively, while the seasonal control elevation is 11 feet.

Each step of the design process is carried out below.

Step A.

From the problem statement, BW = 20 ft, BE = 0 ft, CE = 11 ft, HW_D = 13 ft, TW_D = 9 ft and Q_D = 500 cfs.

Step B.

P = 11 – 0 = 11 ft
H = 13 – 11 = 2 ft
h = 9 – 11 = -2 ft (unsubmerged)

Step C.

Assume a weir crest thickness of t = 2 inches.

Step D.

H/P = 2/11 = 0.18 and H/t = 2/(2/12) = 12 > 1.5. Hence, the weir is acting as a sharp-crested weir.

Step E.

Since H/P = 0.18 < 5, equation C7 applies: C_d = 0.61 + 0.085(0.18) = 0.63.

Step F.

Since h < 0, L = (3)(500)/0.63/[(8)(32.17)(2)^3]$^{1/2}$ = 52.5 ft.

Step G. (skip)

Step H.

At an elevation of 11 ft, the channel width = 20 + (2)(2)(11-0) = 64 ft. This implies that a transition will be needed to reduce the channel width to 52.5 feet at the weir location. Alternatively, the weir can be over-designed to a length of 64 ft since the extra weir length may be cheaper than the cost of a channel transition. However, this will result in less attenuation of the peak discharge at the structure and may result in storm flows downstream that are higher than those that were passed historically by the permanent structure under the same storm conditions.

B. <u>Example 2</u>

After completing the weir design of example 1, it was found that structural changes proposed downstream will increase the design tail water stage to 12 ft. By how much will this decrease the design capacity of the weir for the same head water stage?

In this case, h = 12 – 11 = 1 ft, so step G applies. Applying Equation C4 results in
$\Psi = [1 - (1/2)^{3/2}]^{0.385}$ = 0.85. Substituting this result along with the values for H, C_d and L into the equation shown in step G yields Q_D = 425.2 cfs. This is approximately a 15% decrease from the required capacity of 500 cfs.

V.   References

Bos, M. G. (Ed.). 1989. *Discharge Measurement Structures*, International Institute for Land Reclamation and Improvement, Wageningen, The Netherlands.

Brater, E. F. and H. W. King. 1976. *Handbook of Hydraulics, Sixth Edition,* McGraw-Hill, New York, NY.

Falvey, H. T. 2003. *Hydraulic Design of Labyrinth Weirs*, ASCE, Reston, Va.

Howe, J.W., G.C. Shieh and A.O. Obadia. 1955. Aeration demand of a weir calculated. Civil Engineering Vo1.25, NOS, p.289. Easton, Pa. &Personal Communication, 1972 (Howe).

Kindsvater, C. E. and R. W. Carter. 1957. Discharge Characteristics of Rectangular Thin-Plate Weirs.

Ramamurthy, A. S., U. S. Tim and M. V. J. Rao. 1987. Flow Over Sharp-Crested Plate Weirs. *J. Irrigation and Drainage Engineering,* ASCE, 113(2), 163-172.

Rehbock, T. 1929. Discussion of "Precise Measurements" by K. B. Turner. *Transactions of the ASCE,* 93, 1143–1162.

Swamee, P. K. 1988. Generalized Rectangular Weir Equations. *J. Hydraulic Engineering*, ASCE, 114(8), 945-949.

Tullis, B. P., J. C. Young and M. A. Chandler. 2007. Head-Discharge Relationships for Submerged Labyrinth Weirs. *J. Hydraulic Engineering,* ASCE, 133(3), 248-254.

Villemonte, J. R. 1947. Submerged Weir Discharge Studies. *Engineering News-Record*, 139(26), 54-56.

Wu, S. and N. Rajaratnam. 1996. Submerged Flow Regimes of Sharp-Crested Weirs. *J. Hydraulic Engineering,* ASCE, 122(7), 412-414.

Appendix D. Hydraulic Design Procedure for Labyrinth Weirs

I.   Background

A.   Introduction

A labyrinth weir can be depicted as a linear weir with its planform axis folded so as to create a series of trapezoids as shown in Figures D1 and D2. This results in a weir with an effective
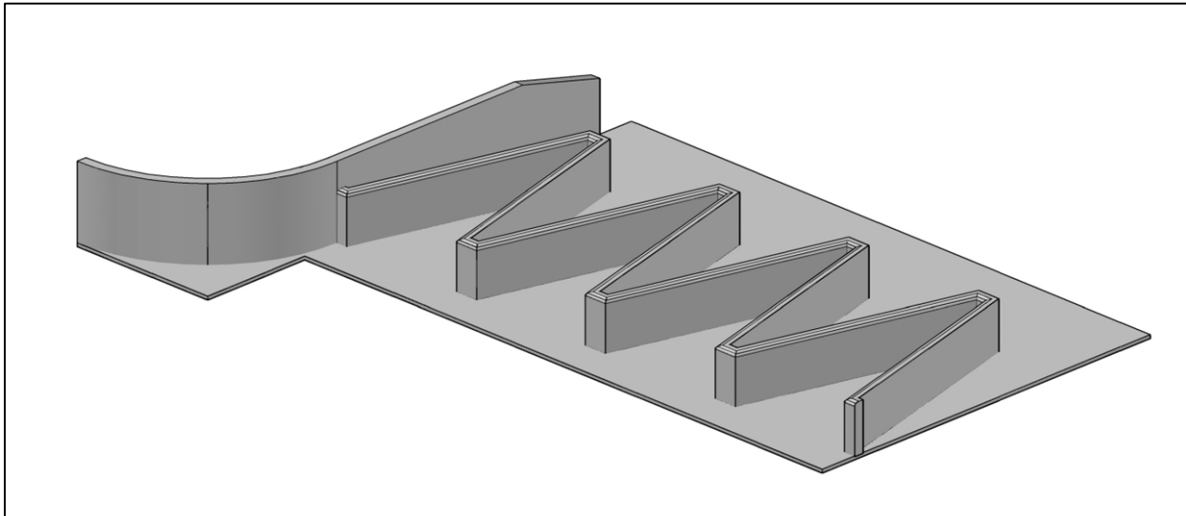
Figure D1. Three-dimensional view of a labyrinth weir (courtesy, Schnabel Engineering)
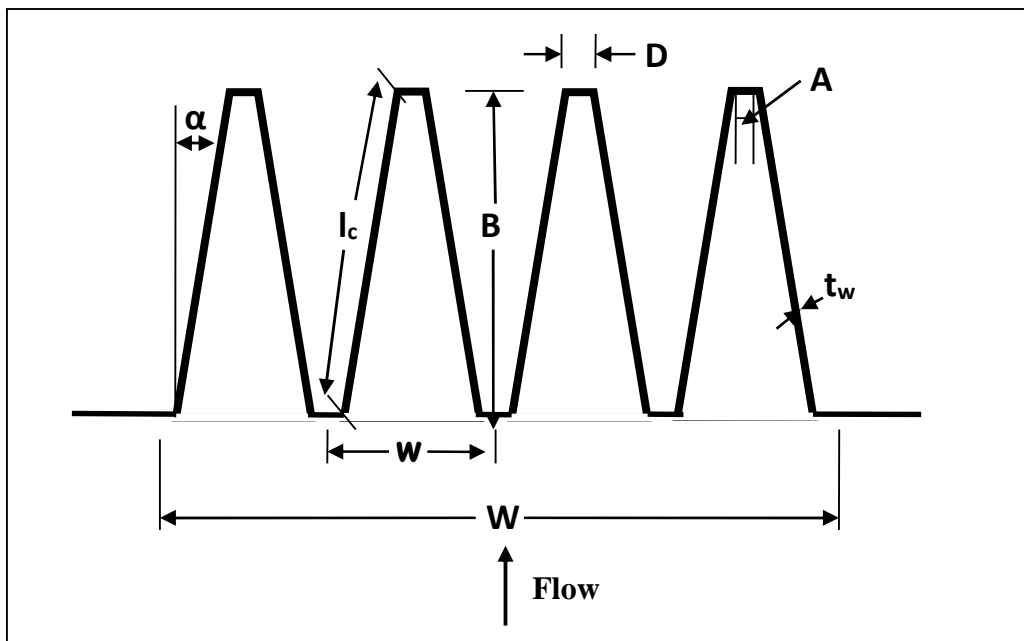
Figure D2. Plan view of a labyrinth weir with pertinent dimensions

length that is much longer than that of a standard linear weir. Consequently, its discharge capacity can be as much as six times greater than that of a linear weir for a given channel width. Alternatively, it can pass the same discharge as a linear weir at a lower upstream head. Shown also in Figure D2 are the dimensions relevant to the hydraulic design and efficiency of the weir. These are, namely

α = the angle between the sidewall and the primary flow direction
W = the total width of the weir perpendicular to the primary flow direction
B = the total depth of the weir parallel to the primary flow direction
w = a width of one cycle = W/N
N = the number of cycles
D = the outer apex width
A = the inner apex width
l_c = the side wall length
t_w = the wall thickness at the crest

B.   Previous Studies

Although labyrinth weirs have never been constructed and used in southern Florida, they have been used extensively in the USA and may turn out to be the most economically or hydraulically efficient outfall structure for sites with head water constraints that make passing the design discharge problematic (see, for example, Sitompul et al. 1995). Labyrinth weirs were incorporated into the outlet works of Ute dam (Houston, 1983) by the U.S. Bureau of Reclamation in order to provide the desired storage while increasing the discharge capacity to pass the inflow design flood. Other examples include Dog River Dam (Frizell, 2003); Lake Townsend Dam (Tullis and Crookston, 2008); the Avon and Woronora dams constructed by the Metropolitan Water Sewerage and Drainage Board of Sydney, Australia (Darvas, 1971); the Maguga (Van Wyk, 2006) dam; and the Bospoort (ARQ, 2006) Dam. To date, there are estimated to be approximately 100 labyrinth weir structures in the United States.

The hydraulic characteristics of labyrinth weirs have been studied over the years by various researchers while some investigators have proposed hydraulic design procedures. The hydraulic behavior of labyrinth weirs was studied by Taylor (1968) through physical experimentation. Hay and Taylor (1970) used the results of Taylor (1968) to develop the first hydraulic design guidelines. Around the same time, Darvas (1971) had carried out hydraulic model studies of several prototypes and proposed alternative design guidelines. Physical modeling carried out later by Houston (1982) was used to verify and expand the results of Hay and Taylor (1970) so that design curves applicable to Ute dam could be developed. Discrepancies between the USBR experimental results and those of Hay and Taylor (1970) were noted. This was attributed to differences in the definition of upstream head used by the two sets of investigators which directly relates to differences in the approach flow conditions (Falvey, 2003).

Subsequent analyses carried out by Lux and Hinchliff (1985) and physical modeling by Tullis et al. (1995) led to the development of two additional hydraulic design guidelines specific to

labyrinth weirs constructed with a quarter-round crest shape (see also Falvey, 2003). The hydraulic performances of selected labyrinth weir designs predicted by each of these two sets of design criteria were evaluated by Paxson and Savage (2006) through numerical modeling with CFD. In this evaluation, both design procedures were applied to the design configuration of the labyrinth weir at Hyrum dam (Houston, 1983) installed within a channel. The hydraulic performance of the weir predicted by each procedure was then compared to that predicted by the CFD modeling. While both design approaches showed good agreement with the modeling results, better agreement with less bias was achieved with the design approach proposed by Tullis et al. (1995). Other applications of the design methodologies developed by Lux and Hinchliff (1985) and Tullis et al. (1995) are provided by Paxson et al. (2011).

Additionally, Falvey (2003) compared the discharge coefficients obtained through measured data for a number of labyrinth spillways located around the world to the corresponding discharge coefficients obtained from the design curves developed by Tullis et al. (1995). In most cases, agreement between the two sets of discharge coefficients was very good. Falvey (2003) attributed any large deviations to differences in inlet flow conditions or errors in published dimensions or flow properties.

While most of the preceding investigations considered only unsubmerged weir flow, a procedure was developed by Tullis et al. (2007) that conveniently corrects head water stages computed under unsubmerged conditions so as to account for downstream submergence. Although Taylor (1968) used the Villemonte (1947) equation to correct for submergence, Tullis et al. (2007) found that this approach, applied to labyrinth weirs, generally overestimated the increase in upstream head for a given discharge caused by downstream submergence. Hence, it is recommended that the approach by Tullis et al. (2007) be used to compute submerged flow over labyrinth weirs as opposed to the conventional approach by Villemonte (1947) for linear weirs.

Additional and more recent studies of flow over labyrinth weirs have been carried out at the Utah Water Research Laboratory by Willmore (2004) and Crookston (2010). These investigations extended the previous efforts by Tullis et al. (1995) and considered additional weir crest shapes and labyrinth wall angles. Furthermore, these efforts were later supplemented through an investigation by Carollo et al. (2012) that quantified unsubmerged flow over sharp-crested labyrinth weirs. The research carried out by Crookston (2010) has been disseminated via Crookston and Tullis (2013a,b) and Crookston and Tullis (2012a,b,c). These publications provide the most recent and comprehensive hydraulic design guidelines for labyrinth weirs. These guidelines are reflected in the design procedure explained in sections II and V below. Although Crookston and Tullis (2013a) includes design information of quarter- and half-round crest shapes, the procedure outlined herein focuses on the half-round shaped weir crests since they were found to be advantageous at lower heads. Additionally, it is assumed that the proposed labyrinth weir will be sited in a straight channel. Other approach conditions, including reservoir applications, were also investigated by Crookston (2010) and the associated results can be used to specify a similar design procedure, if necessary. Finally, since the use of a sharp-crested labyrinth weir may be preferred in some cases, a separate design procedure for this type of weir that is based on the results of Carollo et al. (2012) is provided in sections III and VI.

II. Computation of Flow Over a Labyrinth Weir with a Half-Round Shaped Crest

A. Unsubmerged Flow

1. Computation of Flow

Crookston and Tullis (2013a) indicate that the discharge over a labyrinth weir can be stated as

$$Q = \frac{2}{3}\, C_d\, L_C\, \sqrt{2gH_T^3} \tag{D1}$$

where L_C is the total length of the weir crest, H_T is the total upstream hydraulic head (potentiometric head plus velocity head) above the weir crest, and C_d is a dimensionless discharge coefficient. Denoting the height of the weir crest above the channel floor as P, the coefficient C_d was presented by Tullis et al. (1995) and Crookston (2010) as a function of the head water ratio H_T/P and the sidewall angle α (Figure D2). This function was expressed by Crookston and Tullis (2013a) as

$$C_d = a \left(\frac{H_T}{P}\right)^{\left[b\left(\frac{H_T}{P}\right)^c\right]} + d \tag{D2}$$

where a, b, c and d are parameters determined through physical experiments. Crookston and Tullis (2013a) provide the values for these parameters (Table D1) for $6° \leq \alpha \leq 35°$. Equation D2 is depicted graphically in Figure D3. If a value of C_d is needed for a value of α that lies between two of the nominal values shown in Table D1, linear interpolation between the computed $C_d(\alpha)$ values for the nominal α values is acceptable. Although the experimental data presented by Crookston (2010) supports the curves for H_T/P up to about 1.0, additional work has been performed by Crookston et al. (2013) for H_T/P up to 2.0.

Table D1. Values of regression parameters for half-round labyrinth weirs (from Crookston, 2010)

α (º)	a	b	c	d
6	0.009447	-4.039	0.3955	0.1870
8	0.017090	-3.497	0.4048	0.2286
10	0.029900	-2.978	0.4107	0.2520
12	0.030390	-3.102	0.4393	0.2912
15	0.031600	-3.270	0.4849	0.3349
20	0.033610	-3.500	0.5536	0.3923
35	0.018550	-4.904	0.6697	0.5062

2. Cycle Efficiency

In Figure D3, it is apparent that, for H_T/P greater than about 0.1, C_d increases as α increases. In contrast, for a given base area of the structure (W x B), the total length of the weir crest (L_c) will increase as α decreases. According to Equation D1, increasing either C_d or L_c will increase the
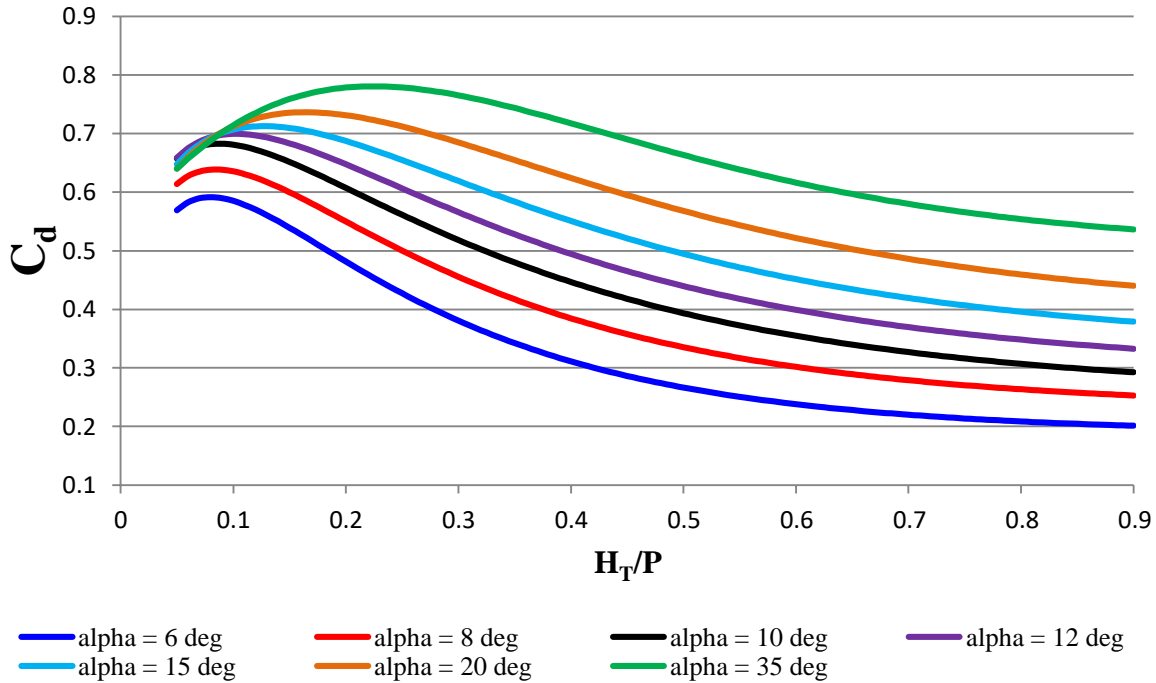
Figure D3. C_d vs. H_T/P (reconstructed from Crookston, 2010)

capacity of the structure. Crookston (2010) recommends that both of these factors be considered when designing a labyrinth weir since the longer weir lengths can compensate for the reduction in C_d with decreasing α. To help understand this concept, Crookston and Tullis (2013a) introduced the concept of a cycle efficiency ε' defined by

$$ε' = C_d \, L_{c\text{-cycle}} / w \qquad\qquad (D3)$$

where $L_{c\text{-cycle}}$ is the weir crest length per cycle. That is, $L_{c\text{-cycle}} = L_c / N$. Cycle efficiency is representative of the discharge per cycle and was computed by Crookston and Tullis (2013a) for each of the C_d values shown in Figure D3. The results are shown in Figure D4. In this effort, the values of $L_{c\text{-cycle}}$ used in Equation D3 were the unit cycle lengths of the physical models.

According to Figure D4, ε' increases with decreasing α and this trend becomes more evident as H_T/P decreases. Furthermore, it is readily apparent that, for a given α, ε' becomes optimal at smaller values of H_T/P. In particular, cycle efficiency is maximized from about $H_T / P = 0.1$ for α = 6° to about $H_T/P = 0.2$ for α = 35°. Moreover, Figure D4 demonstrates that the increases in weir length that result from smaller values of α are less beneficial at higher values of H_T / P. These results suggest that a cost analysis should be performed to evaluate an optimal ε' and labyrinth geometry. Crookston (2010) indicates that hydrodynamic interference between nappes is a primary reason as to why cycle efficiency decreases as H_T/P increases. Similarly, as H_T/P increases, ε' decreases more rapidly for the smaller values of α where nappe interference is more significant. This is discussed further below.
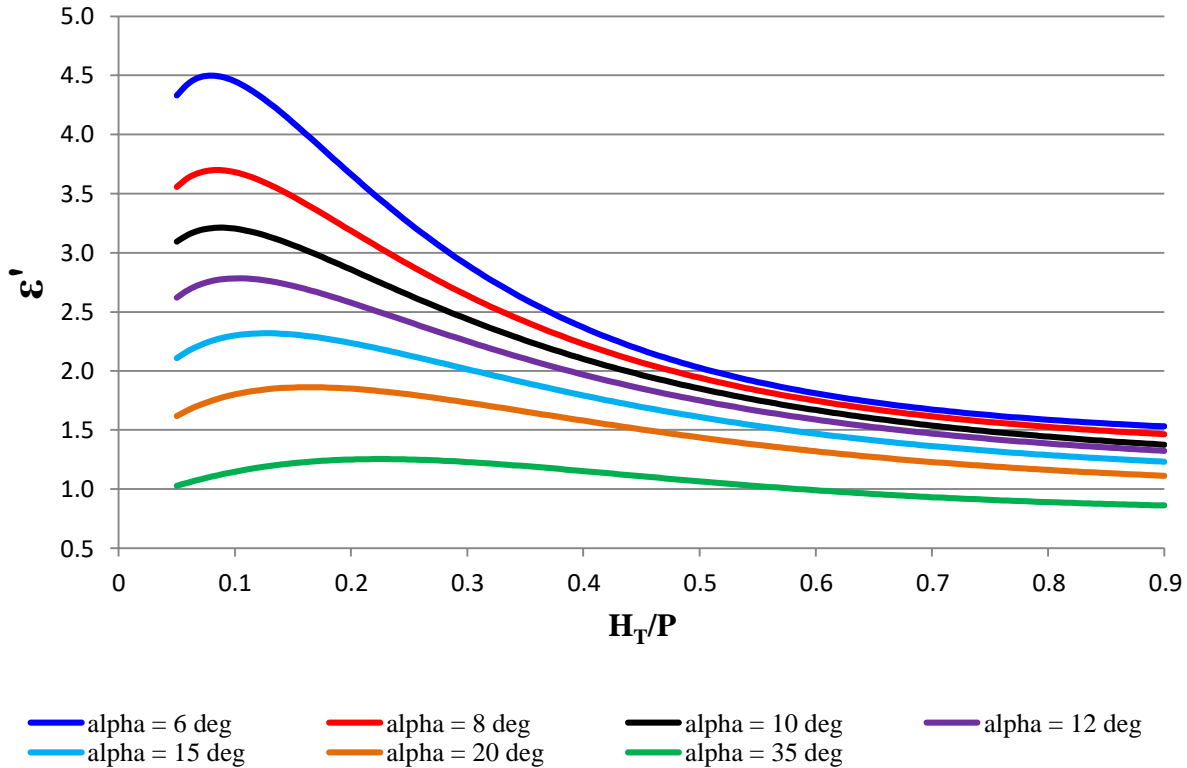
Figure D4. ε' vs. α and H_T/P (reconstructed from Crookston, 2010)

3. *Nappe Interference*

As indicated above, the effects of nappe interference are inherently reflected in the empirical values of C_d determined by Crookston and Tullis (2013a). However, Crookston and Tullis (2013a) found that nappe interference can cause two labyrinth weir designs with common sidewall angles and weir lengths, but with a different number of cycles, to exhibit different head-discharge characteristics. Crookston and Tullis (2012c) demonstrate that nappe interference is most significant near the upstream apexes of the weir. Furthermore, they indicate that for a given value of α, t_w, A, H_T and P, the distance downstream of an apex (measured perpendicular to the apex) over which nappe interference occurs, hereafter referred to as B_{int}, is essentially independent of the value of B. As a result, if two geometrically similar weirs have the same value of L_c but different values of N, the weir with the greater number of cycles (i.e. the greater number of apexes) will incur nappe interference over a greater portion of its length. Through physical model tests, Crookston and Tullis (2012c) found that the ratio B_{int}/B can be expressed as

$$\frac{B_{int}}{B} = 2.038 \left[(5.155 \times 10^{-7})^{1/\alpha} \left(\frac{H_T}{P} \right)^{1.307} \right] + 0.03916, \quad 6° \leq \alpha \leq 35° \; and \; \frac{H_T}{P} \geq 0.1 \quad (D4)$$

The primary concern here regarding nappe interference is that if the geometry (e.g., sidewall length) of a cycle is appreciably smaller than that tested by Crookston (2010), nappe interference may affect a greater portion of the weir length and the value of C_d may be over estimated by the procedure discussed above. As an example, for $\alpha = 15°$ and $H_T/P = 0.5$, Crookston and Tullis (2012c) found that increasing the number of cycles from one to two while maintaining L_c and the other geometric properties caused the value of B_{int}/B to increase from 0.26 to 0.66. This resulted in a value of C_d determined through the design procedure that was 13% higher than the experimentally determined value. Hence, for a given geometric design, L_c and H_T/P, it appears that as the number of cycles is increased and B is reduced, B_{int}/B increases to a point where the effective value of C_d for the weir begins to decrease materially from its design value.

For design purposes, it may be more intuitive to compare the nappe interference length measured along the weir crest to l_c, the length of a single weir crest (Figure D2). Crookston and Tullis (2012c) denote the former quantity as L_d, where $L_d = B_{int} \cos(\alpha)$. In the findings mentioned above where B_{int}/B was increased from 0.26 to 0.66, the corresponding increase in L_d/l_c was from approximately 0.24 to 0.62. Thus, under the conditions of their experiments where L_d was about 25% of l_c, the investigators found negligible difference between the experimental and design values of C_d. In contrast, the experimental and design values of C_d differed by 13% when the length of L_d covered about 60% of l_c. While these results would not necessarily be the same under a different set of experimental conditions, they nonetheless suggest that for a hydraulically optimal labyrinth, L_d should be a small fraction of l_c. For design purposes, $L_d/l_c \leq 0.25$ is suggested.

4. Nappe Behavior

Nappe behavior should be considered in the design of a labyrinth weir so as to identify the potential of nappe vibration, pressure fluctuations, or nappe instability at the design flow rate or under typical operations. Of particular interest to the designer is the unstable nappe behavior that was identified to occur over certain ranges of H_T/P. Unstable nappe behavior can in some cases produce unwanted structural side effects. The affected ranges of H_T/P are provided in Table D2 as a function of α. For each angle shown, the weir should, if possible, be designed so that the associated unstable range of H_T/P is avoided (Crookston and Tullis, 2012c). However, in certain situations an economically optimal design may result in a value of H_T/P that lies within an unstable range. In such a case it is possible that the unstable nappe may not impose against the weir pressure fluctuations that are of sufficient magnitude to cause structural damage. Additionally, it may be possible to resolve adverse nappe conditions through remedial measures such as crest modifications, a staged crest, or a modified apron. This information is discussed in detail in Crookston and Tullis (2013b).

5. Other Design Constraints

The design equations and methods presented in the preceding sections are based on experimental data for specific flow conditions and labyrinth geometries. These include

Table D2. Ranges of H_T/P resulting in unstable nappe operation (from Crookston, 2010)

α (degrees)	Unstable Range for H_T/P
6	None
8	None
10	0.325 – 0.326
12	0.329 – 0.385
15	0.332 – 0.577
20	0.363 – 0.599
35	0.411 – 0.460

$$2 \leq w/P \leq 4 \tag{D5a}$$
$$A = t_w \tag{D5b}$$
$$t_w = P/8 \tag{D5c}$$
$$0.05 \leq H_T/P \leq 1.0 \tag{D5d}$$

There is some flexibility, however, in the value of t_w to accommodate structural design requirements (e.g. battered walls are often used where P is large). Once C_d is determined in the manner explained above and the total weir length L_c is computed with Equation D1, the other labyrinth weir dimensions can be determined from the planform geometry. The required expressions are

$$D = A + 2t_w \tan(45^0 - \alpha/2) \tag{D6a}$$
$$B = \tfrac{1}{2}(L_c/N - A - D)\cos(\alpha) + t_w \tag{D6b}$$
$$l_c = (B - t_w)\sec(\alpha) \tag{D6c}$$
$$w = 2l_c \sin(\alpha) + A + D \tag{D6d}$$

Although this methodology is recommended for the design and analyze labyrinth weirs, in large applications there may be merit to a physical or numerical model study to verify hydraulic performance and to include site specific conditions. The predictive accuracy of the design method may decrease for weirs that are geometrically dissimilar to those tested by Crookston (2010).

Designing a labyrinth weir using the preceding information is generally a trial-and-error process. This will be demonstrated by example in later sections. Design examples are also provided by Tullis et al. (1995), and Crookston and Tullis (2013a). As is the case for most water control structures, a successful design balances hydraulic optimization with project costs.

B. Submerged Flow

The design equations and data presented in the preceding section pertain to unsubmerged flow over a labyrinth weir crest. If the nappe becomes submerged due to a tail water stage that is higher than the weir crest, additional modifications to the flow computation procedure are needed. Submerged flow over a linear weir is commonly computed by first determining the

discharge rate under unsubmerged conditions and then multiplying it by a flow reduction factor. This factor is a function of the tail water submergence and the upstream head. Villemonte's equation (Villemonte, 1947) is frequently used in engineering practice to compute the flow reduction factor. For submerged flow over labyrinth weirs, however, Falvey (2003) found that Villemonte's equation has limited accuracy in predicting the effects of submergence on the discharge rate. This conclusion was based in part on the experimental data published by Taylor (1968). Labyrinth weirs are influenced less by submergence than are linear weirs.

Instead of determining a flow reduction factor that can be used to correct the discharge rate computed with Equation D1 under submerged conditions, Tullis et al. (2007) proposed that a dimensionless magnification factor for the upstream head, H^*/H_T, be used to determine the increase in upstream head caused by downstream submergence. H^* denotes the total upstream energy head with respect to the weir crest under submerged conditions. If H^* is a specified design condition, the corresponding value of H_T that would result in the same discharge rate under unsubmerged conditions is obviously less than H^*. By conducting submergence tests on several labyrinth weir configurations with various discharge rates and submergence levels, Tullis et al. (2007) found that these two quantities are related through the following expressions:

$$\frac{H^*}{H_T} = 0.0332 \left(\frac{H_d}{H_T}\right)^4 + 0.2008 \left(\frac{H_d}{H_T}\right)^2 + 1 \quad for \;\; 0 \leq \frac{H_d}{H_T} \leq 1.53 \qquad \text{(D7a)}$$

$$\frac{H^*}{H_T} = 0.9379 \left(\frac{H_d}{H_T}\right) + 0.2174 \quad for \;\; 1.53 < \frac{H_d}{H_T} \leq 3.5 \qquad \text{(D7b)}$$

$$H^* = H_d \quad for \;\; 3.5 < \frac{H_d}{H_T} \qquad \text{(D7c)}$$

In Equations D7, H_d denotes the total downstream energy head measured from the weir crest. Both H^* and H_d are known quantities since they are based on known or specified conditions upstream and downstream, respectively, of the weir. Under the conditions of their experiments, Tullis et al. (2007) found that Equations D7 are substantially more accurate than Villemonte's equation when used to predict the increase in upstream energy head due to downstream submergence. He also proposed additional submergence relationships for linear weirs.

The value of H_T corresponding to H^* can be determined by solving Equation D7a or D7b. However, since H_T is initially unknown, it may not be clear as to which of these two equations applies. Unless the value of H_d/H^* dictates which range H_d/H_T lies in (since $H_d/H_T > H_d/H^*$), it is advisable to first solve Equation D7b and then ascertain whether or not H_d/H_T falls into the specified range. If the computed value of H_d/H_T is less than 1.53, then Equation D7a should be solved for H_T. For convenience, this equation can be restated as

$$k_1(H_T{}')^4 + k_3(H_T{}')^2 - k_4 H_T{}' + 1 = 0 \;\; for \; 0 \leq (H_d \, H_T') \leq 1.53 \qquad \text{(D7d)}$$

where $H_T{}' = 1/H_T$, $k_1 = 0.0332 H_d{}^4$, $k_3 = 0.2008 H_d{}^2$, and $k_4 = H^*$. This is a linear, fourth-degree polynomial whose roots can be conveniently determined using Excel, Mathematica or other

mathematical software. This equation will generally have four roots. The correct root is the one that is real, positive and satisfies the restriction $0 \leq (H_d\ H_T') \leq 1.53$. The value of H_T is then simply $1/H_T'$. Once H_T is determined, the discharge under submerged conditions can be computed with Equations D1 and D2.

At high submergence levels ($H_d/H_T > 3$), Tullis et al. (2007) found that $H^* = H_d$. In this case, the discharge is no longer controlled by the weir. These investigators also found that the effects of submergence on the upstream head do not become significant until H_d/H_T exceeds 0.5.

The required steps of the design procedure for a labyrinth weir with a half-round crest are given in section V.

III.   Computation of Flow Over a Labyrinth Weir with a Sharp Crest

If the proposed labyrinth weir is to have a sharp crest, the design principles presented in this section should be applied. All design equations and supporting data were obtained from Carollo et al. (2012) who utilized data acquired from their own hydraulic model tests (P = 3.9 inches) along with previous laboratory test results published by Gentilini (1940). Unfortunately, the results of this investigation only address unsubmerged flow. Also, s*ince the results of this investigation are relatively new and may have had limited applications, the design equations given in this section should be used with discretion*.

Carollo et al. (2012) determined that the discharge Q over a triangular, sharp-crested labyrinth weir installed in a straight channel is given by

$$\frac{Q}{Q_n} = 1 + \frac{\frac{2l_c}{w} - 1}{5.988\left(\frac{H}{w}\right)^{1.419} + 1} \tag{D9}$$

where H is the upstream hydraulic head with respect to the weir crest and Q_n is the corresponding discharge over a linear weir of length W. Carollo et al. (2012) specify Q to be in the direction opposite to that shown in Figure D1 and refer to the term $2l_c/w$ as the *magnification ratio*. In order to maintain consistency with the procedure used by Carollo et al. (2012) to develop the above equation, Q_n should be computed with Rehbock's formula, which can be written as

$$Q_n = \left[0.402 + 0.054\frac{H+0.0011}{P}\right]\sqrt{2g}\, W(H + 0.0011)^{1.5} \tag{D10}$$

Based on the experimental conditions inherent to the investigation by Carollo et al. (2012), it is recommended that the proposed design procedure be subject to the following constraints (refer to Figure D1):

$$D = 0 \text{ (i.e. a triangular planform)} \tag{D11a}$$
$$1.15 \leq 2l_c/w \leq 2.0 \tag{D11b}$$

$$0.3 \leq w/P \leq 1.5 \qquad\qquad (D11c)$$
$$0.1 \leq H/w \leq 1.2 \qquad\qquad (D11d)$$

It should be noted that constraint D11b implies $30° \leq \alpha \leq 60°$. The steps for the design procedure that is based on Equations D9 and D10 along with constraints D11 are given in section VI.

IV.   Site Constraints

There are a number of site features that can influence both the economic and hydraulic feasibility of a labyrinth weir. These include the dimensions of the discharge channel or outfall, the design discharge and downstream backwater effects that may submerge the weir. Throughout the design process, the engineer should remain aware of any constraints imposed by these factors.

V.   Hydraulic Design Tasks for a Half-Round Weir Crest

Once the design discharge (Q_D), head water stage (HW_D) tail water stage (TW_D) and desired control elevation (CE) have been established, the tasks listed below should be performed in the order given.

A. Obtain the approach channel floor elevation (BE) along with the bottom width (BW). Assume that the head water stage upstream of the weir (HW) is equal to the design head water stage (HW_D). Similarly, assume that the tail water stage downstream of the weir (TW) is equal to the design tail water stage (TW_D).

B. Compute the velocity head in the upstream approach channel ($V_u^2/2g$) at the designated head water stage and design discharge. Similarly, compute the velocity head downstream of the proposed weir location at the designated tail water stage ($V_d^2/2g$).

C. Compute the following:

   $HW_T = HW + V_u^2/2g$ (upstream EGL elevation)

   $TW_T = TW + V_d^2/2g$ (downstream EGL elevation)

   $P = CE - BE$ (the weir height measured from the upstream channel floor)

   $H_d = TW_T - CE$ (the downstream energy head measured from the weir crest)

   $t_w = P/8$ (the wall thickness at the weir crest)

D. If $H_d > 0$, proceed directly to step E below. Otherwise, compute the upstream energy head measured from the weir crest under unsubmerged flow conditions (H_T) as follows:
   $H_T = HW_T - CE$

Omit step E and proceed directly to step F.

E. Compute the total upstream energy head measured from the weir crest under submerged flow conditions (H^*) from

$$H^* = HW_T - CE$$

and, using the computed values of H^* and H_d along with Equations D7, compute H_T.

F. Compute H_T/P using the value of H_T obtained from either step D or E. It is recommended that the condition $0.05 \leq H_T/P \leq 1.0$ be satisfied.

G. Select an initial value for the labyrinth weir sidewall angle α (Figure D1). Use Figure D4 and Table D2 for guidance.

H. Select an initial value for N (the total number of labyrinth cycles).

I. Set $A = t_w$.

J. Compute $C_d(\alpha)$ using Equation D2, the value of H_T / P determined in step F, and the parameter values given in Table D1.

K. Compute L_c using Equation D1 along with the design discharge, the value of H_T determined in either step D or E, and the value of C_d computed in step J.

L. Use Equations D6 to compute D, B, l_c and w.

M. Compute w/P.

N. Determine B_{int} using the value of B computed in step L and Equation D4. Compute $L_d = B_{int} \cos(\alpha)$ and L_d/l_c.

O. Determine if $2 \leq w/P \leq 4$ and $L_d/l_c \leq 0.25$. If these criteria are not satisfied, choose a different value of N or adjust the value of α and repeat steps J – N. Iterate as needed until each of these criteria is satisfied.

P. Compute $W = Nw$.

Q. Design the channel transitions needed upstream and downstream of the weir. The transition should include vertical side walls upstream of the weir that are long enough to ensure that the approach flow is relatively straight and uniform. Refer to Appendix I for guidelines.

R. Design any channel stabilization measures needed downstream of the weir.

S. Develop a cost estimate of the weir structure that includes the results of steps Q and R.

T. Repeat steps G – R as desired in order to develop several labyrinth weir designs. This is necessary to determine the design configuration that is most cost-effective.

The procedure for designing a labyrinth weir with a half-round crest is summarized in Figure D5. It should be noted that in the above procedure, H_T and H_d are based on the velocity heads in the primary channel. In many situations, the computed weir base width W will be different than the primary channel bottom width, necessitating a different channel cross section immediately upstream and downstream of the weir. This implies that H_T and H_d will deviate from the values used in the calculations. Consequently, in a strict sense this would require that the preceding computations involving either H_T or H_d be repeated in order to determine what (if any) changes to the design would result. Fortunately, in most south Florida applications the velocity heads will not be appreciable and should have only a small influence on the final design. In exceptional cases, though, the procedure demonstrated above can be iterated until negligible changes in the final design are obtained.

VI.   Hydraulic Design Tasks for a Sharp Weir Crest

Once the design discharge (Q_D), head water stage (HW_D) tail water stage (TW_D) and desired control elevation (CE) have been established, the tasks listed below should be performed in the order given.

A. Perform step A given in section V.

B. Compute P = CE – BE and H = HW – CE.

C. Select an initial value for the labyrinth weir sidewall angle α (Figure D1). Recall that $30^\circ < \alpha < 60^\circ$ (this will satisfy constraint D11b).

D. Select an initial value for N = the total number of labyrinth cycles.

E. Compute the magnification ratio $2l_c/w = \csc(\alpha)$

F. Determine by trial & error the base weir width W using Equation D9, Equation D10 and the relation w = W/N .

G. Verify that constraints D11c and D11d are satisfied. If not, select a new trial value for α or N and repeat steps E and F.

H. Compute $l_c = \frac{1}{2}\, w\csc(\alpha)$, $B = l_c\cos(\alpha)$ and $L_c = 2\, l_c N$.

I.   Design the channel transitions needed upstream and downstream from the weir. The transition should include vertical side walls upstream of the weir that are long enough to ensure that the approach flow is as straight and uniform as possible. Refer to Appendix I for guidelines.

J.   Design any channel stabilization measures needed downstream of the weir.

K.   Develop a cost estimate of the weir structure that includes the results of steps I and J.

L.   Repeat steps C – K as desired in order to develop several labyrinth weir designs. This is necessary to determine the design configuration that is most cost-effective.

The procedure for designing a sharp-crested labyrinth weir is summarized in Figure D6.

VII.   Design Example for a Labyrinth Weir with a Half-Round Weir Crest

A. Example 1

Design a labyrinth weir with a half-round crest for the conditions specified below.

A bypass channel with a bottom width of 50 feet, a bottom elevation of 0 feet, a top-of-bank elevation of 15 feet and 2:1 side slopes carries a design discharge of 2500 cfs. The design head water and tail water stages for the proposed structure location are 13 and 9 feet, respectively, while the seasonal control elevation is 11 feet.

Each step of the design process is carried out below. As stated, Q_D = 2500 cfs, HW_D = 13 feet, TW_D = 9 feet and CE = 11 feet.

Step A.

As given in the problem statement, BW = 20 feet, BE = 0 feet. Also, set HW = 13 feet and TW = 9 feet.

Step B.

Given the channel geometry along with the specified head and tail water stages, the velocity heads corresponding to the design discharge were determined to be $V_u^2/2g$ = 0.1 ft and $V_d^2/2g$ = 0.26 ft.

Step C.

$HW_T = HW + V_u^2/2g = 13 + 0.1 = 13.1$ feet

$TW_T = TW + V_d^2/2g = 9 + 0.26 = 9.26$ feet

$P = CE - BE = 11 - 0 = 11$ feet

$H_d = TW_T - CE = 9.26 - 11 < 0$

$t_w = P/8 = 11/8 = 1.375$ feet

Step D.

$H_T = HW_T - CE = 13.1 - 11 = 2.1$

Step E (omit since $H_d < 0$).

Step F.

$H_T/P = 2.1/11 = 0.191$. Since $0.05 \leq 0.191 \leq 0.9$, the constraint $0.05 \leq H_T/P \leq 1.0$ is satisfied.

Step G.

For $H_T/P = 0.191$, Figure D4 indicates that the cycle efficiency is significantly higher for $\alpha = 6^0$ than it is for the other angles. Also, according to Table D2, the nappe should be stable. Hence, $\alpha = 6^0$ appears to be a worthwhile initial selection.

Step H.

Try an initial value of $N = 2$.

Step I.

Set $A = t_w = 1.375$ feet.

Step J.

Using Equation D2 and Table D2 with $\alpha = 6^0$ and $H_T/P = 0.191$ results in $C_d = 0.492$.

Steps K-O.

$L_c = 312.35'$, $D = 3.85'$, $B = 76.44'$, $l_c = 75.47'$, $w = 21.00'$, $B_{int} = 7.70'$, $L_d = 7.66'$, $w/P = 1.91$, $A = 1.375' < 0.08(21.00) = 1.68$, and $L_d/lc = 0.10 < 0.25$. Note that w/P is just slightly below the lower limit of 2.

Step P.

$W = Nw = (2)(21) = 42$ feet.

Step Q.

Given W = 42 feet, BW = 50 feet and a top width of 94 feet at CE = 11 feet, the channel transition required for this design will be somewhat extensive. Other designs should be considered as well.

Steps R-S (Omitted here)

Step T.

The procedure above was repeated for α = 8, 10, 20 and 35 degrees. The resultant weir dimensions are shown in Table D3.

Table D3. Results of design example 1

α(°)	N	A < 0.08w	L_c	D	B	l_c	w	W	B_{int}	L_d	2 < w/P < 4	L_d/l_c < 0.25
6	2	1.375	312.35	3.85	76.44	75.47	21.00	42.01	7.70	7.66	1.91	0.10
8	2	1.375	274.82	3.77	66.87	66.13	23.55	47.10	7.90	7.82	2.14	0.12
10	2	1.375	249.64	3.68	60.35	59.88	25.85	51.71	8.14	8.01	2.35	0.13
20	2	1.375	209.54	3.30	48.41	50.05	38.91	77.82	9.35	8.79	3.54	0.18
35	3	1.375	197.92	2.81	26.68	30.90	39.62	118.87	6.26	5.13	3.60	0.17

From Table D3, it is apparent that the design based on α = 35° yields the shortest total weir length (~198 feet). However, the total weir length for α = 20° is only about 12 feet longer (~210 feet) while its base width is about 78 feet compared to approximately 119 feet for α = 35°. Given the channel bottom with of 50 feet along with a top width of 94 feet at the control elevation, it appears that α = 20° yields a geometric design that is more amenable to the channel dimensions and would minimize transition costs. It may be the best choice for this application.

B. Example 2

In the previous example, what would have been the design value of H_T if the design tail water stage was 12 feet instead of 9 feet?

In this case the downstream velocity head $V_d^2/2g = 0.12$ and $H_d = 12 + 0.12 - 11 = 1.12$. In addition, the upstream head now reflects submerged conditions, so $H^* = HW_T - CE = 2.1$ feet. Solving Equation D7a by trial and error yields $H_d / H_T = 0.573$ and $H_T = 1.96$ feet. This value of H_T represents the upstream energy head that would produce the same discharge rate under unsubmerged conditions. The weir would then be designed as demonstrated above with this value of H_T.

VIII.   Design Example for a Sharp-Crested Labyrinth Weir

Design a labyrinth weir with a sharp crest for the same conditions specified for the design example given in the previous section.

Step A

As in the previous example, BW = 50 feet, BE = 0 feet, HW = 13 feet and TW = 9 feet.

Step B

As before, P = 11 – 0 = 11 feet. H = 13 – 11 = 2 feet.

Step C

Select a trial value of $\alpha = 30°$.

Step D

Select a trial value of N = 10.

Step E

Compute $2l_c/w = \csc(30°) = 2.00$

Step F

Solving Equations D9 and D10 for W and w by trial and error yields W = 152.8 feet and w = 15.28 feet.

Step G

w/P = 1.39 and H/w = 0.13. These satisfy the constraints $0.3 \leq w/P \leq 1.5$ and $0.1 \leq H/w \leq 1.2$.

Step H

$l_c = (1/2)(15.28)\csc(30°) = 15.28$ ft; B = $(15.28)\cos(30°) = 13.23$ ft; $L_c = (2)(15.28)(10) = 305.60$ ft.

```
                              Begin

      ┌──────────────────┐                    ┌──────────────────┐
      │ Obtain design Q, │                    │   Compute L_c    │◄──┐
      │  HW, TW, CE,     │                    └──────────────────┘   │
      │   BE, BW         │                             │             │
      └──────────────────┘                    ┌──────────────────┐   │
               │                              │ Compute D, B, l_c, w │ │
      ┌──────────────────┐                    └──────────────────┘   │
      │ Compute V_u²/2g, │                             │             │
      │     V_d²/2g      │                    ┌──────────────────┐   │
      └──────────────────┘                    │ Compute w/P, B_int, │ │
               │                              │      L_d/l_c      │   │
      ┌──────────────────┐                    └──────────────────┘   │
      │Compute HW_T, TW_T,│                            │             │
      │   P, t_w, H_d    │                        2 ≤ w/P ≤ 4,       │
      └──────────────────┘              no      A ≤ 0.08w,           │
               │                      ◄───────  L_d/l_c ≤ 0.25?       │
          H_d > 0?                                    │              │
     yes ◄────┴────► no                              yes             │
      │                   │              ┌──────────────────┐        │
┌─────────────┐  ┌─────────────┐         │ Compute W = Nw   │        │
│Compute H*, H_T│  │ Compute H_T │        └──────────────────┘        │
└─────────────┘  └─────────────┘                │                    │
      │                 │             ┌──────────────────────┐        │
      └────────┬────────┘             │ Design channel transition │   │
       ┌──────────────┐               │ and stabilization measures│   │
       │Compute H_T/P │               └──────────────────────┘        │
       └──────────────┘                        │                      │
               │                      ┌──────────────────┐            │
   no     0.05 ≤ H_T/P ≤ 1.0?         │Develop cost estimate│          │
  Stop ◄──────┴──────                 └──────────────────┘            │
               │ yes                           │                      │
       ┌──────────────┐              yes   Additional design?          │
       │  Select α, N │◄───────────────────                           │
       └──────────────┘                        │ no                   │
               │                              End                      │
       ┌──────────────┐                                                │
       │Compute A = t_w│                                               │
       └──────────────┘                                                │
               │                                                       │
       ┌──────────────┐                                                │
       │Compute C_d(α) │───────────────────────────────────────────────┘
       └──────────────┘
```
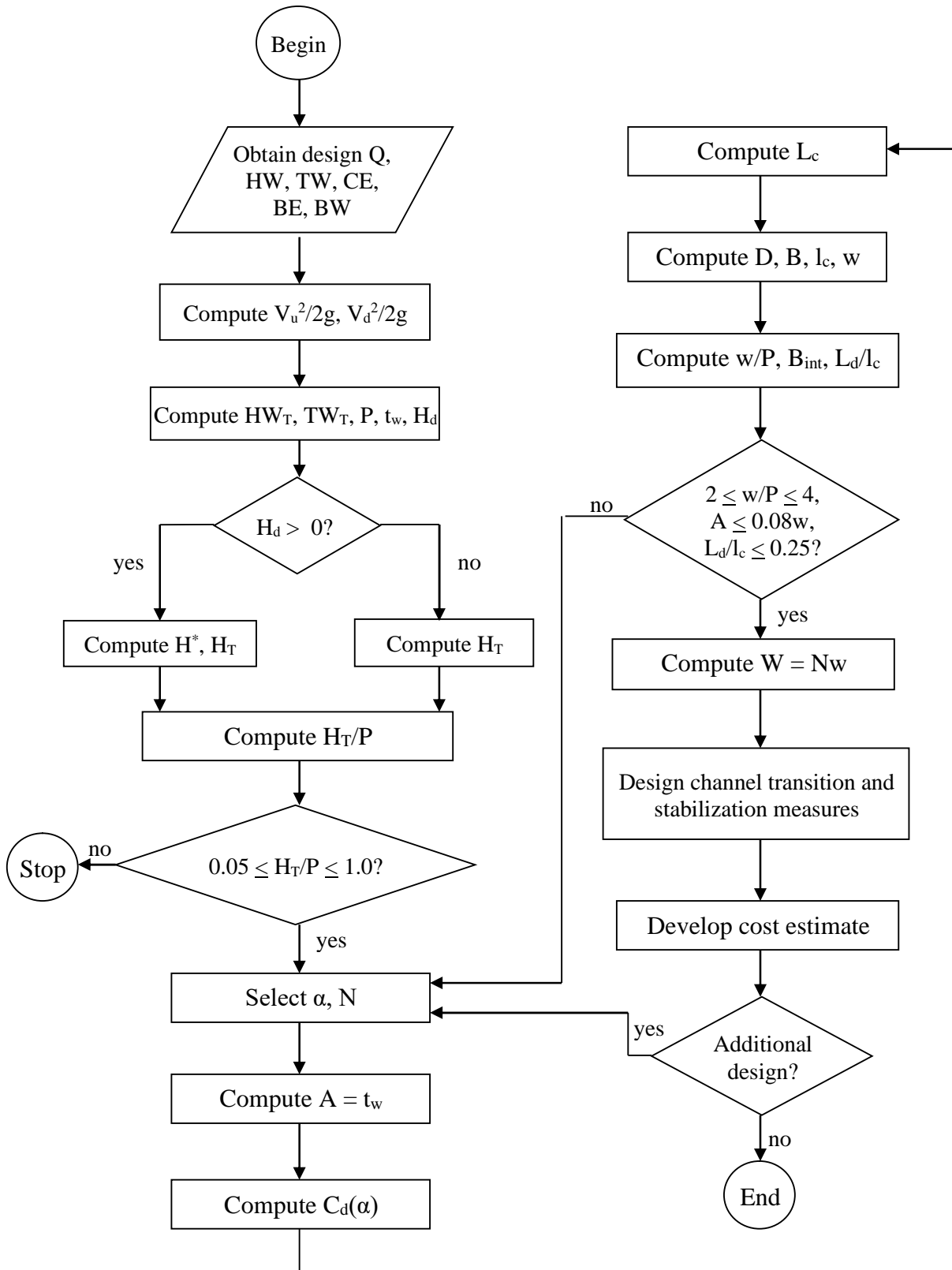
Figure D5. Hydraulic design process for a labyrinth weir with a half-round crest

Begin

Obtain design Q, HW, TW, CE, BE, BW

Compute H, P

Select α, N

Compute $2l_c/w$

Compute W, w

$0.3 \leq w/P \leq 1.5$
$0.1 \leq H/w \leq 1.2$
?

no

yes

Compute B, l_c, L_c

Design channel transition and stabilization measures

Develop cost estimate

Additional design?

yes

no

End
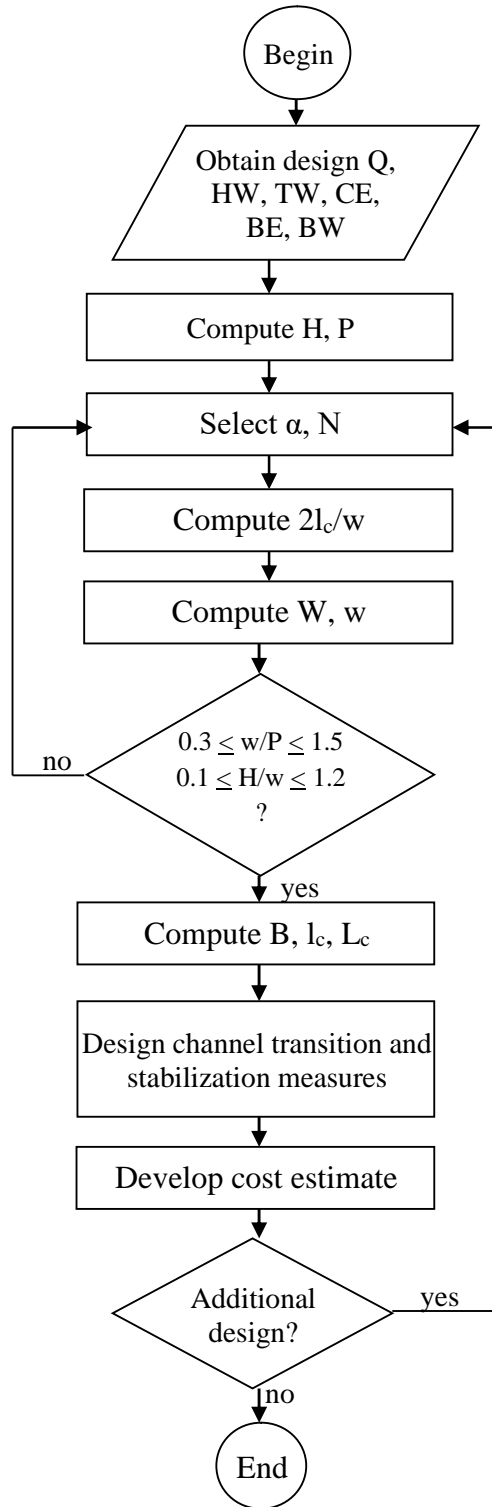
Figure D6. Hydraulic design process for a labyrinth weir with a sharp crest

Step I

Since W = 152.8 ft > BW = 50 ft, a channel transition will be required.

Steps J - K

Omitted here.

Step L

The design process was repeated with several combinations of α and N. The results are shown in Table D4. While the design resulting from trial 3 results in the shortest weir length, it also requires the widest channel cross section at the weir location. Trial 1 yields a total weir length that is about 30 feet longer along with a base width that is over 150 feet shorter. In this case it is likely that the savings in channel transition costs will more than offset the cost of the longer weir wall length.

Table D4. Trial designs of a sharp-crested labyrinth weir

Trial	N	α(^{0})	W	B	L_c
1	10	30	152.8	13.23	305.60
2	13	45	203.4	7.82	287.65
3	15	60	239	4.60	276

IX.   References

Carollo, F. G., V. Ferro and V. Pampalone. 2012. Experimental Investigation of the Outflow Process over a Triangular Labyrinth-Weir. *J. of Irrigation and Drainage Engineering,* ASCE, 138(1), 73-79.

Crookston, B. 2010. Labyrinth Weirs. Ph.D Dissertation, Utah State University, Logan, Utah, 197 pp.

Crookston, B. M., G. S. Paxson, B. M. Savage, & B. P. Tullis. 2013. Increasing hydraulic design flexibility of labyrinth spillways. *ICOLD 2013 International Symposium.* Seattle, Wash.

Crookston, B. M. and B. P. Tullis. 2011. The Design and Analysis of Labyrinth Weirs. 31st Annual USSD Conference: 21st Century Dam Design – Advances and Adaptations, San Diego, CA, April 11-15, pp. 1667-1681.

Crookston, B. M. and B. P. Tullis. 2012. Labyrinth Weirs: Nappe Interference and Local Submergence. *J. of Irrigation and Drainage Engineering,* ASCE, 138(8), pp. 757-765.

Crookston, B. M. and B. P. Tullis. 2012a. Arced labyrinth weirs. *J. of Hydr. Engrg., ASCE,* 138(6), pp. 555-562.

Crookston, B. M. and B. P. Tullis. 2012b. Discharge efficiency of reservoir-application-specific labyrinth weirs. *J. Irrig. Drain. Engr., ASCE,* 138(6), pp. 773-776.

Crookston, B. M. and B. P. Tullis. 2013a. Hydraulic design and analysis of labyrinth weirs. Part 1: Discharge relationships. *J. Irrig. Drain. Engr., ASCE,* 139(5), pp. 363-370.

Crookston, B. M. and B. P. Tullis. 2013b. Hydraulic design and analysis of labyrinth weirs. Part 2: Nappe aeration, instability, and vibration. *J. Irrig. Drain. Engr., ASCE,* 139(5), pp. 371-377.

Darvas, L. (1971). Discussion of performance and design of labyrinth weirs, by Hay and Taylor. *J. of Hydraulic Engineering,* ASCE, 97(80), 1246-1251.

Falvey, H. T. 2003. *Hydraulic Design of Labyrinth Weirs*, ASCE, Reston, Va.

Gentilini, B. 1940. Stramazzi con cresta a piñata obliqua e a zig-zag. *Memorie e Studi del Regio Politecnico di Milano,* 48, (in Italian).

Hay, N., and Taylor, G. (1970). Performance and Design of Labyrinth Weirs. *J. of Hydraulic Engineering,* ASCE, 96(11), 2337-2357.

Houston, K. (1983). Hydraulic Model Study of Hyrum Dam Auxiliary Labyrinth Spillway. Report No. GR-82-13, U.S. Bureau of Reclamation, Denver, CO, 29 pp.

Lux, F. and Hinchliff, D. 1985. Design and Construction of Labyrinth Spillways. 15th Congress ICOLD, Vol. IV, Q59-R15, Lausanne, Switzerland, 249-274.

Paxson, Greg, Dave Campbell and Joe Monroe. 2011. Evolving Design Approaches and Considerations for Labyrinth Spillways. 31st Annual USSD Conference: 21st Century Dam Design – Advances and Adaptations, San Diego, CA, April 11-15, 22 pp.

Paxson, Greg and Bruce Savage. 2006. Labyrinth Spillways: Comparison of Two Popular U.S.A. Design Methods and Consideration of Non-Standard Approach Conditions and Geometries. International Junior Researcher and Engineer Workshop on Hydraulic Structures, Report CH61/06, The University of Queensland, Brisbane, Australia, pp. 37-46.

Sitompul, A. T., J. J. Sharp and M. Iwra. 1995. The Use of Labyrinth Weirs for Water Level Control. *Water International*, IWRA, 20(1), 46-51.

Taylor, G. (1968). The performance of labyrinth weirs. Ph.D. Thesis, University of Nottingham, Nottingham, England.

Tullis, P., Amanian, N., and Waldron, D. 1995. Design of Labyrinth Weir Spillways. *J. of Hydraulic Engineering,* ASCE*,* 121(3), 247-255.

Tullis, B. P., J. C. Young and M. A. Chandler. 2007. Head-Discharge Relationships for Submerged Labyrinth Weirs. *J. Hydraulic Engineering,* ASCE, 133(3), 248-254.

Villemonte, J. R. 1947. Submerged Weir Discharge Studies. *Engineering News-Record*, 139(26), 54-56.

Willmore, C. 2004. Hydraulic Characteristics of Labyrinth Weirs. M.S. Report, Utah State University, Logan, Utah.

Appendix E. Hydraulic Design Procedure for Sheet Pile Weirs

I.   Background

A.   Characteristics

Weirs are often constructed of Z-section sheet piles due to their pricing, availability and constructability. Examples of this type of weir are shown are Figures E1 and E2. A weir constructed of sheet piles will resemble a linear weir folded along its axis so as to create a sinusoidal pattern of trapezoids. The resultant planform can vary from nearly flat to a series of rectangles that are nearly square (Figure E1). In general, the planform of a sheet pile weir will be comprised of a sinusoidal pattern of trapezoids, where the dimensions will vary with manufacturer and specifications.

Figure E1. Sheet pile weir in the Santa Margarita River (from USBR, 2004)

Figure E2. Compound sheet pile weir (from Girard and Clopper, undated)

B.   Flow Over Sheet Pile Weirs

   1. Unsubmerged Flow

Hydraulic analyses of flow over sheet pile weirs are almost nonexistent in the literature. The only documented study that explicitly addresses the characteristics of flow over the Z-section sheet pile described previously was carried out by Rice and Gwinn (1981). Their effort involved the development of flow rating equations for the former drop structure S-13 located on Otter Creek in Okeechobee County. Defining the head H as the distance between the upstream water surface and the weir crest, the investigators used a rating equation of the form

$$Q_u = CLH^{3/2} \tag{E1}$$

where Q_u is the discharge over the weir under unsubmerged conditions and L is the length of the weir. This is a standard equation used to compute flow over sharp-crested weirs (see, for example, Brater and King, 1976). However, they indicate that experimental data of weir discharge over straight, linear weirs can only be used to predict flow over a sheet pile weir at very low or very high heads. At very low heads, the effective length can be taken as the

sinusoidal length of the weir crest while at high heads, the channel width at the weir crest elevation would be the appropriate choice for L. In the transition from low to high flows, the effective weir length will gradually decrease from the sinusoidal length to the channel width. This phenomenon is not reflected in experimental data of linear weir flows.

Using data acquired from physical model experiments carried out at the USDA Water Conservation Structures Laboratory in Stillwater, OK, Rice and Gwinn (1981) determined that the relationship between C and H for the former S-13 structure can be approximated by

$$C = A + BLog_{10}(H + E) \qquad (E2)$$

where A, B and E are regression parameters determined from experimental data. Table E1 provides the values of these parameters for various prototype head ranges. Additionally, the crest height (above channel bottom) of the prototype was approximately 0.5 foot. Denoting this value as P, the range of H/P associated with each head range is also shown.

Table E1. Values of parameters in Equation E2 (from Rice and Gwinn, 1981)

H (ft)	H/P (approx.)	A	B	E
< 0.04	< 0.02	10.57	2.847	-0.0128
0.04 – 2.04	0.08 – 4.08	4.959	-1.761	0
2.04 – 4.0	4.08 – 8.0	4.709	-0.955	0

Equations E1 and E2 along with the parameter values in Table E1 can be used to estimate the free-flow discharge over a sheet pile weir under limited conditions. First, the weir planform should not be too different from the one examined by Rice and Gwinn (1981). A half cycle of this Z-section sheet piling is depicted schematically in Figure E3. Second, the approach conditions should reflect those of a straight channel. Third, it should be noted that the former S-13 was a drop structure as opposed to a conventional weir. In particular, the approach flow depth was relatively shallow, resulting in H/P values that are higher than those typically experienced by a weir acting a water control structure. More specifically, H/P for a sheet pile weir will typically be less than 1. Hence, for H > 2 feet, the parameters given in the last row of Table E1 may not be reliable if H/P < 4. Furthermore, as indicated previously, the results obtained by Rice and Gwinn (1981) have apparently not been verified by other investigations. Consequently, the design equations and data presented above should be used with caution and only when design values of H and H/P are within the ranges shown. It is recommended that stage and flow data be acquired at future installations of sheet pile weirs in order to improve the reliability of this design procedure.

2. *Submerged Flow*

If the stage downstream of the weir exceeds the weir crest elevation, flow across the weir will occur in a submerged state. Rice and Gwinn (1981) demonstrated that the Villemonte (1947) correction factor can be used to account for downstream submergence. The procedure for

determining and applying this correction factor to computed unsubmerged flows is discussed in Appendix C.

II.   Site Constraints

There are a number of site features that can influence both the economic and hydraulic feasibility of a sheet pile weir installation. These include the dimensions of the discharge channel or outfall, subsurface conditions, the design discharge rate and downstream backwater effects that may impede weir discharges. Throughout the design process, the engineer should remain aware of any constraints imposed by these factors.

III.   Hydraulic Design Tasks

Once the design discharge (Q_D), head water stage (HW_D), tail water stage (TW_D) and desired control elevation (CE) have been established, the tasks listed below should be performed in the order given.

A. Obtain the approach channel floor elevation (BE) along with the bottom width (BW).

B. Compute the following:

    $P = CE – BE$ (the weir height measured from the upstream channel floor)

    $H = HW_D - CE$

    $h = TW_D – CE$

C. Compute H/P. If H and H/P do not fall within the ranges indicated in Table E1, this design procedure should not be used and another type of weir design should be considered.

D. Compute the discharge coefficient C using Equation E2 and Table E1.

E. If $h > 0$, proceed to step F. Otherwise, compute

$$L = \frac{Q_D}{CH^{3/2}}$$

    A transition may be needed to modify the channel width to L at elevation CE. Additionally, design, if necessary, the aeration devices needed to provide the required ventilation under the nappe. Refer to the appropriate section of these guidelines.

    Proceed next to step G.

F. Compute the submergence correction factor ψ based on the procedure outlined in Appendix C for sharp-crested weirs. Then compute

$$L = \frac{Q_D}{\psi C H^{3/2}}$$

A transition may be needed to modify the channel width to L at elevation CE.

G. Design the apron, the upstream and downstream transitions (if required), and any other structural improvements to the channel that are needed.

H. Complete a cost estimate and note any anticipated maintenance problems.

The procedure for designing a sheet pile weir is summarized in Figure E3 and demonstrated by example in the next section.

IV.   Design Example

Design a sheet pile weir for the same bypass channel and design conditions specified for the design example given in Appendix A. For convenience, these conditions are repeated here:

A bypass channel with a bottom width of 20 feet, a bottom elevation of 0 feet, a top-of-bank elevation of 15 feet and 2:1 side slopes carries a design discharge of 500 cfs. The design head water and tail water stages for the proposed structure location are 13 and 9 feet, respectively, while the seasonal control elevation is 11 feet.

Each step of the design process is carried out below.

Step A

From the problem statement, BE = 0 and BW = 20.

Step B

P = CE – BE = 11 – 0 = 11 ft
H = 13 – 11 = 2 ft
h = 9 – 11 < 0

Step C

H/P = 2/11 = 0.182

```
                    ┌─────────┐
                    │  Begin  │
                    └────┬────┘
                         │
                         ▼
              ╱─────────────────────╲
             ╱   Obtain design Q,     ╲              ┌──────────────────────┐
            ╱       HW, TW, CE         ╲────────────▶│    Compute ψ, L      │
            ╲                          ╱             └──────────┬───────────┘
             ╲────────────────────────╱                        │
                         │                                     ▼
                         ▼                           ┌──────────────────────┐
              ╱─────────────────────╲                │  Design additional   │
             ╱     Obtain BE, BW      ╲──────────────▶│    improvements      │
             ╲────────────────────────╱              └──────────┬───────────┘
                         │                                      │
                         ▼                                      ▼
            ┌──────────────────────┐                 ┌──────────────────────┐
            │   Compute P, H, h    │                 │   Develop cost       │
            └──────────┬───────────┘                 │     estimate         │
                       │                             └──────────┬───────────┘
                       ▼                                        │
                    ╱──────╲     no    ┌──────┐                 ▼
                   ╱  H, H/P ╲─────────▶│ Stop │            ┌───────┐
                   ╲ in range?╱         └──────┘            │  End  │
                    ╲────────╱                              └───────┘
                       │ yes
                       ▼
            ┌──────────────────────┐
            │     Compute C        │
            └──────────┬───────────┘
                       │
                       ▼
                    ╱──────╲     yes
                   ╱  h ≥ 0? ╲───────────────────────────┐
                   ╲────────╱
                       │ no
                       ▼
            ┌──────────────────────┐
            │     Compute L        │
            └──────────┬───────────┘
                       │
                       ▼
            ┌──────────────────────┐
            │ Design nappe aeration│
            └──────────────────────┘
```
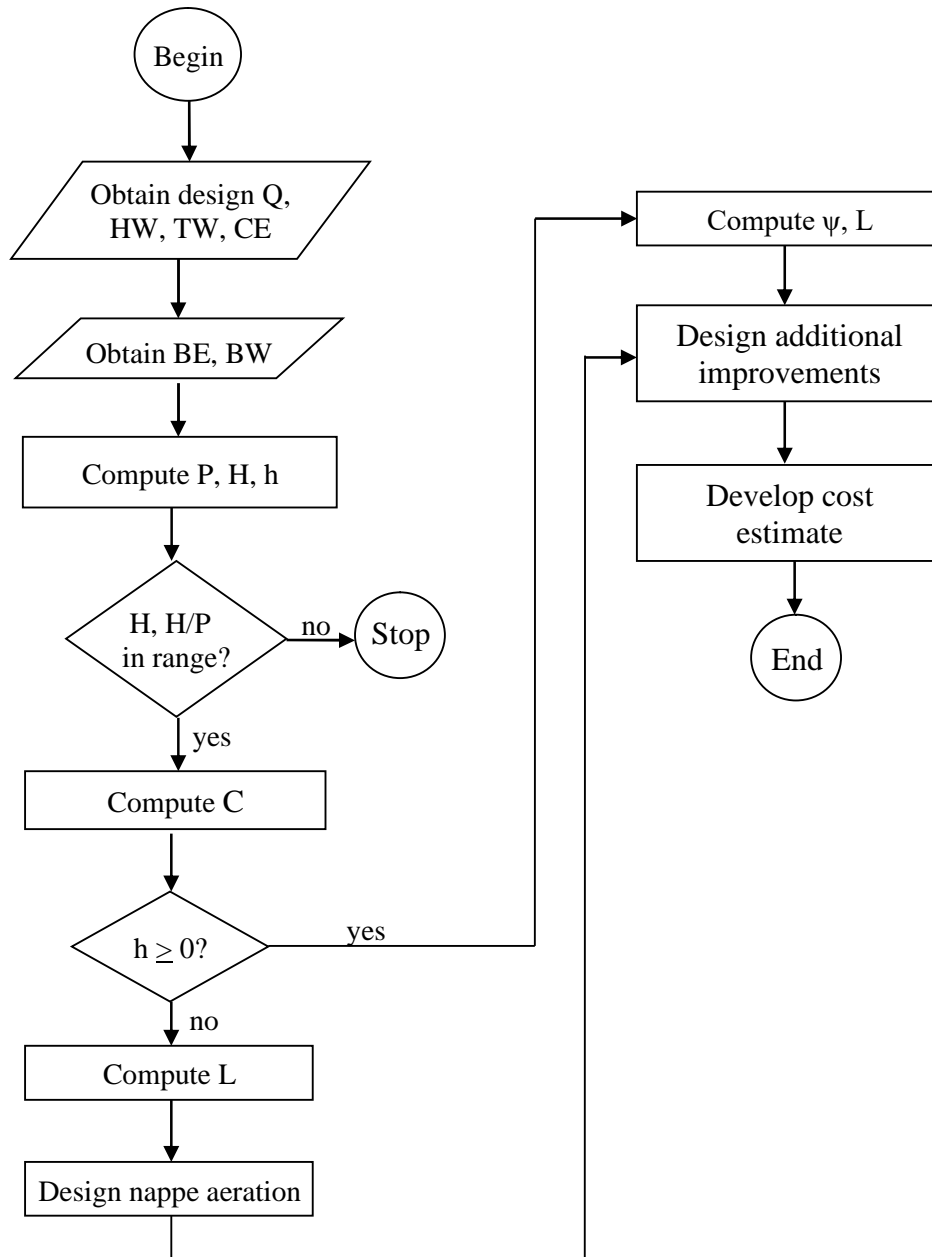
Figure E3. Sheet pile weir design process

Step D

According to Table E1, for H = 2 ft and H/P = 0.182, A = 4.595, B = -1.761 and E = 0. From Equation E2, C = 4.959 – 1.761Log$_{10}$(2) = 4.43.

Step E

From Equation E1, L = 500/4.43/2$^{3/2}$ = 39.91 ≈ 40 ft. At an elevation of 11 feet, the channel width is 20 + (2)(2)(11-0) = 64 ft. This implies that a transition will be needed to reduce the channel width to 52.5 feet at the weir location. Alternatively, the weir can be over-designed to a length of 64 ft since the extra weir length may be cheaper than the cost of a channel transition. However, this will result in less attenuation of the peak discharge at the structure and may result in storm flows downstream that are higher than those that were passed historically by the permanent structure under the same storm conditions.

Step F

Omit since h < 0

Steps G, H (omit here)

V.   References

Brater, E. F. and H. W. King. 1976. *Handbook of Hydraulics, Sixth Edition,* McGraw-Hill, New York, NY.

Girard, L. G. and P. E. Clopper. Undated. Sims Bayou: Articulating Concrete Blocks Enhance Erosion Control Installations. Unpublished report by Ayres Associates, Fort Collins, CO, 12 pp.

Rice, C. E. and W. R. Gwinn. 1981. Rating of Z-Section, Steel-Sheet Piling Drop Structures. *Transactions of the ASAE,* 24(1), 107-112.

USBR. 2004. Proposed Obermeyer Modifications to O'Neill Diversion Weir on Santa Margarita River, California. United States Bureau of Reclamation, Technical Service Center, Denver, CO, 15 pp.

Villemonte, J. R. 1947. Submerged Weir Discharge Studies. *Engineering News-Record*, 139(26), 54-56.

Appendix F. Hydraulic Design Procedure for Broad-Crested Weirs

I.   Introduction

Broad-crested weirs have been widely used for water control purposes over the last century. In general, they are structurally more stable and simpler to construct than sharp-crested weirs, and are less susceptible to tail water effects. Furthermore, they can be constructed in a variety of profile and cross-sectional shapes, including rectangular, trapezoidal, triangular and parabolic. Roadway embankments and levees often function as broad-crested weirs when over topped during a flood event (Yarnell and Nagler, 1930; Fritz et al., 2008).

For economic reasons, a broad-crested weir serving as a temporary by-pass structure will most likely be constructed as an earth embankment covered with erosion-resistant material. Consequently, the scope of this appendix is limited to the hydraulic design of broad-crested weirs with a trapezoidal profile.

Unsubmerged flow over a trapezoidal weir is depicted in Figure F1. The upstream energy grade line is at a distance H_T above the weir crest with mean approach velocity V_u while the hydraulic grade line is situated at a height H above the crest. The weir is constructed with a top width of L_w and a height P above the channel floor. Flow passes through critical depth at some location along the weir crest and terminates in a hydraulic jump (often submerged) near the downstream toe. The tail water depth is d and its water surface is a distance h below the weir crest. If h were to increase above the crest elevation, flow over the weir would eventually become submerged.

II.   Background

A. Research by Kindsvater (1964)

Experimental investigations of flow over trapezoidal broad-crested weirs have not been nearly as plentiful or widespread as research on sharp-crested weir flow. One of the most extensive and classical studies of flow over roadway embankments was conducted at the hydraulics laboratory of the Georgia Institute of Technology by Kindsvater (1964). The two primary objectives of this research were to (i) investigate the essential discharge characteristics of both submerged and unsubmerged flow along with their relationships to embankment form and roughness, and (ii) better define the relationship between unsubmerged flow and the boundary layer on the roadway. Additionally, the investigators identified the various regimes of flow that can exist under both unsubmerged and submerged conditions. Additionally, they noted the headwater ranges where either embankment form or roughness controls the unsubmerged flow characteristics.

According to Kindsvater (1964), flow over a highway embankment can be classified as either free flow or submerged flow. Under free flow conditions, flow over the embankment crest passes through critical depth and is unimpeded by tail water. Furthermore, free flow can be subcategorized as either plunging flow, which results in a submerged hydraulic jump on the downstream slope, or surface flow, where flow separates from the roadway surface at the

downstream shoulder and creates a flow zone along the tail water surface. Additionally, the brief transition between this latter subclassification of free flow and submerged flow is referred to by Kindsvater (1964) as *incipient submergence*. Submerged flow, as defined in the study, is always characterized by surface flow downstream. Detailed descriptions and experimental photographs of the various flow regimes over a highway embankment are provided by Kindsvater (1964).

B. Research by Fritz and Hager (1998)

Fritz and Hager (1998) identified four primary flow regimes for discharges over embankments that are trapezoidal with 2:1 side slopes. First, they classified free flow as the condition where flow passes through critical depth somewhere on the weir crest and then accelerates along the downstream face and passes through a hydraulic jump (referred to as an *A-jump*) at the toe of the embankment. With increasing tail water, the free flow condition transitions into a second flow classification that is comprised of both a plunging jet along the downstream face of the embankment and a surface roller. As the tail water continues to rise, it produces a third flow regime that is characterized by surface wave flow, where flow primarily occurs along the free surface and is accompanied by a bottom recirculation zone. The fourth flow condition is classified as surface jet flow and is analogous to the third flow condition. The primary difference between the third and fourth flow regimes is that the downstream water surface is nearly horizontal without waves. Additional discussions of each of these flow conditions are provided in a later section.

It is also of interest that the investigators found that upstream heads can be unaffected by tail water levels that are as high as 80% of the upstream water levels measured with respect to the weir crest. This verifies that broad-crested weirs are less affected by submergence than are sharp-crested weirs.

C. Research by Sargison and Percy (2009)

Sargison and Percy (2009) experimented on trapezoidal broad-crested weirs with varying side slopes. They developed and tested physical models with upstream and downstream faces whose slopes varied from 0H:1V to 2H:1V. They found that the weir discharge was much more sensitive to the upstream side slope than to the downstream side slope. Additionally, their results indicate that within the range of upstream heads tested, the discharge was highest for the weir design with a 2H:1V side slope on the upstream face and a side slope of 1H:1V on the downstream face. The discharge coefficients obtained by these investigators for this weir design were, however, lower than those obtained by Fritz and Hager (1998) for the symmetrical weir design with 2H:1V side slopes.

D. Research by Wang, Hao and Tan (2010)

The primary objective of this effort was to measure the velocity fields both upstream and downstream of a trapezoidal embankment for varying approach velocities and tail water levels at two different model scales. Velocity measurements were acquired using Particle Image Velocimetry. The velocity vector plots constructed using the experimental results appear to be

consistent with the results obtained by Fritz and Hager (1998). The relationship between certain characteristics of the velocity fields and approach Froude number was also investigated.

E. Application of Previous Research to Hydraulic Design Guidelines

The results of the investigations by Kindsvater (1964) and Fritz and Hager (1998) appear to be the most applicable to the development of the hydraulic design guidelines proposed here. Fritz and Hager (1998) emphasize the importance of predicting flow types in engineering applications. The various flow regimes identified by Kindsvater (1964), however, do not all appear to precisely coincide with those specified by Fritz and Hager (1998). In particular, Kindsvater (1964) states that submerged discharges result in surface flows downstream of the weir. In contrast, the definition of submerged flow used by Fritz and Hager (1998) includes the occurrence of either a plunging jet or a surface jet downstream of the weir. Fritz and Hager (1998) also identified a transition zone between these two flow regimes that depends on the head and tail water levels along with the weir crest length. Furthermore, the objectives of each study differ. The primary objectives of the Kindsvater (1964) study were to (i) determine the relationship between road embankment geometry and roughness to prominent discharge characteristics, and (ii) to define the relationship between free-flow discharge and the boundary layer on the roadway. The results were intended to improve the accuracy of flood discharge computations over roadways. The primary objectives of the Fritz and Hager (1998) study were to analyze flow conditions over embankment weirs and develop equations that can be useful in hydraulic design. In particular, equations that can be used to characterize the downstream velocity field were provided along with expressions for determining the discharge coefficient and submerged flow correction factor.

Despite these differences, both studies identified the four flow conditions discussed by Fritz and Hager (1998). The investigation by Fritz and Hager (1998), however, is more directly applicable to the development of a hydraulic design procedure for trapezoidal embankment weirs that are symmetrical with conventional 2H:1V side slopes.

F. Conceptualization of Flow Over a Trapezoidal Weir

Figures F1 – F3 portray a general conceptualization of discharge over a trapezoidal embankment. In Figure F1 the discharge occurs as unsubmerged overflow and results in a hydraulic jump at the downstream toe of the weir. This is referred to as an *A-jump* by Fritz and Hager (1998). Depending on the tail water stage, the hydraulic jump may be submerged. In Figure F2, the tail water stage is at or above the weir crest but still low enough to allow a plunging jet to form along the downstream side of the weir. A surface roller forms above the jet to a distance L_r from the toe of the embankment. As the tail water rises, the plunging jet eventually transitions to a surface jet as depicted in Figure F3. In this case, a bottom recirculation zone forms below the surface jet over a length L_R from the weir crest.

The velocities within both the recirculation zone (Figure F3) and the plunging jet (Figure F2) are of interest since they could potentially result in erosion of the channel bottom and downstream face of the weir. The hydraulic conditions depicted in Figure F1 are not expected to occur often

in southern Florida due to the low channel slopes and high tail water conditions commonly encountered at water control structures. However, in certain cases where an embankment is subjected to a hurricane storm surge, it is possible that the flow conditions portrayed in Figure 1 could be temporarily realized (H. Fritz, personal communication, July 17, 2013). This flow condition would be the most critical for erosion of the embankment given the higher velocities along the downstream slope and at the toe.

G. Discharge Equations

Unsubmerged flow over a trapezoidal embankment weir can be expressed as (Fritz and Hager, 1998)

$$Q = C_d L \sqrt{2gH_T^3} \qquad (F1)$$

where L is the length of the embankment perpendicular to the flow and C_d is an empirical discharge coefficient that offsets any simplifying assumptions made in the derivation of Equation F1. Fritz and Hager (1998) indicate that if $H_T/P > 1/6$, the approach velocity head should be multiplied by a correction coefficient of 5/3. This is needed to account for the effects of both a nonuniform approach velocity distribution and the larger values of H_T/P. They also found that the discharge coefficient C_d varies with the dimensionless relative crest length ξ defined by

$$\xi = \frac{H_T}{H_T + L_w} \qquad (F2)$$

where $0 < \xi < 1$, H_T is the total upstream hydraulic head and L_w is the embankment crest length (Figure F1). An empirical relationship between C_d and ξ developed by Fritz and Hager (1998) is given by

$$C_d = 0.43 + 0.06\sin[\pi(\xi - 0.55)] \qquad (F3)$$

Equations F1 – F3 can be used to compute unsubmerged flow over a trapezoidal weir.

The modular limit separating free and submerged flow can be expressed in terms of the ratio of the downstream head to the upstream head (Figures F2-F3). In this case, h denotes the height of the tail water surface above the weir crest. Denoting this threshold value of h as h_L, the modular limit y_L is expressed as

$$y_L = \frac{h_L}{H} \qquad (F4)$$

Through experimentation, Fritz and Hager (1998) found that

$$y_L \approx 0.85 - 0.5\xi \qquad (F5)$$

To compute flow under submerged conditions, the conventional flow reduction factor ψ given by
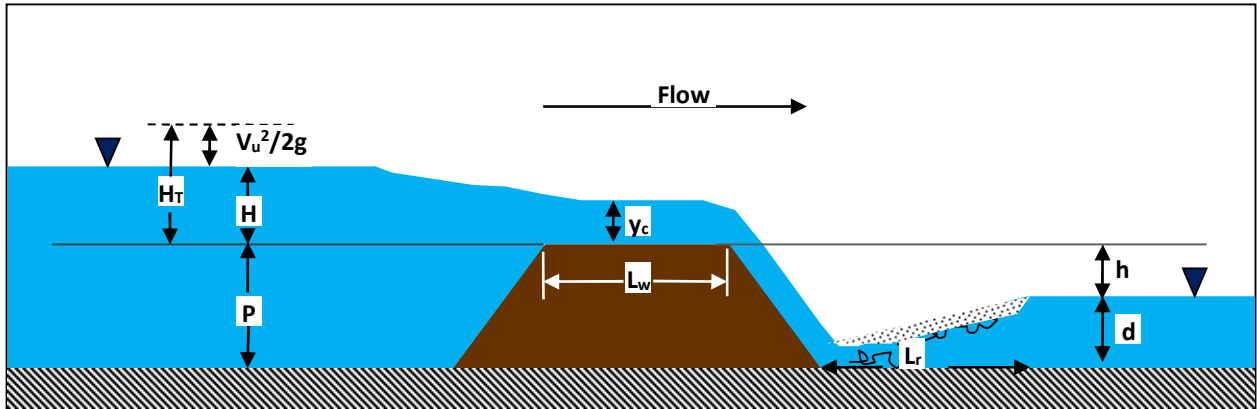
$$\psi = \frac{Q_s}{Q} \qquad (F6)$$

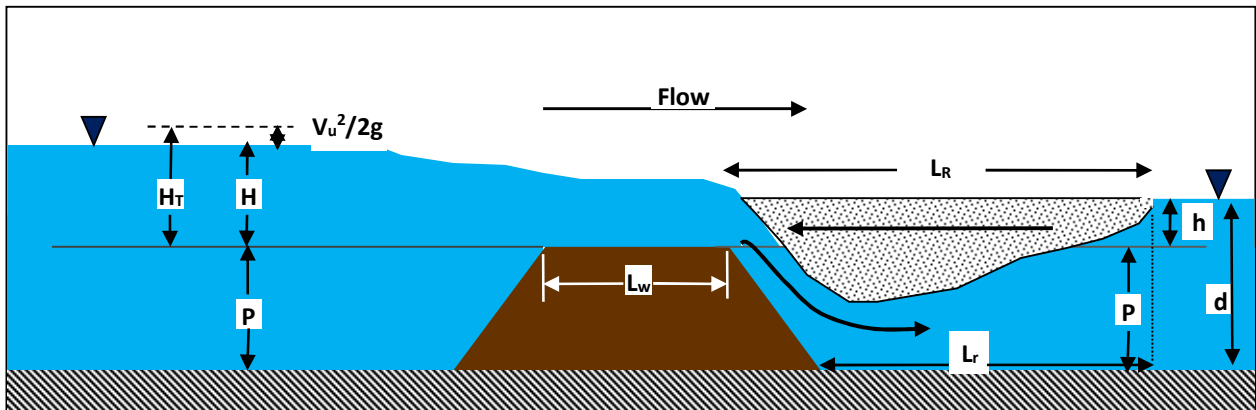**Figure F1. Free flow over a trapezoidal weir (Fritz and Hager, 1998)**

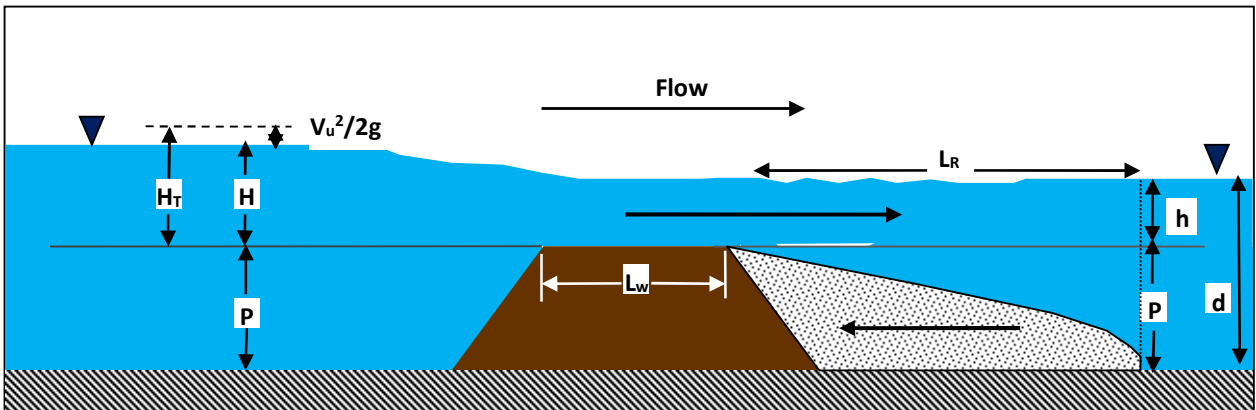**Figure F2. Discharge through a plunging jet over a trapezoidal weir (Fritz and Hager, 1998)**

Figure F3. Discharge through a surface jet over a trapezoidal weir (Fritz and Hager, 1998)

is used, where Q_s denotes flow under submerged conditions and the unsubmerged flow Q is computed with Equation F1. Denoting the submergence ratio h/H as y_t, Fritz and Hager (1998) introduced the nondimensional parameter Y_t defined as

$$Y_t = \frac{y_t - y_L}{1 - y_L} \tag{F7}$$

and proposed the following normalized representation of ψ as a function of Y_t:

$$\psi = (1 - Y_t)^{1/n} \tag{F8}$$

Their experimental results yielded the relationship between ξ and the exponent n given in Table F1. These data along with Equations F1 – F8 can be used to compute submerged flow over a trapezoidal weir with 2H:1V side slopes and variable embankment crest lengths.

Table F1. n versus ξ

ξ	n
0.25	7
0.67	6
1.0	4

H. Tail Water Hydrodynamics

Fritz and Hager (1998) also investigated the characteristics of the tail water velocity field for each of the flow regimes shown in Figures F2 and F3. As mentioned previously, if the discharge over the embankment is a plunging jet, this type of flow will eventually transition into a surface jet. Fritz and Hager (1998) found that a transition exists between these two flow conditions and that the tail water range demarking this transition region is a function of ξ. Denoting the tail water level within this transition range as h_T, it can be expressed in nondimensional form as $y_T = h_T / H$. Fritz and Hager (1998) determined through experimentation that the relationship between y_T and ξ is as shown in Figure F4. Note that y_T is not single-valued for any given ξ. When the tail water rises, the stage at which a plunging jet becomes a surface jet is higher than the stage at which a surface jet becomes a plunging jet as the tail water falls.

Shown also in Figure F4 for reference is Equation F5. For $\xi \geq 0.4$, it can be seen that a plunging jet can occur during either unsubmerged or submerged flow. Under limited tail water ranges when $\xi \leq 0.2$, a surface jet can occur under either unsubmerged or submerged flow conditions.

From the preceding discussions, it is evident that the possible flow regimes under design conditions must be established before any determination of downstream velocities and erosion potential can be made. The information discussed below can then be used to assess the velocities that impact the channel bottom.

1. Velocity Field of a Plunging Jet

Downstream of a plunging jet, Fritz and Hager (1998) found that the length of the surface roller L_r measured downstream from the toe of the embankment can be estimated from
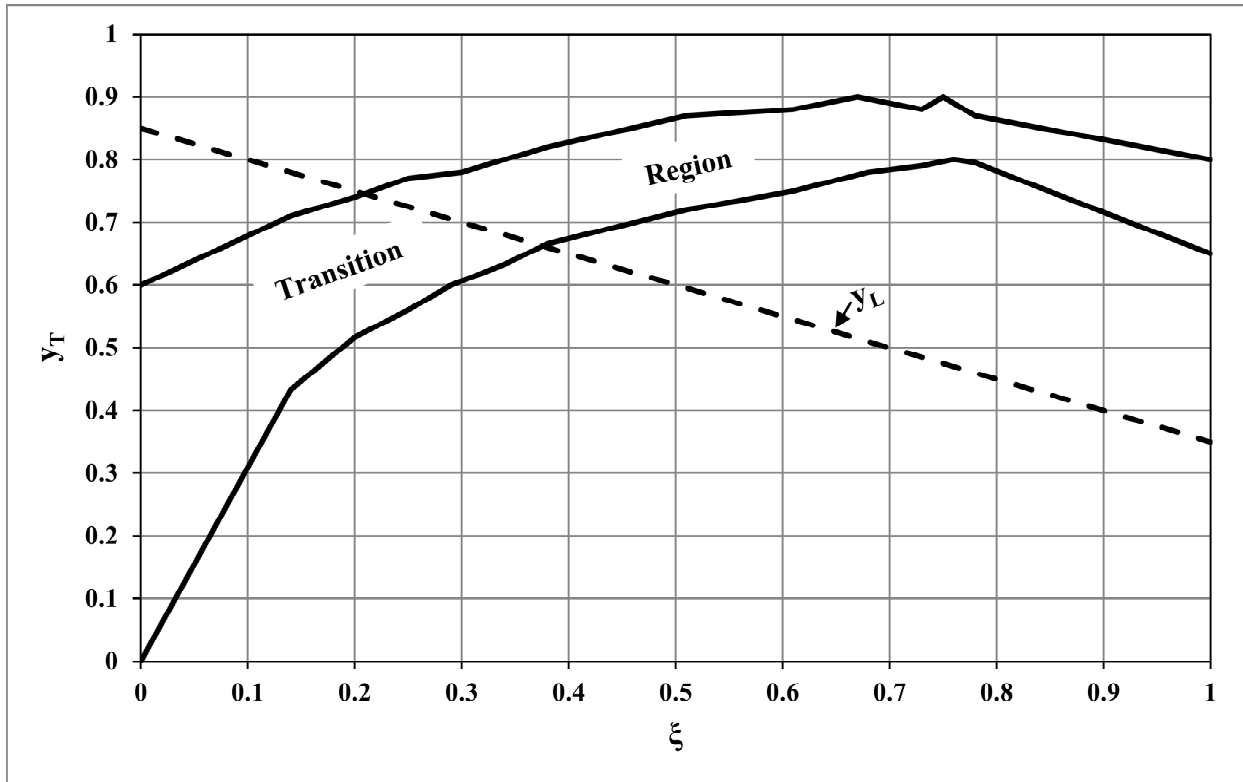
Figure F4. Transition region between plunging and surface jets (Fritz and Hager, 1998)

$$L_r \approx 4.3d \tag{F9}$$

where d is the downstream tail water depth. The uncertainty of L_r computed with Equation F9 is $\pm$ 10%. This distance can be used as an estimate of the channel length over which erosion control measures should be installed. In their study, the investigators found that, at the end of the roller, the maximum forward velocity was only 10% greater than the ambient tail water velocity in the downstream channel. Furthermore, the approach (or absolute maximum) velocity u_A within a plunging jet at the top of the embankment was specified as

$$u_A = \sqrt{gd\left(1 - \frac{h}{H}\right)} \tag{F10}$$

The tail water velocity in the downstream channel u_d is simply

$$u_d = \frac{Q}{(BW+zd)d} \tag{F11}$$

In Equation F11, BW is the downstream channel bottom width and z is the channel side slope. Designating x_R as the downstream distance from the edge of the embankment crest (or, in the case of an A jump, the downstream toe), Fritz and Hager (1998) determined that the maximum

streamwise velocity u_M at any location between the embankment and the downstream edge of the surface roller is given by

$$u_M = (u_A - u_d)e^{-2.3\chi^2} + u_d \qquad (F12)$$

where $\chi = x_R/L_R$ for a plunging jet or x_R/L_r for an A jump. The maximum streamwise velocity in a plunging jet will occur near the bottom of the jet, at the top of the boundary layer. From this point, the streamwise velocity will decrease in the vertical direction. At the top of the jet (i.e. at the interface with the surface roller), the streamwise velocity will be zero since velocities within the surface roller are in the reverse direction (i.e. < 0). Consequently, the mean velocity of the plunging jet can be taken to be approximately ½ $u_M.$

Since u_M decreases with χ, Equations F10 – F12 can be used to determine the maximum and average streamwise velocities for various segments of the downstream channel between $\chi = 0$ and $\chi = 1$. The required stabilization measures can then be designed for each segment.

2. *Velocity Field of a Surface Jet*

The length L_R of a surface jet recirculation zone (Figure F3) is given by (Fritz and Hager, 1998)

$$L_R = 6.8d\ (1 - h/H)^{1/6} \qquad (F13)$$

In this case, the maximum backward velocity within the recirculation zone is of interest for design purposes since it is the recirculation zone and not the jet that is in contact with the channel bottom and downstream face of the embankment. The absolute maximum backward velocity u_a was found in the study to be

$$u_a = -0.25\sqrt{gd(1 - \tfrac{h}{H})} \qquad (F14)$$

The magnitude of absolute maximum backward velocity in this recirculation zone is therefore 25% of the magnitude of the absolute maximum forward velocity (u_A) within a plunging jet. The maximum backward streamwise velocity u_m at a specified downstream location $0 \leq x_R \leq L_R$ was determined by the investigators to be

$$u_m = 2u_a\sqrt{\chi(1 - \chi)} \qquad (F15)$$

As was the case for $u_M,$ u_m will occur at the top of the boundary layer for the channel bottom. Furthermore, the backward streamwise velocity will be zero at the top of the recirculation zone since the velocities within the surface jet are in the opposite direction. Therefore, the average backward velocity within the recirculation zone can be approximated as ½ u_m. Since $|u_m| < |u_M|$, the channel stabilization measures required for a surface jet will be less extensive than those required by a plunging jet.

3. Limitations of Design Equations

Equations F9 – F15 are based on a limited amount of data acquired by Fritz and Hager (1998), Kindsvater (1964) and Hager (1992). Despite their apparent usefulness, it is not known if these equations have had any application in engineering practice. Prior to their study, Wang et al. (2010) indicated that the velocity and vorticity distributions within the vicinity of an embankment weir have received little attention by researchers and practitioners. For these reasons it is recommended that they be used with discretion along with an appropriate factor of safety. Additional research through physical and numerical modeling is needed to improve the techniques presented here for estimating velocities downstream of an embankment weir.

III.   Site Constraints

There are a number of site features that can influence both the economic and hydraulic feasibility of a broad-crested weir installation. These include the dimensions of the discharge channel or outfall, the design discharge rate and downstream backwater effects that may submerge weir discharges. Throughout the design process, the engineer should remain aware of any constraints imposed by these factors.

IV.   Hydraulic Design Tasks

Once the design discharge (Q_D), head water stage (HW_D), tail water stage (TW_D) and desired control elevation (CE) have been established, the tasks listed below should be performed in the order given.

A. Obtain the approach channel floor elevation (BE) along with the bottom width (BW).

B. Specify the weir crest width based on traffic crossing requirements, geotechnical design requirements or other site constraints. Preferably, L_w should be as small as possible.

C. Compute the following:

P = CE – BE (the weir height measured from the upstream channel floor)

H = HW_D - CE

h = TW_D – CE

L = the channel width at elevation CE

A_u = the upstream wetted area at stage HW_D

$V_u = Q_D / A_u$

D. Compute:

$HW_T = HW_D + V_u{}^2 / 2g$

$H_T = HW_T - CE$

$H = HW_D - CE$

E. Compute H_T / P. If $H_T / P \leq 1/6$, proceed to step F. Otherwise, compute $V^2{}_{ucr} / 2g = {}^5/_3 V_u{}^2 / 2g$ and then recompute HW_T and H_T (from step D) using $V^2{}_{ucr} / 2g$ in place of $V_u{}^2 / 2g$.

F. Compute ξ with Equation F2.

G. Compute C_d using Equation F3.

H. Compute the following:

y_L with Equation F5

$d = TW_D - BE$

$h_L = Hy_L$ (from Equation F4)

I. If h (from step C) $< h_L$, flow is unsubmerged. Set $Q_u = Q_D$ and proceed to step K.

J. If h (from step C) $\geq h_L$, flow is submerged. Set $Q_s = Q_D$ and compute:

$y_t = h / H$

Y_t using Equation F7

ψ using Equation F8 and Table F1

$Q_u = Q_s / \psi$ (from Equation F6)

K. Use Equation F1 and the value of Q_u to compute the required weir length L_{req}. If L_{req} is significantly different from L (from step C), design a channel transition that changes the channel width at the weir location from L to L_{req} at elevation CE. The transition design should include a section of straight channel both upstream and downstream of the weir.

L. If $h \geq 0$, use the values of y_t and ξ along with Figure F4 to determine whether the design discharge over the weir occurs as a plunging or surface jet.

M. Compute the length of the recirculation zone using either Equation F9 or F13. Locate its end in the downstream channel.

N. Divide the floor between the weir crest and the end of the recirculation zone into increments of 10 feet (or other incremental length as deemed appropriate).

O. If discharge over the weir occurs as a plunging jet, determine the maximum streamwise velocity and average jet velocity at the beginning of each increment demarked in step N. Use the procedure discussed in section II.H.1. If the only flow regime expected to occur is a surface jet, determine the maximum backward streamwise velocity and average backward velocity at the beginning of each increment using the approach given in section II.H.2.

P. Design the stabilizing features for both the downstream side of the weir embankment and the downstream channel using the results of step O. Refer to the appropriate section of the guidelines.

The procedure for designing a broad-crested trapezoidal weir is summarized in Figure F5. Design examples based on this procedure follow.

V. Design Examples.

A. Example 1

Design an embankment weir for the same bypass channel and design conditions specified for the design example given in Appendix A. For convenience, these conditions are repeated here:

A bypass channel with a bottom width of 20 feet, a bottom elevation of 0 feet and 2:1 side slopes carries a design discharge of 500 cfs. The design head water and tail water stages for the proposed structure location are 13 and 9 feet, respectively, while the seasonal control elevation is 11 feet.

Each step of the design process is carried out below.

Step A.

From the site description, BE = 0 and BW = 20 ft.

Step B.

To accommodate vehicular traffic, set L_w = 10 ft.

Step C.

P = CE – BE = 11 – 0 = 11 ft; H = 13 – 11 = 2 ft

```
                    ( Begin )
                       │
                       ▼
           / Obtain design Q,        /
          /   HW, TW, CE            /
                       │
                       ▼
           / Obtain BE, BW /
                       │
                       ▼
           │ Establish L_w │
                       │
                       ▼
           │ Compute P,H,h,L,A_u,V_u │
                       │
                       ▼
           │ Compute HW_T, H_T, H │
                       │
                       ▼
           │ Compute ξ │
                       │
                       ▼
           │ Compute C_d │
                       │
                       ▼
           │ Compute y_L, d, h_L │
                       │
                       ▼
              ◇ h ≥ h_L? ◇ ──no──► │ Q_u = design Q │
                       │
                      yes
                       │
                       ▼
           │ Compute y_t,Y_t,ψ,Q_u │


           │ Compute L_req │
                       │
                       ▼
           │ Determine Flow Regime │
                       │
                       ▼
           │ Compute L_r or L_R │
                       │
                       ▼
           │ Divide recirculation
             zone into
             increments │
                       │
                       ▼
           │ Compute maximum
             streamwise and
             average velocities │
                       │
                       ▼
           │ Design channel
             transition and
             stabilization
             features │
                       │
                       ▼
                    ( End )
```
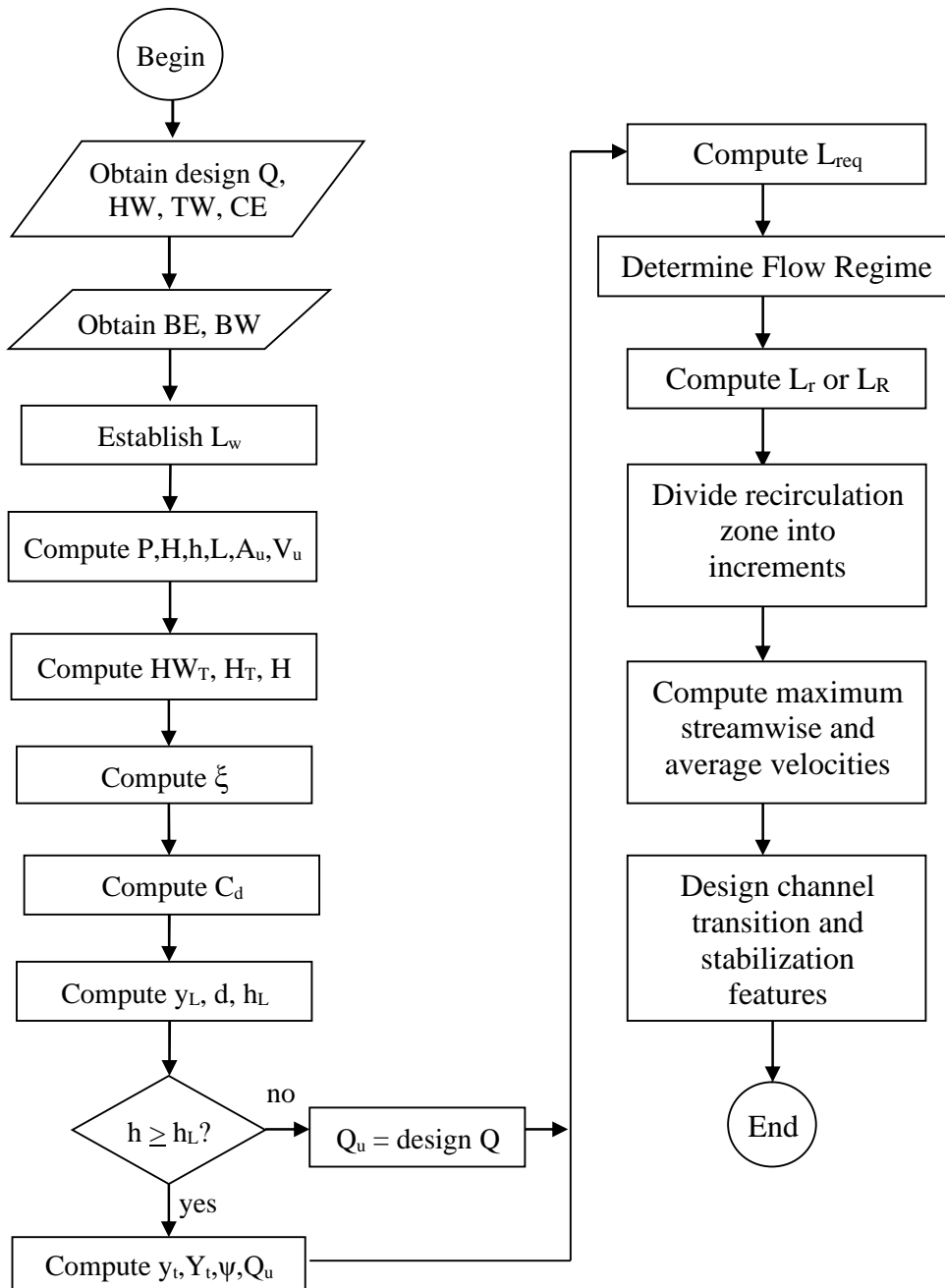
Figure F5. Broad-crested weir design process

$h = 9 - 11 < 0$

$L = BW + 2zP = 20 + (2)(2)(11) = 64$ ft.

$A_u = [20 + (2)(13)](13) = 598$ ft^2

$V_u = Q_D / A_u = 500/598 = 0.84$ ft/s

Step D.

$HW_T = 13 + (0.84)^2/2g = 13.01$ ft

$H_T = 13.01 - 11 = 2.01$ ft

$H = 13 - 11 = 2$ ft

Step E.

$H_T/P = 2.01/11 = 0.183 > 0.167$, so $V_{ucr}^2/2g = 5/3V_u^2/2g = 0.02$ ft.

Hence, $HW_T = 13 + 0.02 = 13.02$ ft and $H_T = 13.02 - 11 = 2.02$ ft.

Step F.

$\xi = H_T/(H_T + L_w) = 2.02/12.02 = 0.17$

Step G.

$C_d = 0.43 + 0.06\sin[\pi(0.17 - 0.55)] = 0.37$

Step H.

$y_L = 0.85 - 0.5(0.17) = 0.77$

$d = 9 - 0 = 9$ ft

$h_L = (2)(0.77) = 1.53$ ft

Step I.

$h = -2 < 1.53$, so flow is clearly unsubmerged and $Q_u = Q_D = 500$ cfs.

Step J. N/A

Step K.

L_{req} = 500/0.37/[2g(2.02)^3]$^{1/2}$ = 58.68 ft < L = 64 ft from step C. A mild transition can be constructed to narrow the channel to the required width or the weir crest length can be left at 64 ft to save construction costs. The latter option would result in the loss of some attenuation of peak discharges. Furthermore, there will be some additional error in the results based on this length since the tail water depth is not constant over the entire weir length.

Step L.

As indicated previously, flow over the weir occurs as a plunging jet since h < 0. Figure F4 is therefore not needed.

Step M.

From step H, d = 9 ft. The downstream toe of the embankment is located at x_R = (11 − 0)(2) = 22 feet. From Equation F9, the length of the recirculation zone is L_r = (4.3)(9) = 38.7 ft, which occurs at x_R = 22 + 38.7 = 60.7 ft = L_R.

Step N.

For the purpose of designing channel stabilization measures, compute velocities at x_R = 0, 10, 20 30, 40, 50 and 60 feet.

Step O.

Following the process outlined in section II.G.1, u_A = [(32.17)(11)]$^{1/2}$ = 18.81 ft/s, u_d = 500 / {[20 + (2)(9)](9)} = 1.46 ft/s, and u_M is computed using Equation F12 for the values of x_R determined in step N. Recalling that χ = x_R / L_R, substitution of the values of u_A, u_d and x_R into Equation F12 yields u_M = 18.81, 17.76, 14.98, 11.35, 7.85, 5.10 and 3.29 ft/s at x_R = 0, 10, 20 30, 40, 50 and 60 feet, respectively. Since the average jet velocity is taken to be one-half of the maximum streamwise velocity, u_{ave} = 9.41, 8.88, 7.49, 5.68, 3.93, 2.55 and 1.65 ft/s at the same values of x_R.

Step P.

The velocities determined in step O can be used to design the stabilization features for the downstream side of the weir and the downstream channel over a length of L_r. The design technique used will determine whether the average or maximum streamwise velocities will be considered. Given the results of step O, the downstream side of the embankment should be protected against an average jet velocity of about 9 ft/s while the channel floor should be able to withstand an average jet velocity of about 7 ft/s over the first 10 feet and up to about 5 ft/s thereafter. An appropriate factor of safety can be applied to each of these design velocities.

B. Example 2

Design an embankment weir for the same conditions stated in Example 1 except for a tail water stage of 12.6 feet.

Steps A – H

The results are the same as those determined in Example 1 except now h = 12.6 – 11 =1.6 ft and d = 12.6 ft.

Step I

Since h = 1.6 > h_L = 1.53, discharge over the weir now occurs as submerged flow. Proceed with step J.

Step J

$Q_s = Q_D = 500$ cfs

$y_t = h/H = 1.6/2.0 = 0.8$

$Y_t = (y_t – y_L) / (1 – y_L) = (0.8 – 0.77) / (1 – 0.77) = 0.13$

For $\xi = 0.17$, assume n ≈ 7 (table F1). $\psi = (1 – Y_t)^{1/n} = (1 - 0.13)^{1/7} = 0.98$

$Q_u = Q_s / \psi = 500/0.98 = 510.2$ cfs. This is what the unsubmerged flow would be at the design head water stage if the weir is long enough to pass 500 cfs under submerged conditions at the design head water and tail water stages.

Step K

$L_{req} = 510.2/0.37/[2g(2.02)^3]^{1/2} = 59.88$ ft ≈ 60 ft < L = 64 ft from step C. A mild transition can be constructed to narrow the channel to the required width or the weir crest length can be left at 64 ft to save construction costs. The latter option would result in the loss of some attenuation of peak discharges.

Step L

From Figure F4, for $\xi = 0.17$ the maximum value of y_T of the transition range is about 0.7. Since this is less than $y_t = 0.8$, discharge over the weir occurs as a surface jet.

Step M

From Equation F13, $L_R = (6.8)(12.6)(1-1.6/2)^{1/6} = 65.52$ ft from $x_R = 0$ at the weir crest edge. L_R will be overestimated in this case since d is less than 12.6 ft over the length of the weir that spans

the channel side slopes.

Step N

Starting at the downstream edge of the weir crest, compute velocities within the bottom recirculation zone at x_R = 0, 10, 20, 30, 40, 50 and 60 ft.

Step O

From Equation F14, u_a = -0.25[(32.17)(12.6)(1-1.6/2)]$^{1/2}$ = -2.25 ft/s. From Equation F15, u_m = -4.5[$\chi(1-\chi)$]$^{1/2}$, where $\chi = x_R/L_R$. Recall that $u_m < 0$ since it is in the negative x_R direction. Evaluating this expression for each location identified in Step N yields $|u_m|$ = 0.0, 1.62, 2.07, 2.24, 2.20, 1.91, and 1.25 ft/s. Average velocities within the recirculation zone are approximately one-half of these values.

Step P

Based on the results of step O, a channel lining that is designed for a velocity of 2.5 ft/s should suffice throughout the required length.

VI.   References

Kindsvater, C. E. 1964. Discharge Characteristics of Embankment-Shaped Weirs. *Geologic Survey Water Supply Paper 1617-A*, U. S. Government Printing Office, Washington, D.C.

Fritz, H. M. and W. H. Hager. 1998. Hydraulics of Embankment Weirs. *Journal of HydraulicEngineering, 124(9), 963-971.*

Fritz, H. M., C. Blount, R. Sokoloski, J. Singleton, A. Fuggle, B. G. McAdoo, A. Moore, C. Grass, B. Tate. 2008. Hurricane Katrina Storm Surge Reconnaissance**,** *J. Geotechnical and Geoenvironmental Engrg., ASCE*, 134(5):644-656, doi:10.1061/(ASCE)1090-0241(2008)134:5(644).

Sargison, J. E. and A. Percy. 2009. Hydraulics of Broad-Crested Weirs with varying Side Slopes. *Journal of Irrigation & Drainage Engineering, 135(1), 115-118.*

Wang, Xi-kun, Zhi-yong Hao and Soon Keat Tan. 2010. Hydrodynamics of Trapezoidal Embankment Weirs. *Proceedings of the 9th International Conference on Hydrodynamics*, Shanghai, China, October 11-15, 2010, pp. 386-390.

Yarnell, D. L., and F. A. Nagler. 1930. Flow of flood water over railway and highway embankments." *Public Roads,* 11(2),30-34.

Appendix G. Hydraulic Design Procedure for Temporary Pump Stations

I.   Introduction

Temporary pump stations may be needed where a permanent pump station is out of service, or may be the best alternative for a by-pass structure in situations where a permanent structure is taken out of commission and it is not feasible to construct a by-pass channel around it. For example, in 2010 the temporary pumps shown in Figure G1 were installed at the S-6 site in order to offset the loss in capacity incurred while one of the primary pumps was taken out of service. Figure G2 displays the temporary pump station that was placed into operation at S-60 while the spillway was undergoing repairs. In both cases, the temporary pump stations were comprised of submersible pumps driven by hydraulic motors.

Figure G1. Temporary pump station at S-6 (head water at left, tail water at right)

Figure G2. Temporary pump station at S-60 (head water at right, tail water at left)

Temporary pump stations installed at District structures so far often resemble the designs illustrated above. While this type of installation may often be advantageous in regards to affordability, adaptability and setup, it has been demonstrated to be sometimes unreliable due to frequent clogging of the pump intakes, inefficiencies in pump performance and reliance on manual operation. This would be undesirable in applications where the pump station is to maintain a designated level of service over several months to a year. In such cases other pump station designs should be considered.

The purposes of the guidelines presented here are to (i) introduce other alternative pump station designs that can be implemented on a temporary basis; and (2) to present a recommended hydraulic design procedure that can be followed for any pump station, temporary or permanent, that is be classified as "small" in accordance with District engineering standards. Such a procedure should yield a conservative design for a temporary pump station so as to help maximize mechanical reliability and predictability of discharge rates. It should be emphasized, though, that the guidelines presented here only address the hydraulic design aspects of a pump station. The engineer should refer to existing guidelines for the mechanical, electrical and structural design processes associated with a pump station. Moreover, any facet of pump station hydraulic design that is not explicitly addressed here should conform to existing standards. In particular, in situations where any criteria or specifications stated in these guidelines conflict with those stated in Section 11212 of the District Engineering Specifications, the latter shall take precedence unless directed otherwise by the project engineer.

II. Background

A. Hydraulic Design Principles

Before applying the design guidelines and procedures contained in this appendix, the engineer should be familiar with the hydraulic principles associated with pump performance, operation and efficiency along with the concepts of total dynamic head (TDH), total static head (TSH), specific speed, suction specific speed, net positive suction head (NPSH), cavitation and best efficiency point (BEP). An understanding of the pump affinity laws is also recommended. Useful references on these subjects include Jones et al. (2006), Lobanoff and Ross (1985), Smith (2001) and various standards sponsored by the Hydraulic Institute (HI).

B. Design Objectives

Conventionally, the primary focus of the hydraulic design process for a pump station has been to select a pump that can produce the design discharge rate at a specified TDH and efficiency. The design flow rate is usually the peak discharge that needs to be passed in order to maintain a targeted level of service or satisfy a project objective. However, the objective of a temporary pump station is generally to by-pass a primary structure while maintaining the same level of service for all flows up to a discharge with a specified recurrence interval. It should also operate in an efficient and reliable manner for all flows that are smaller than the design discharge rate. This is important since these smaller discharges will be pumped much more frequently than the design flow. In fact, the design discharge may never occur during the short service life of the

pump station. If a pump frequently operates under unfavorable conditions, it may deteriorate or sustain damages that could prevent it from performing as intended under design conditions. Therefore, it should be verified during the design process that each pump will operate only under the hydraulic conditions recommended by the manufacturer.
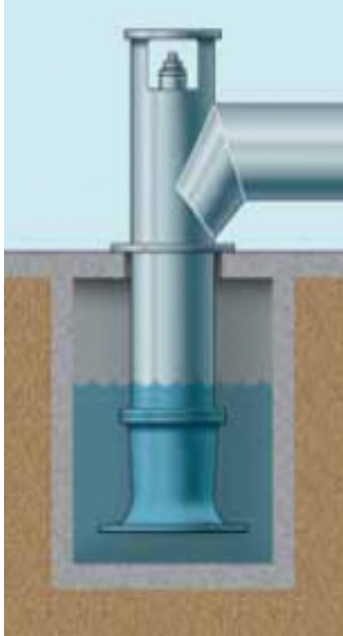
C.   Pump Design

Centrifugal pumps are the most common type of pump used in water management pump stations. At District pump stations, vertical axial flow pumps (a subcategory of centrifugal pumps) are typically used. In this type of pump, water is accelerated by propellers through a cylindrical casing before being discharged through a 90-degree bend (Figure G3). The bottom of the casing terminates in a bell-shaped opening that serves as the pump intake.

These guidelines only address the application of this type of pump. Given their successful and long-term implementations at District facilities, this restriction is considered to be conservative. Furthermore, it is assumed that pumps will be of a constant speed since the cost of a variable speed pump is less likely to be justifiable for a temporary installation.

Figure G3. General schematic of a vertical axial-flow pump installation (courtesy of the FlowServe Corporation)

D.   Pump Inlet Design

The hydraulic conditions surrounding a pump intake can have a significant effect on pump performance. Therefore, specifying the hydraulic design of the inlet structure or wet well for a pump station is one of the most critical facets of the entire design process. Only two wet well types will be considered in these guidelines since they should be adequate for most temporary applications. The first can be classified as open or unconfined, where the pump intake is simply submerged in an open water body to a specified depth from the surface and distance from the bottom. A screen or other protective device can be installed on or around the intake opening in order to prevent floating debris, fish or other objects from entering the pump. An example of a temporary pump station with this type of inlet design is S-332B, which discharges water from the L-31N borrow canal. It is shown in Figure G4. It should be noted, however, that this particular pump station is much larger and has a longer service life than a temporary pump station which is intended to remain in operation for a year or less.

The second type of pump inlet structure of interest is a rectangular wet well with certain modifications needed to achieve a smooth and stable transition of flow from the water body to the pump intake. Based on information obtained through hydraulic models, the HI (1998) has specified a standard design for a rectangular wet well with a single pump intake. Dimensions are expressed in terms of the pump intake diameter. A multi-projection view of this design is provided by Jones et al. (2006) and is displayed in Figure G5. The fillets and curtain wall shown

are located and dimensioned so as to minimize flow instabilities, vortex formations and unevenness in the flow field at the pump intake bell. Additional background information on this design is given by Jones et al. (2006).

Figure G4. Inlet structure for pump station S332B

Although not shown in Figure G5, the HI (1998) recommends the installation of a trash rack or screen at the entrance to the rectangular wet well. In addition to protecting the pump intake from debris and other objects, a properly designed trash rack installed at this location can help the flow entering from the outer water body to become straighter and more uniform. The engineer should refer to existing District guidelines when designing trash racks.

It should be reiterated that the rectangular wet well design discussed above is intended for a single pump intake. The HI (1998) also presents similar designs intended for multiple pump intakes. In such designs, walls separating the pumps are often needed to make the flow to each pump more uniform. Under certain conditions, achieving an even distribution of the total inflow to the pumps can be problematic. Consequently, for conservative design, only single-pump wet wells will be considered here.
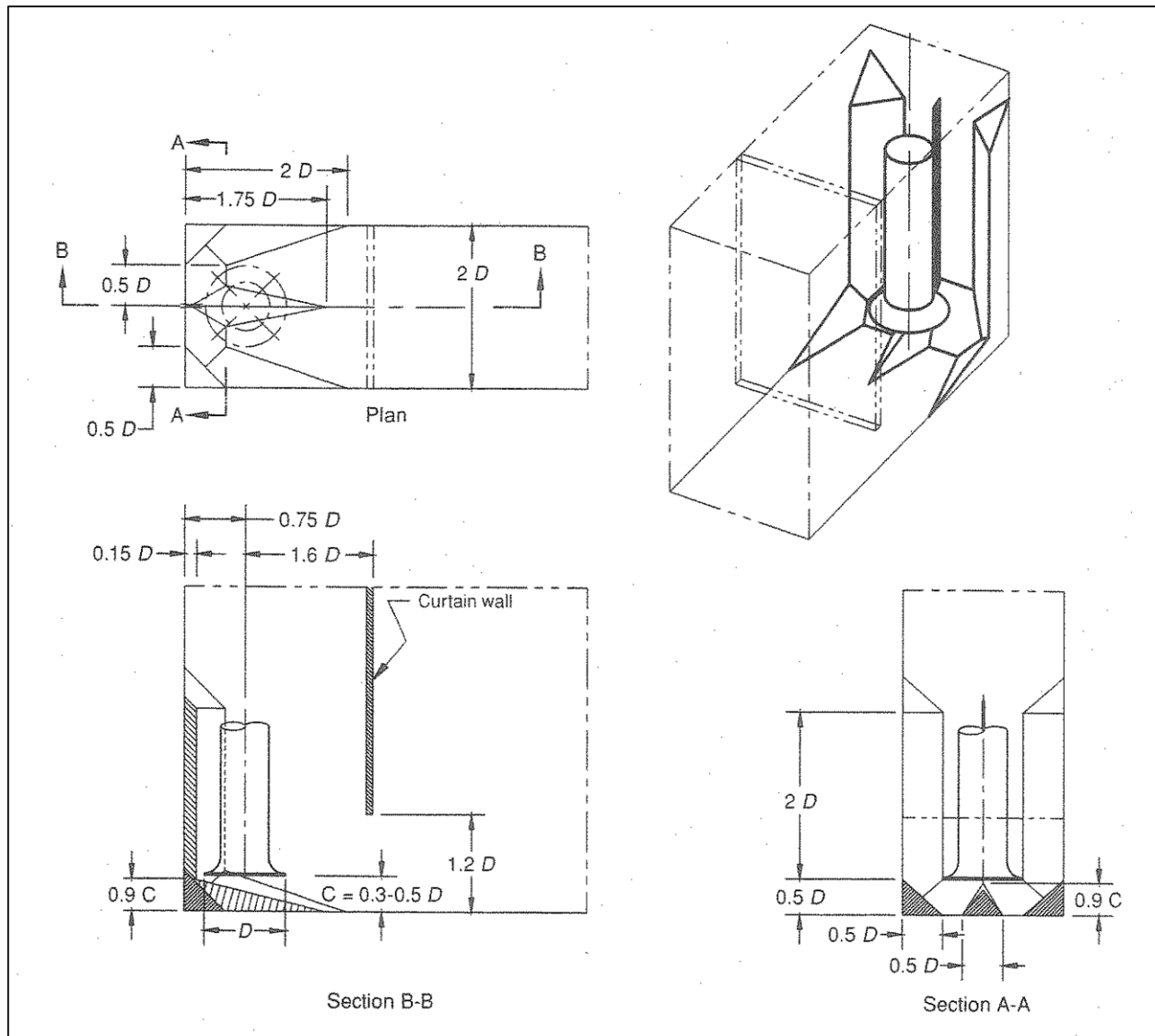
Figure G5. Standard HI design of a rectangular wet well with a single pump
(reprinted from *Pumping Station Design*, 3rd ed., Jones et al., ch. 12, p. 12.5, 2006 with permission
from Elsevier and courtesy of the Hydraulic Institute, Parsippany, NJ 07054, www.Pumps.org)

III.   Hydraulic Design Tasks

Once the design discharge (Q_D), design head water stage (HW_D) and design tail water stage
(TW_D) have been established, the tasks listed below should be performed in the order given.

   A. Determine the desired ranges of target head water and tail water stages for the permanent
       structure. The upstream range is demarked by the seasonal low head water (SLHW) and
       the seasonal high head water (SHHW). Similarly, the downstream range is bound by the
       seasonal low tail water (SLTW) and the seasonal high tail water (SHTW).

B. Using the mean daily flow data in DBHYDRO, select a representative number of wet or dry seasons (depending on which season is under consideration in the design process) that capture the expected range of mean daily flows through the permanent structure. Compute the seasonal average daily flow (Q_{MDF}) that was passed by the permanent structure during this time frame. In determining Q_{MDF}, only days when the mean daily flow was greater than zero should be considered. A pump will be selected for the purpose of passing this flow rate. Q_{MDF} is assumed to be representative of the smaller, day-to-day flows that must be passed by the temporary pump station. Such flows are usually handled by a single pump whose operation will account for 80 – 90% of the total station operation time (Jones et al, 2006). Two identical, alternating pumps should be used for this purpose. The "On" elevation for these pumps should be set to SHHW and the "Off" elevation should be set to SLHW.

C. Select the number of pumps n_p that will be installed to pass the design discharge rate Q_D while neglecting any contribution from the daily flow pump sized in step B. The number of pumps will depend on availability, pricing, site conditions and the distance between the SHHW and HW_D. This distance divided by n_p should not be less than one foot. It is recommended that each of these pumps operate over a headwater interval of at least one foot in order to avoid excessive pump cycling. To help simplify and minimize the cost of station maintenance, it is recommended that these pumps be identical with a design capacity $Q_p = Q_D / n_p$. It is standard practice to include one additional stand-by pump as well.

During storm event discharge operations, the first of these pumps will trigger on at a head water stage of SHHW + $(HW_D – SHHW)/n_p$ and off at SHHW. The second pump would then commence pumping at a head water stage of SHHW + $2(HW_D – SHHW)/n_p$ and cease operation when the head water stage falls to SHHW + $(HW_D – SHHW)/n_p$. This pattern of on/off trigger elevations would then continue to the last pump in sequence that would turn on at a stage of HW_D and off at SHHW + $(n_p – 1)(HW_D – SHHW)/n_p$. As is customary practice, the pumps should alternate in sequence on a regular basis in accordance with a specified protocol (see step R).

D. For the pump handling the frequent flows, the following range of total static heads is assumed for normal operations:

$$TSH_1 = MAX(0, SLTW – SHHW) \quad \text{(seasonal lowest)}$$

$$TSH_2 = SHTW – SLHW \quad \text{(seasonal highest)}$$

During pumping under storm conditions, a different range of total static head values will be encountered. In order to simplify and economize the design of this pump as much as possible, it should not need to be operative under storm conditions. This will allow the installation of electronic controls that will turn the pump off if its operating point moves outside of the Allowable Operating Range (AOR) of the pump performance curve. Designating the TDH associated with the upper limit of this range as TDH_u and the TDH

at the lower limit as TDH_l, it can be easily shown using conservation of energy that the pump will operate within the AOR if

$$TDH_l - 8Q_l^2/g\pi^2D_p^4 \leq P_p/\delta + P_{elev} - HW \leq TDH_u - 8Q_u^2/g\pi^2D_p^4 \qquad (G1)$$

where Q_l and Q_u are the flow rates associated with TDH_l and TDH_u, respectively; D_p, P_{elev} and P_p are the diameter, centerline elevation and pressure at, respectively, the pump discharge; and HW is the head water stage. The pressure at the pump outlet can be monitored with a pressure sensor. The monitored values of P_p and HW can be temporarily stored in a Remote Terminal Unit (RTU) or Programmable Logic Controller (PLC), where the condition in Expression (1) can be evaluated. If this condition is not met, the pump can be turned off. Subsequent restarting of the pumps can then be delayed for a specified amount of time or until the storm water flow pumps turn off, if they are operative at the time.

E. For the storm event pumps, the values of TSH_3 and TSH_4 given below can be assumed to represent the minimum and maximum, respectively, static heads that any of these pumps will operate against.

$$TSH_3 = TW_D - HW_D$$
$$TSH_4 = TW_D - SHHW$$

Steps F – L below should be performed for each pump, as applicable:

F. Establish the pump location and discharge line configuration. Develop plan and profile sketches while adhering to the following:

- At the downstream end of the discharge pipe, the centerline elevation should be less than SLTW.

- If possible, the pipe should be sloped toward the outlet throughout its length in order to minimize backflow through the pump after shutoff. Otherwise, a check valve should be installed 5 pipe diameters downstream of the pump.

- Where possible, all 90-degree elbows and bends should have a long radius.

- The pump should have its own independent discharge line.

G. Select the pipe material and determine the diameter of the discharge pipe. Ideally, the pipe should be sized so that the mean velocity is 3.5 – 4 ft/s at the design flow. This restriction will help to keep the pipe clean internally while also lessening the undesirable effects of any transients that may occur. A maximum velocity of 10 ft/s is recommended. Note also that since the actual discharge from each pump will not be exactly equal to its nominal capacity, the pipe velocities should be recomputed, if necessary, after the

intersections of the system curves with the pump performance curves have been determined (see steps M and N).

H. Estimate the possible range of hydraulic roughness ε for the discharge pipe. Values for hydraulic roughness are widely available in the literature and can sometimes be obtained from pipe manufacturers. For convenience, the values given in Table G1 can be used for the pipe materials indicated. These values were derived from the Hydraulic Institute (1990) and Wallingford and Barr (2006).

I. From the results of step F, identify all appurtenances and fittings located between the pump discharge and the pipe outlet. Estimate from the literature a range for the local head loss coefficient K of each appurtenance. Values provided by Jones et al. (2006) for common fittings are provided in Table G2, where the subscript "1" refers to the flow upstream of the fitting while the subscript "2" denotes the downstream flow. Unless stated otherwise, the local head loss is based on the higher of the two velocity heads. According to Jones et al. (2006), these K values have an uncertainty of at least -20% to 30%.

Table G1. Ranges of ε for selected pipe materials

Pipe Material	ε (inches)		
	low	medium	high
PVC	0.00006	0.0012	0.024
Steel (unlined)	0.0006	0.0012	0.0024
DI (cement-lined)	0.0006	0.0012	0.0024

Table G2. Local head loss coefficients for selected fittings

Appurtenance		*K*
Bellmouth Entrance		0.05
Submerged Exit		1
Elbow	90^0, long radius	0.18
	45^0, standard	0.18
Increaser	conical	$\frac{1}{4}\,[1- (D_1/D_2)^4]$
	abrupt	$[1- (D_1/D_2)^2]^2$
Reducer	conical	0.03 ± 0.01
	abrupt	$\frac{1}{2}\,[1- (D_2/D_1)^2]$

J. Determine the required outer diameter D of the pump intake bell. It should be sized so that the intake velocity falls within the ranges given in Table G3. However, the HI (1998) recommends an optimal velocity of 5.5 ft/s while Jones et al. (2006) indicate that the near-maximum desirable velocity should be 5 ft/s. Given this, it is recommended that the engineer first determine the actual bell diameter needed to achieve a velocity of 5.5 ft/s and then select the next largest nominal size. Under no circumstances should the velocity

through the pump bell be less than the minimum value shown in Table G3. Note: the velocities shown in Table G3 are based on the outer diameter of the pump bell even though the actual wetted area is determined by the inner diameter.

Table G3. Recommended pump intake bell velocities (HI, 1998; Jones et al., 2006)

Flow Rate (cfs)	Allowable Velocity Range (ft/s)
< 11	2 - 9
11 – 44.5	3 - 8
> 44.5	4 - 7

K. If the inlet is to be of the unconfined type shown in Figure G4, the intake bell will require a minimum amount of submergence in order to suppress the formation of vortices. According to HI (1998), this minimum submergence S is

$$S/D = 1.0 + 2.3F_B \qquad\qquad (G2)$$

where F_B is the Froude number of the flow within the pump bell and S is the required depth of water above the bell rim. At this step, F_B is based on the velocity determined in step J.

A minimum clearance between the canal bottom and the pump bell is also required to suppress submerged vortices. HI (1998) recommends that this clearance be at least 5D where the suspension of bottom sediments and debris is of concern. Considering typical dimensions of District canals, adhering to this recommendation may often be problematic. In these cases, riprap or other stabilization measures may need to be installed on the channel floor in the vicinity of the pump inlet. If the suspension of bottom debris is not a concern, the required clearance can be reduced to 0.3D to 0.5D.

As indicated previously, a bar screen surrounding the pump intake (such as that illustrated in Figure G4) should be designed according to established guidelines. In the absence of any clogging, head losses though the bar screen will usually be negligible.

L. If the inlet is to be a rectangular wet well, it should be dimensioned as specified in Figure G5. The required submergence is the same as that required for an unconfined inlet and can be computed using Equation G2. Furthermore, according to HI (1998), the mean velocity of the flow field approaching the pumps should not exceed 1.5 ft/s. In some cases, an approach bay of width 2D and depth S + C (Figure G5) will result in a higher mean velocity. The simplest remedy for this is to increase the submergence. If this is not desirable or feasible, the wet well entrance width can be increased as needed to decrease the mean entrance velocity to 1.5 ft/s. HI (1998) provides the design criteria for such a modification, and the engineer should consult this reference before proceeding.

Additionally, HI (1998) indicates that the trash rack should be installed flush with the upstream edges of the wet well walls (i.e. at the immediate entrance) and at a distance of

at least 4D from the pump bell centerline. If it is not economical to install a self-cleaning trash rack, the bar screen should instead be installed a distance of at least 5D away from the pump centerline. This will help to protect the pump from nonuniformities in the approach flow caused by temporary clogging of the screen.

M. For the routine flow pump, four system curves should be computed for the intake and discharge system designed in steps F – L. A system curve depicts the relationship between flow rate and TDH. That is, each point on the curve represents a discharge rate and the total head that will be required to move that flow through the system. The first curve should be based on TSH_1 along with head losses computed using the minimum ε and K values. Similarly, the second system curve is based on TSH_2 and the maximum ε and K values. The third system curve will reflect the average static head and average head losses. Finally, the fourth curve should be representative of pump start-up conditions where the static head is equal to the discharge line summit elevation minus SHHW. In this case, computed head losses should be at their maximum values. If the discharge line is installed as recommended, the highest point should occur at the pump discharge.

The first three of these curves are conceptualized as shown in Figure G6. In each case, head losses within the intake components designed in either step K or L will usually be negligible in the absence of any clogging at the intake screen.
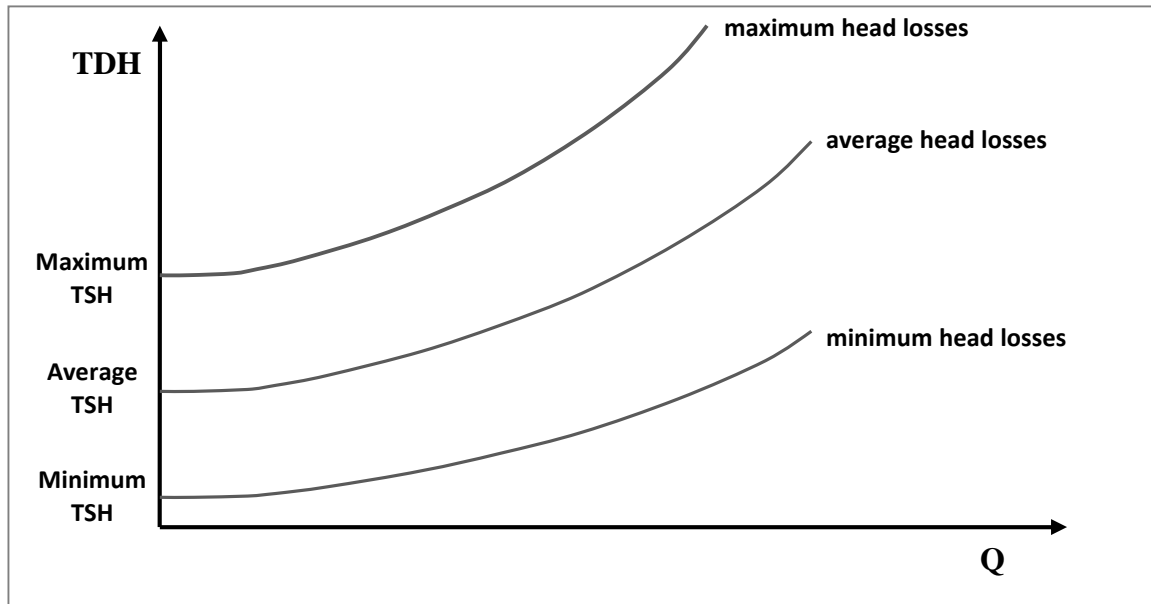
Figure G6. Conceptualization of system curves

N. For the storm event pumps, four system curves should be computed for the intake and discharge systems designed in steps F – L. The first system curve should be based on TSH_3 along with the minimum expected head losses. The second system curve will be computed with TSH_4 along with the maximum expected head losses while the third system curve consists of a static head equal to the average of TSH_3 and TSH_4 along with

average dynamic head losses. The fourth should be representative of startup conditions as discussed in step M and will be based on maximum head losses along with a static head equal to the discharge pipe summit minus $[SHHW + (HW_D - SHHW)/n_p]$.

O. Compute the Net Positive Suction Head Available (NPSHA) at the pump impeller under the minimum expected head water stage. Assuming negligible head losses between the upstream water surface and the pump inlet, the NPSHA is

$$NPSHA = H_{bar} + h_s - H_{vap} \qquad\qquad (G3)$$

where H_{bar} is the barometric pressure head, h_s is the height of the water surface above the eye of the pump impeller, and H_{vap} is the vapor pressure head of the water at the maximum expected temperature. Generally, $H_{bar} \approx 33.9$ feet and $H_{vap} \approx 1$ foot at 75^0. In the event that head losses upstream of the pump intake are not negligible, they should be subtracted from the right side of Equation G3. This will be necessary if partial clogging of the intake screen is expected. In such a situation, NPSHA would be a function of discharge and should be plotted along with the system curves.

P. For the pump designated to pass the daily flows, the design point should be taken as Q_{MDF} at a TDH that is computed using the average of TSH_1 and TSH_2 along with the average head losses. The highest discharge rate will occur at the intersection of the pump performance curve with the system curve that was computed using the minimum static head and minimum dynamic head losses. Given these concepts, the following criteria should be met:

1. The intersection of the pump performance curve with the system curve that is based on TSH_1 and minimum head losses should occur within the pump's Preferred Operating Region (POR). Similarly, the intersection of the pump performance curve with the system curve that is based on TSH_2 and maximum head losses should also occur within the POR. It is best that the POR be defined by the pump manufacturer. Otherwise, it can be (conservatively) estimated to occur from 80% to 115% of the discharge associated with the BEP.

2. The discharge associated with the intersection of the pump performance curve with the system curve that is based on the average of TSH_1 and TSH_2 along with average dynamic losses should preferably be within 5% of the pump's BEP discharge. Furthermore, the discharge associated with this operating point should be greater than or equal to Q_{MDF}.

3. At the BEP, the pump's efficiency should meet or exceed a specified minimum.

4. The operating points defined in criterion 1 should not produce a velocity in the discharge line or pump intake that is excessive. A maximum of 10 ft/s in the discharge line is recommended.

5. The intersection of the pump performance curve with the system curve representing start-up conditions should lie within the AOR. While such conditions will persist for only a very short time and will not be steady, this step will help to ascertain that the pump will not experience excessive vibrations during startup. Additionally, since the criteria specified in step D will turn the pump off if the operating point moves outside of the AOR, the operating point determined in this step should lie within the AOR by an acceptable margin so that the pump does not intentionally turn off during startup. If this point does not lie within the AOR by an acceptable margin, the pump may still be acceptable given the relatively short duration of the startup process. In such a situation, the pump manufacturer should be consulted and additional logic that overrides the criteria specified in step D during startup will have to be included in the RTU or PLC.

6. The NPSHA should exceed the Net Positive Suction Head Required (NPSHR, specified by the manufacturer) by an acceptable safety margin throughout the projected operating range. It is best that this safety margin be provided by the pump manufacturer. Otherwise, as a conservative safety factor, within 15% of the BEP the NPSHA should exceed the NPSHR by at least 5 feet or 35% of the NPSHR, whichever is greater. Beyond 15% of the BEP, NPSHA should exceed NPSHR by at least 80%.

7. The suction specific speed S_s should be between 8,000 and 12,000 (U.S. customary units). This parameter is given by

$$S_s = n(Q_{BEP})^{0.5} / (NPSHR_{BEP})^{0.75} \qquad \text{(G4)}$$

where n is the pump speed (rpm) while Q_{BEP} (gpm) and $NPSHR_{BEP}$ (ft) are the discharge and NPSHR, respectively, at the BEP.

The primary objective of this step is to identify candidate pumps that satisfy the above requirements. Some pump manufacturers have web-based software linked with electronic catalogs that can be used to locate candidate pumps that satisfy specified requirements. The specifications that can be entered into the application as search criteria will vary with the pump manufacturer. The engineer should include as many of the above criteria as possible and then manually check the omitted ones after candidate pump curves have been obtained. Moreover, this selection process should be carried out using electronic catalogs of at least two reputable pump manufacturers. A case example of this process is provided by Jones et al. (2006).

Depending on the engineer's familiarity and experience with the selected pump models, it may be desirable to forward the candidate pumps along with the system specifications developed in steps A-O to the engineering departments of the pumps' manufacturers. The pump manufacturers can then provide independent evaluations and selection recommendations.

Q. Unlike the pump that is designated to pass the frequent flows occurring on a day-to-day basis, the pumps designated to handle the design storm flows will operate far less frequently. In fact, depending on the hydrologic conditions that exist during the service life of the temporary pump station, it's even possible that they will not be operated at all. Consequently, the hydraulic design criteria for these pumps need not be as stringent as those indicated in Task P.

The criteria proposed here address the first pump in sequence since it will operate over the widest range of static heads. Since all n_p pumps will cycle and potentially operate first in sequence, the same criteria obviously apply to each pump. The criteria listed below should be satisfied by the pump selected for this application.

1. The intersection of the pump performance curve with the system curve that is based on the average static head along with the average expected head losses should have an associated discharge rate that equals or exceeds Q_p/n_p.

2. The discharge associated with the operating point identified in criterion 1 should preferably fall within 5% of the pump's BEP discharge. This operating point should, however, at least lie within the POR. This will help to ensure reliable pump operation during the peak of the storm event.

3. The operating point defined by the intersection of the performance curve with the system curve that is based on TSH_3 along with the minimum expected head losses should lie within the pump's AOR.

4. The operating point defined in criterion 3 should not produce a velocity in the discharge line or pump intake that is excessive.

5. The operating point defined by the intersection of the performance curve with the system curve that is based on TSH_4 along with the maximum expected head losses should lie within the pump's AOR.

6. Refer to criterion 6 given in step P.

7. Refer to criterion 7 given in step P.

As explained in step P, the primary objective at this point is to identify candidate pumps that satisfy the above requirements. Follow the same process explained in step P using the electronic catalogs and selection software provided by at least two pump manufacturers. If necessary, forward the candidate selections to the engineering departments of the pumps' manufacturers for independent evaluations and recommendations.

R. Establish the pump sequencing for the storm event pumps. The operation sequence should be changed after each storm event that incites operation of the design storm pumps. This will help to "balance the work load" between the pumps during the service life of the station. Table G4 provides some suggested sequencing schemes that can be implemented during the first five storm events. In the unlikely event that more than five events occur during the life of the pump station, the given schemes can be repeated.

Table G4. Suggested pump sequencing schemes (Smith, 2001)

n_p	Storm Event Number				
	1	*2*	*3*	*4*	*5*
2	1-2	2-1	1-2	2-1	1-2
3	1-2-3	3-1-2	2-3-1	1-2-3	3-1-2
4	1-2-3-4	4-1-2-3	3-4-1-2	2-3-4-1	1-2-3-4

The hydraulic design procedure outlined above is summarized in Figure G7.

IV.   Maintenance Considerations

Considering the short service life of the proposed pump station, certain features and design steps that are normally included in the design of a permanent pump station were either not considered or considered optional in these guidelines. First, it was recognized that a self-cleaning trash rake for the intake screen may not be economically justified. A pump station constructed without this feature may then require more frequent inspections and manual cleaning by field station staff. Second, it should be noted that a one-foot minimum interval separating the different storm water pump trigger stages was arbitrarily specified. As discussed, this requirement is to ensure that none of the pumps cycle on and off too frequently since water level sensors might be susceptible to wave actions that can erroneously trigger a pump cycle. Moreover, frequent cycling can occur if canal stage draw down occurs too rapidly. However, a detailed hydraulic analysis of the approach canal would be needed to identify the potential for this problem beforehand. In cases where this is not feasible, pump cycle times should be monitored after the facility installation is complete and trigger stages adjusted as needed to satisfy the manufacturer's requirements.

V.   Design Example

Design a temporary pump station that can pass a design discharge of 200 cfs that is associated with a design head water stage of 9 feet and a design tail water stage of 17 feet. Additionally, the seasonal average daily flow is 35 cfs. Upstream of the permanent structure, the targeted range for seasonal water control is 6 – 7 feet while it is 12 – 13 feet downstream of the structure. Each seasonal flow pump will discharge to a PVC pipe that is approximately 200 feet long, is installed along land surface and includes four 45^0 elbows. A similar configuration will be used for the discharge lines connected to the storm event pumps, except other pipe materials may be considered. The land surface elevation near the permanent structure is 19 feet. Assume that the pump inlet will be open as depicted in Figure G4.

Start

Determine SLHW, SHHW, SLTW, SHTW

Determine Q_{MDF}

Determine n_p, Q_p and on/off trigger stages

Compute TSH_i, $i = 1,4$

i : 2
1 = routine pump
2 = event pump

establish pump sequencing

End

Locate pump and design discharge line

Determine pump intake bell diameter

Design intake works

Construct system curves

Compute NPSHA, S_s

Select & evaluate candidate pumps

Consult manufacturers; final selection
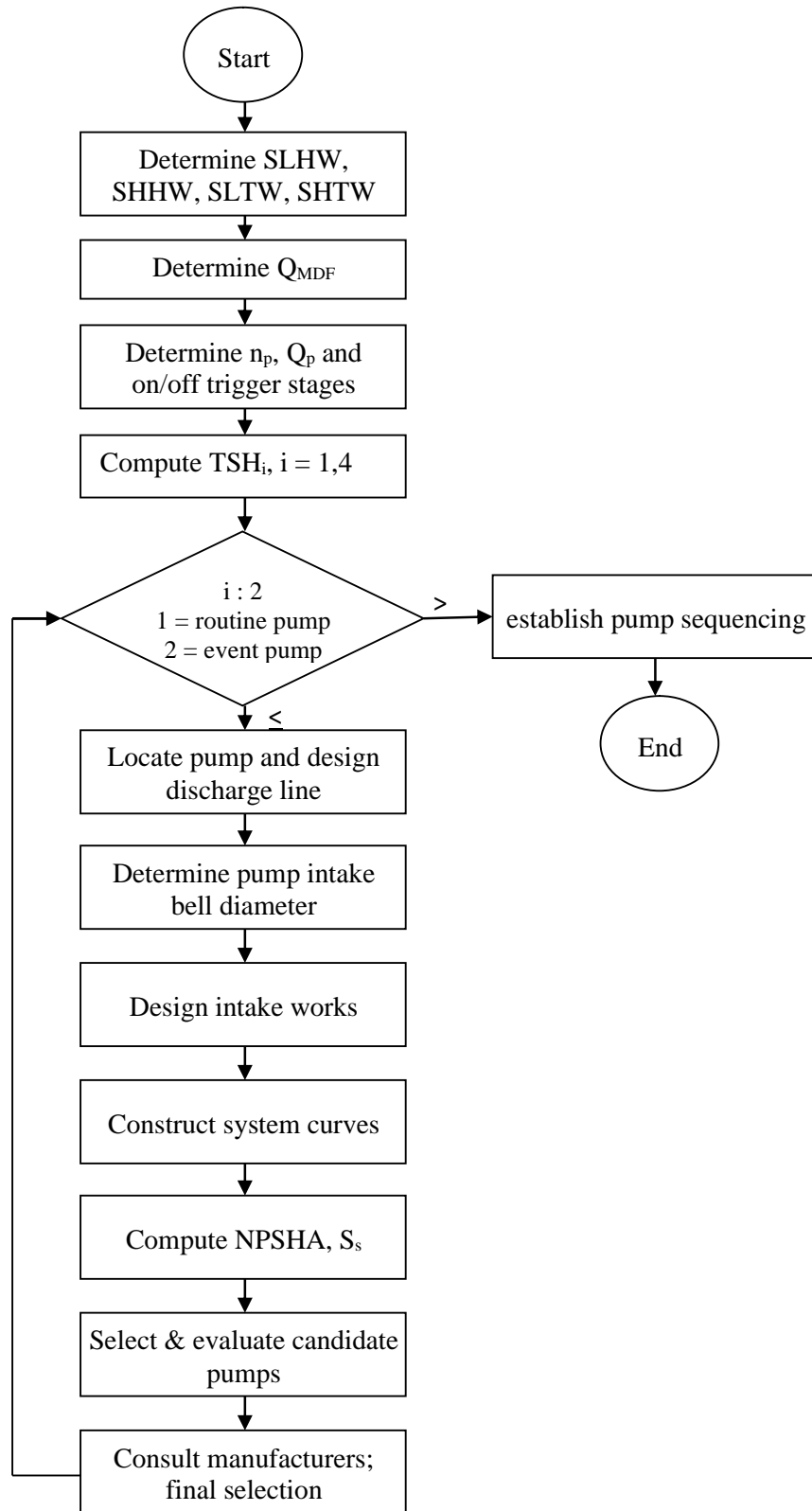
Figure G7. Summary of hydraulic design procedure for a pump station

Step A

According to the information given above, SLHW = 6 ft, SHHW = 7 ft, SLTW = 12 feet and SHTW = 13 feet.

Step B

The seasonal average daily flow was indicated to be 35 cfs. Two identical pumps, each with this capacity will be needed for routine flow operations, where the operation of each pump is alternated. The "on" elevation for each pump is 7 ft (SHHW) while its "off" elevation is 6 ft (SLHW).

Step C

During storm event operations, the design head water stage range is 7 – 9 feet. If the minimum operational range for each pump is 1 foot, then three identical pumps can be specified for this situation. The first in sequence will trigger on at 8 feet and will continue operating until the head water recedes to 7 feet. The second pump will commence operations when the head water stage reaches 9 feet and will turn off when the head water stage falls to 8 feet. The third will serve as a stand-by unit. All three pumps, however, should be included in an operating sequence (see step R).

Steps D and E

According to the results of steps A – C, $TSH_1 = 12 – 7 = 5$ ft; $TSH_2 = 13 – 6 = 7$ ft; $TSH_3 = 17\text{-}9 = 8$ ft; and $TSH_4 = 17 – 7 = 10$ ft.

Step F

As indicated, the crown of each discharge pipe at its downstream end should be set no higher than SLTW = 12 feet. If possible, each pipe should be sloped downward continuously between its upstream end (set at approximately 19 feet) and its outlet.

Step G

Based on a pipe manufacturer's data, a 36" PVC pipe with a working pressure of 125 psi has a nominal internal diameter of 35.80 inches. This translates to a cross sectional area of 6.99 ft^2. A flow rate of 35 cfs through this pipe yields a velocity of 5 ft/s. Since this velocity is satisfactory, the stated pipe size can be used.

The design flow rate for each of the storm water discharge pipes is 200/2 = 100 cfs. 48 inches is the largest nominal size of PVC pipe rated for pressurized flow, where the actual inner diameter is about 47.49 inches. For 100 cfs, this results in a velocity of about 8 ft/s. Since this value is less than the recommended maximum of 10 ft/s, it will be considered acceptable. The velocities computed here, however, reflect the design discharge rates. The actual flow rates may be

different, depending on the pump characteristics. These pipe flow velocities can be recomputed later, if necessary, once the actual discharge rates are known more precisely.

Step H

From Table G1, ε for PVC pipe has minimum, average and maximum values of 0.00006, 0.0012 and 0.024 inches, respectively.

Step I

From Table G2, the nominal value of K for a 45° elbow is 0.18. Given an inherent uncertainty of -20% to 30%, this K value can range from 0.14 to 0.23.

Step J

A discharge of 35 cfs and a target velocity of 5.5 ft/s imply that a pump bell diameter equal to 2.85 feet is required. A nominal bell size of 36" would then result in an intake velocity of about 5 ft/s which is acceptable and within the range of 3 – 8 ft/s given in Table G3. Similarly, the storm event pump discharge of 100 cfs will require a bell diameter of 58 inches to achieve a velocity of 5.5 ft/s.

Step K

For a pump bell diameter of 36 inches and a velocity of 5 ft/s, $F_B = 5.0/[(32.17)(3.0)]^{1/2} = 0.51$. The minimum required submergence of the pump bell is then $S = (3.0)[1.0 + (2.3)(0.51)] = 6.51 \approx 7$ feet. In order to avoid suspending bottom sediments, a bottom clearance of $(5)(3) = 15$ feet will be required. Given the bell submergence requirement of 7 feet, such a bottom clearance is not likely to be feasible. If stabilization measures are installed along the channel bottom near the pump intake, the bottom clearance can be reduced to about $0.5D = (0.5)(3.0) = 1.5$ feet. A bar screen should also be designed according to existing guidelines and installed around the pump intake.

Similarly, a pump bell diameter of 58 inches and a velocity of 5.5 ft/s implies that $F_B = 4.83/[(32.17)(5.5)]^{1/2} = 0.36$. The minimum required submergence of the pump bell is then $S = (4.83)[1.0 + (2.3)(0.36)] = 8.8 \approx 9$ feet. In order to avoid suspending bottom sediments, a bottom clearance of $(5)(4.83) = 24$ feet will be required. Such a bottom clearance seems highly infeasible. If stabilization measures are installed along the channel bottom near the pump intake, the bottom clearance can be reduced to about $0.5D = (0.5)(4.83) = 2.4$ feet. A bar screen should also be designed according to existing guidelines and installed around the pump intake.

Step L

N/A

Step M

The four system curves shown in Figure G8 were constructed for the piping and appurtenances associated with the daily flow pump. Each curve was constructed with the total static head and dynamic head losses indicated. In constructing the system curve that reflects startup conditions, the discharge line summit was assumed to be at an elevation equal to land surface plus one-half of the pipe diameter. The green curves depict the estimated range of conditions that each pump will experience under routine, seasonal flow conditions. The purple curve represents the TDH that each pump will have to move water against momentarily during startup.
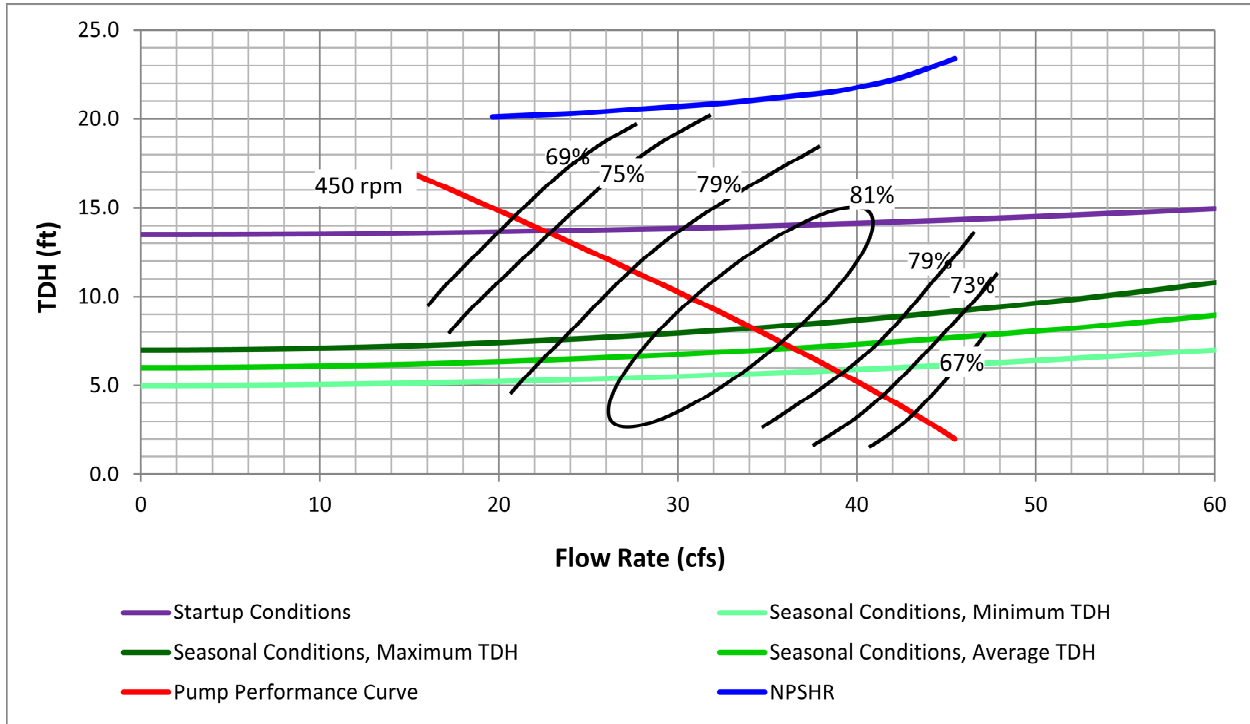

Figure G8. Pump and system performance curves for the routine flow pump

Also shown in Figure G8 are hypothetical curves that specify the TDH vs. Q relationship for the pump, the NPSHR vs. Q requirements and the pump efficiency curves. These will be discussed in step P.

Step N

The four system curves shown in Figure G9 were constructed for the piping and appurtenances associated with the storm water flow pump. Each curve was constructed with the total static head and dynamic head losses discussed previously. In constructing the system curve that reflects startup conditions, the discharge line summit was assumed to be at an elevation equal to land surface plus one-half of the nominal pipe diameter. The green curves depict the estimated range of conditions that each pump will experience under storm event conditions. The purple curve represents the TDH that each pump will have to move water against momentarily during startup.

Also shown in Figure G9 are hypothetical curves that specify the TDH vs. Q relationship for each pump, the NPSHR vs. Q requirements and the pump efficiency curves. These will be discussed in step Q.
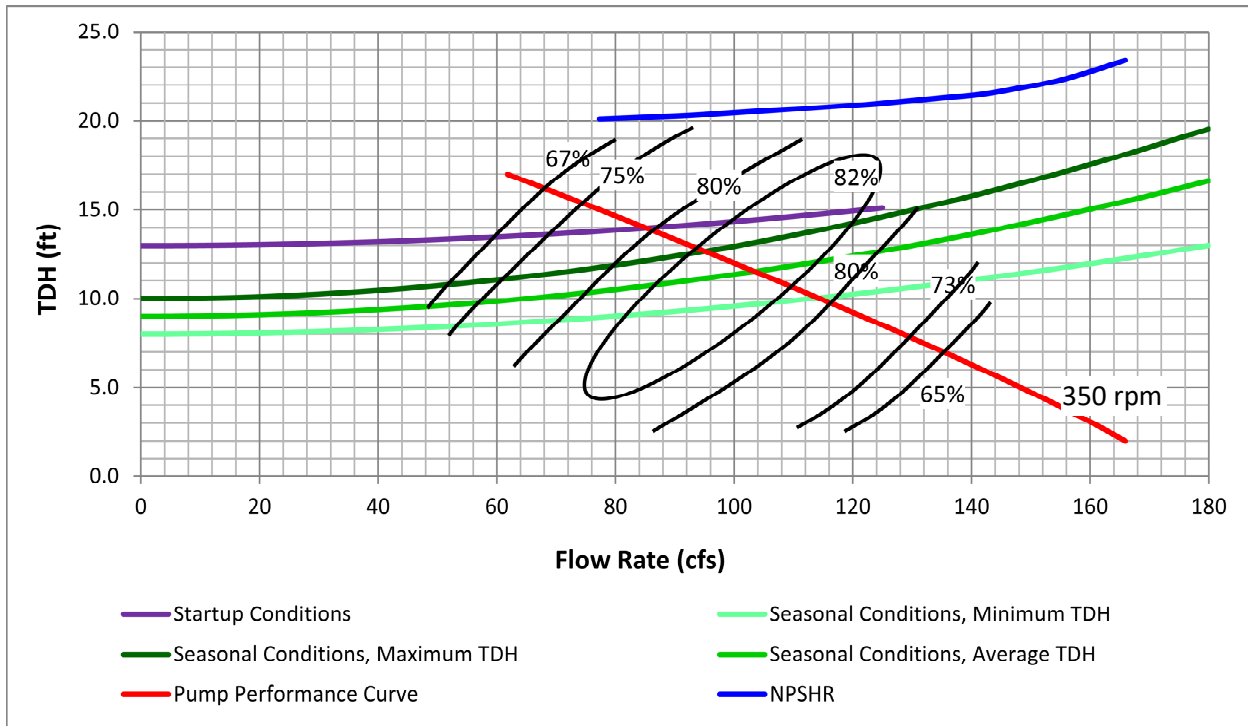
Figure G9. Pump and system performance curves for the storm water flow pumps

Step O

Given the required submergence depth of 7 feet and an estimated intake bell height of 1 foot, the minimum height of the water surface above the eye of the seasonal flow pump impeller is $h_s = 7 - 1 = 6$ feet. According to Equation G3, with $H_{bar} = 33.9$ feet and $H_{vap} = 1$ foot, NPSHA = 33.9 + 6 – 1 = 38.9 feet.

For the storm event pumps, the required submergence was calculated to be 9 feet. With an estimated bell height of 1 foot, the minimum height of the water surface above the eye of the pump impeller is $h_s = 9 - 1 = 8$ feet. According to Equation G3, with $H_{bar} = 33.9$ feet and $H_{vap} = 1$ foot, NPSHA = 33.9 + 8 – 1 = 40.9 feet.

Step P

Since the BEP of the pump performance curve was not specified either, it is assumed, for the purposes of this example, to be located near the middle of the highest efficiency contour. This corresponds approximately to Q = 33 cfs and TDH = 8.7 feet.

1. In this case, the POR was not specified, so it will be estimated from the BEP. The discharge at the lower limit of the POR is approximately $(0.8)(33) = 26.4 \approx 26$ cfs while the upper limit is estimated to be $(1.15)(33) = 40$ cfs. An examination of Figure G8 indicates that the intersections of the limiting system curves (light green and dark green curves) with the pump performance curve (red curve) yield a discharge range of about 34-39 cfs under the expected operating conditions. These values are within the estimated POR of 26 – 40 cfs, so the selected pump is, so far, acceptable.

2. According to Figure G8, the intersection of the average system performance curve (medium green) with the pump performance curve yields $Q = 36.5$ cfs at TDH = 7.2 feet. A 5% deviation around the BEP discharge of 33 cfs yields a range of 31.35 – 34.65 cfs. The operating point is therefore slightly outside of this range. However, since it is within the POR of 26 – 40 cfs, the pump should be acceptable.

3. The pump efficiency at its BEP is at least 81%, which should be acceptable for a temporary installation.

4. The maximum expected discharge rate of 39 cfs yields a velocity of $(39)(4)/\pi/(35.80/12)^2$ = 5.58 ft/s < 10 ft/s. This velocity is acceptable. Additionally, the velocity through the intake bell is $(39)(4)/9\pi = 5.5$ ft/s.

5. From Figure G8, it is evident that the startup system curve (purple) intersects the pump performance curve at $Q = 22.5$ cfs and TDH = 13.8 feet. While the AOR was not specified in Figure G6, for the purposes of this example it is assumed to be bounded by the minimum efficiency curves provided. Given this, the startup operating point appears to be acceptable and provide a small buffer between it and the limit of the AOR where the shut-off mechanism specified earlier would be incited.

6. From the results of step O, the NPSHA for the daily flow pump was estimated to be 38.9 feet. The discharge range that is within 15% of the BEP is about 28 – 38 cfs. Within these discharge limits, Figure G8 indicates that the NPSHR ranges from 20.5 feet to 21.5 feet. 35% of this upper NPSHR value is 7.5 feet. Since 7.5 > 5, the NPSHA should exceed the NPSHR by at least 7.5 feet within the discharge range of 28 – 38 cfs. Noting that 38.9 > 21.5 + 7.5 = 29 feet, the selected pump satisfies the first requirement. Beyond 15% of the BEP, the maximum NPSHR value within the assumed AOR specified previously is about 22.5 feet. 80% of this value is 18 feet. Hence, beyond 15% of the BEP, NPSHA should exceed NPSHR by at least 18 feet. Since 38.9 – 22.5 = 16.4 feet, this requirement is not met near the upper limit (with respect to discharge) of the AOR. This can be remedied by increasing the submergence depth of the pump intake by 1.6 feet. However, the NPSHR at the upper limit of the expected operating range (39 cfs) is 21.5 feet and 38.9 – 21.5 = 17.4 feet, which is fairly close to 18 feet. Hence, it may be acceptable to dispense with the extra submergence requirement.

7. From Equation G4, the suction specific speed is $S_s = (450)(33/0.1337*60)^{0.5}(8.7)^{0.75}$ = 10,810. Since $8,000 < 10,810 < 12,000$, the specific speed criterion is met.

Step Q

Establishing the BEP in the same manner as in step P results in a BEP located approximately at Q = 100cfs and TDH = 11.3 ft (Figure G9).

1. The intersection of the average system curve (medium green) with the pump performance curve (red) occurs at Q = 108 cfs and TDH = 11.6 ft. This discharge is greater than Q_p/n_p = 200/2 = 100 cfs.

2. The range of discharges that are within 5% of the BEP discharge is 95 – 105 cfs. Establishing the POR in the same manner as in step P1 yields a discharge range of 80 – 115 cfs. While the operating discharge of 108 cfs is 8% above the BEP flow rate of 100cfs, it is within the POR.

3. If the AOR limits are assumed to occur at the minimum specified efficiencies, it is evident from Figure G9 that the intersections of all three system performance curves (green) with the pump performance curve lie well within the AOR.

4. Based on the intersections of the three system performance curves with the pump performance curve, the maximum expected flow rate is about 114 cfs. This yields a discharge pipe velocity of $(114)(4)/\pi/(47.49/12)^2 = 9.3$ ft/s < 10 ft/s. In the intake bell, the velocity is $(114)(4)/\pi/(58/12)^2 = 6.21$ ft/s < 7 ft/s.

5. See sub-step 3 above.

6. From the results of step O, the NPSHA for the storm flow pump was estimated to be 40.9 feet. The discharge range that is within 15% of the BEP is 85 – 115 cfs. Within these discharge limits, Figure G9 indicates that the NPSHR ranges from about 20.2 feet to 20.8 feet. 35% of this upper NPSHR value is 7.3 feet. Since 7.3 > 5, the NPSHA should exceed the NPSHR by at least 7.3 feet within the discharge range of 85 – 115 cfs. Noting that 40.9 > 20.8 + 7.3 = 28.1 feet, the selected pump satisfies the first requirement. Beyond 15% of the BEP, the maximum NPSHR value within the assumed AOR specified previously is about 21.3 feet. 80% of this value is 17 feet. Hence, beyond 15% of the BEP, NPSHA should exceed NPSHR by at least 17 feet. Since 40.9 – 21.3 = 19.6 feet, this requirement is satisfied.

7. From Equation G3, the suction specific speed is $S_s = (350)(100/0.1337*60)^{0.5}(11.3)^{0.75} = 12{,}030$. Since this value is only slightly over the upper limit of 12,000, the pump should be satisfactory.

Step R

Since $n_p = 2$ for the seasonal flow pumps, the alternating sequence given in the first row of Table G4 can be used. However, pump operations will not be alternated with storm events since these

pumps will operate on a more frequent basis. In this case pumps can be alternated after each operation. For the storm event pumps, $n_P = 3$ so the alternating sequence given in the second row of Table G4 can apply. The required controls should be designed accordingly.

VI.   References

Hydraulic Institute. 1998. *American National Standard for Pump Intake Design.* ANSI/HI 9.8, The Hydraulic Institute, Parsippany, NJ.

Jones, G. M., R. L. Sanks, G. Tchobanoglous and B. E. Bosserman. 2006. *Pumping Station Design.* Butterworth-Heinemann, Burlington, MA.

Lobanoff, V. S. and R. R. Ross. 1985. *Centrifugal Pumps: Design and Application.* Gulf Publishing Company, Houston, TX.

Smith, P. N. 2001. Highway Stormwater Pump Station Design. Publication No. FHWA-NHI-01-007(HEC No. 24), USDOT, Federal Highway Administration, Washington, DC, 218 pp.

Wallingford, H. R. and D. I. H. Barr. 2006. *Tables for the Hydraulic Design of Pipes, Sewers and Channels: Volume I.* Thomas Telford Ltd, London, UK.

Appendix H. Hydraulic Design Procedures for Channel Stabilization

I.   Introduction

Structural measures for preventing scour and erosion downstream of a hydraulic structure are needed due to the high velocities and turbulence created by the structure discharge. In particular, such measures should be required for temporary structures as well since downstream scour resulting from a single storm event can compromise the integrity of a structure. The channel stabilization and erosion control techniques commonly used include riprap, gabion baskets and mattresses, articulating concrete blocks (ACB's) and geotextiles. Certain geotextiles can be used as stand-alone devices (e.g. turf reinforcement mats, erosion control blankets) while others serve primarily as filter or drainage sublayers for the aforementioned armored measures (e.g. woven geotextiles, geonets). Examples are shown in Figures H1 through H4.

Figure H1. Channel stabilization with riprap (from NRCS[1], 2007)

Figure H2. Bank stabilization with gabion baskets (from NRCS[3], 2007)

Figure H3. Turf reinforcement mat (from NRCS[2], 2007)

Figure H4. ACB with underlying geotextile (from NRCS[4], 2007)

General design criteria identified in the literature for riprap aprons located on a channel invert downstream of a water control structure will first be presented. In addition, design procedures that were developed for riprap aprons located downstream of specific types of structures will be discussed. Finally, in the sections that follow, general design guidance is given for the stabilization of embankment weirs as well as for the application of ACBs, gabions and geotextiles.

II. Riprap Apron Design Procedures

A. General Riprap Stone-Sizing Procedures for Channel Inverts

Numerous procedures for predicting the failure of riprap aprons and determining minimum stone sizes have been developed for open-channel flow conditions. These include Maynord et al. (1989), Brown and Clyde (1989), Stevens et al. (1976) and Anderson et al. (1970). Other design procedures were developed for sizing riprap within and near stilling basins (e.g. Johns et al., 1993, Peterka, 1958). It is expected, however, that a temporary water control structure will typically discharge to a horizontal apron comprised of riprap since this will usually be the most economical design. Unfortunately, riprap design criteria for flows immediately downstream of a structure are not as plentiful, and the procedures developed for uniform open-channel flow conditions generally are not applicable. In any case, the requirements given in Section 02370 of the District Engineering Standards should be considered and adhered to, where applicable.

According to Reese (1988) and Maynord (2012), the Isbash (1936) method can be applied to the highly turbulent conditions found within a horizontal channel directly downstream of a structure. The design equation for this method can be stated as

$$D_{50} = \frac{V^2}{2g(S_s-1)C^2}$$ (H1)

where

$C = 0.86$ for highly turbulent conditions
S_s = the specific gravity of the riprap stone
V = the average velocity in the channel downstream of the structure
D_{50} = the median stone size of the riprap

The use of an average velocity for V is conservative. Equation H1 can be used to determine D_{50}, which can be specified along with other gradation requirements for the riprap (these will be discussed in a later section).

According to Reese (1988), the Froude Number method is also applicable to sizing riprap under flow conditions characterized by high or uncertain turbulence. This method can be stated as

$$D_{50} = \left[\frac{1.65}{g(S_s-1)}\right]^{3/2} \frac{K_F}{\sqrt{d_h}} V^3$$ (H2)

where

$K_F = 1.0$ for the hydraulic conditions immediately downstream of a structure
d_h = the hydraulic depth downstream of the structure

and the other terms are as previously defined. The empirical nature of these two methods is evident in the fact that they each rely on an empirical constant that adapts them to the hydraulic conditions of interest. Each of the two equations above can be applied under either submerged or unsubmerged structure discharge conditions.

In practice, it is recommended that D_{50} be computed with both Equations H1 and H2 and the higher of the two values used in the design. Furthermore, a factor of safety should be applied to the computed value of D_{50}. In general, this factor of safety will range from 1.1 to 1.5 (NRCS[1], 2007).

Unless the riprap used is of a uniform size, certain gradation requirements should be adhered to. In general, graded riprap performs better and is more economical. Gradation requirements for the riprap along with procedures for determining the length and thickness of the apron will be discussed in a later section.

B. Riprap Stone-Sizing Procedure for a Channel Invert Downstream of a Sharp-Crested Weir or Culvert

Figure H5 depicts a riprap apron sited on a channel floor situated downstream of a sharp-crested weir or culvert outlet with an unsubmerged discharge to a tail water. Under these conditions, Shafai-Bajestan and Albertson (1993) found through hydraulic model experiments that the
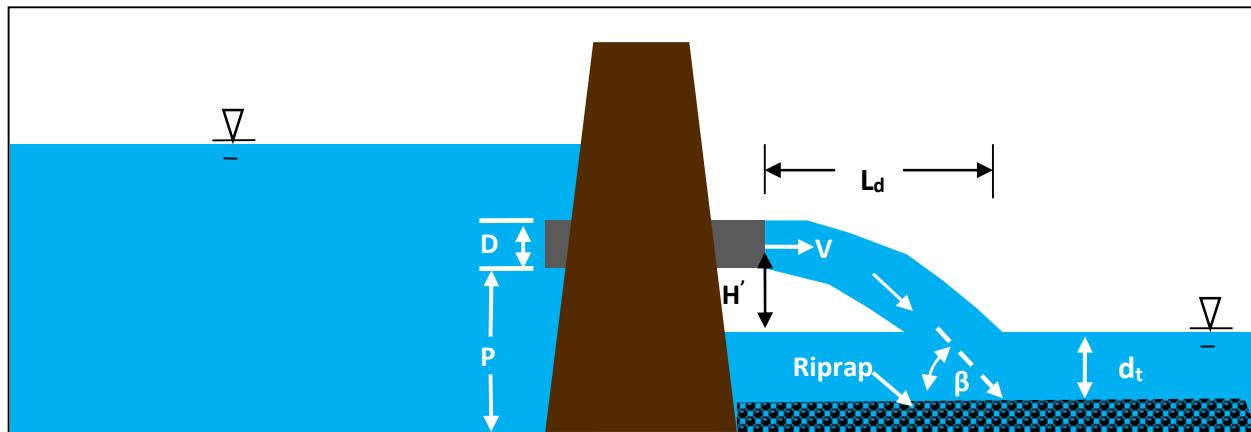

Figure H5. Culvert structure with unsubmerged discharge to tail water

required riprap size for the downstream apron is best expressed in terms of the stone diameter that equals or exceeds 90% of the stone diameters in the riprap. Conventionally, this is denoted as D_{90} and was found to satisfy the relation

$$\frac{V}{\sqrt{g(S_s-1)D_{90}}} = 0.422\left(\frac{d_1}{D}\right) \tag{H3}$$

where

V = the discharge velocity at the pipe outlet or weir crest
S_s = the specific gravity of the riprap stone
D = the culvert diameter or the flow depth on the weir crest
d_1 = the submerged plunge distance traveled by the discharge jet = $d_t / \sin(\beta)$
d_t = the tail water depth
β = the angle at which the discharge jet hits the water surface = $\arccos[V/(2gH' + V^2)^{1/2}]$
H' = the distance from the tail water to either the pipe centerline or half the weir flow depth

The distance from the pipe outlet where the jet strikes the water surface can be conservatively estimated as $V(2H'/g)^{1/2}$ if air resistance is neglected. This implies that the distance L_d from the culvert outlet to the location where the centerline of the submerged jet strikes the riprap is approximately

$$L_d = d_1 + V\sqrt{\frac{2H'}{g}} \tag{H4}$$

As in the previous section, Equations H3 and H4 only apply to the riprap apron on the channel bottom. A factor of safety is normally applied to the computed value of D_{90}.

C. Determining the Riprap Stone Size on Channel Side Slopes

Procedures used to determine riprap sizes for channel bottom aprons cannot be directly used to size the riprap that is to be installed on the adjacent side slopes. In addition to the gravitational force that tends to incite stone movement, riprap placed on side slopes is subjected to different shear stresses. According to Maynord (1988), Carter et al. (1953) defined a tractive force ratio K_s as the ratio between the force on a side slope that will cause incipient stone movement to the corresponding force on a level surface. They showed that it is given by

$$K_s = \sqrt{1 - \frac{\sin^2\theta}{\sin^2\varphi}} \tag{H5}$$

where θ is the side slope angle and φ is the angle of repose for the riprap. Reese (1988) indicates that the factor K_s can be applied to the Froude Number method discussed previously in order to compute the required riprap size for the adjacent channel side slopes. In this case, the velocity V in Equation H2 should be replaced by an effective velocity V_{eff} defined as

$$V_{eff} = \frac{V}{\sqrt{K_s}} \tag{H6}$$

If Equation H2 was not used to compute the stone size for the channel bottom, then V_{eff} should be substituted for V in the equation that was used.

D. Estimating the Required Riprap Apron Length

A somewhat generalized technique for estimating the required apron length can be obtained from USACE HDC 722-4 (1973). The criteria given by this hydraulic design chart were developed by the USACE Waterways Experiment Station and are based on a laboratory study of the development of scour holes in cohesionless material located downstream of culvert outlets. The culverts tested were apparently installed horizontally along the channel invert. It was found that the length, width, depth and volume of the scour hole formed was related to the pipe diameter D (feet), the pipe discharge Q (cfs), the flow duration t (minutes) and the tail water depth Tw (feet). The relationship is given by

$$L_{sm} = C \left(\frac{Q}{D^{5/2}}\right)^{0.71} t^{1/8} \tag{H7}$$

where L_{sm} is the length of the scour hole and C = 2.4 for Tw $\leq$ 0.5D while C = 4.10 for Tw > 0.5D. The scour hole length estimated with Equation H7 could be used as an indicator of the required apron length if an appropriate value of t were used. An inspection of this equation indicates that $\partial L_{sm}/\partial t \sim t^{-7/8}$. The value of $t^{-7/8}$ at t = 2880 minutes is less than 0.1% of its value at 1 minute. If the initial scour rate is taken to be $\partial L_{sm}/\partial t$ at 1 minute, the scour rate then drops to less than 0.1% of its initial value at t = 2880 minutes. Hence, it is reasonable to assume that any increase in L_{sm} beyond t = 2880 minutes can be neglected. So, for design purposes, t = 2880 can be used in Equation H7 when estimating the apron length. An appropriate factor of safety should be applied to L_{sm}.

While it was stated previously that Equation H7 is based on laboratory experiments with horizontal culverts installed on a channel invert, it can still be used to estimate the required riprap apron length for the type of structure depicted in Figure H5. However, the resultant value of L_{sm} would intuitively be conservative since the flow striking the riprap is only partially horizontal. Thus, the apron length would in this case likely be overestimated. This could be offset with a reduced factor of safety.

Another thing to note when applying Equation H7 to the design depicted in Figure H5 is that L_{sm} would only represent the apron length from the point where the plunging jet strikes the riprap to the downstream end of the apron. The total apron length, starting from the structure to the downstream end of the apron, should be set to the sum of equations H4 and H7.

E. Determining the Required Riprap Apron Thickness

Thickness requirements for a riprap apron are discussed in Brown and Clyde (1989) and in USACE (1991). These studies indicate that with significant gradation, isolated pieces of large rock within the apron could protrude into the flow field unless the apron is sufficiently thick. This could result in the removal of smaller stones as the flow is accelerated around larger stones. The following criteria based on both references are proposed for these guidelines:

1. The apron thickness shall be equal to $1.5D_{100}$ or $2.25D_{50}$, whichever quantity is greater.

2. For practical purposes, the apron thickness shall not be less than 1 foot.

3. If the riprap is placed underwater, the layer thickness shall be increased by 50%.

Both of the references cited above specify a minimum apron thickness of D_{100} or $1.5D_{50}$, whichever quantity is greater. However, USACE (1991) indicates that a minimum thickness of $1.5D_{100}$ should be used in highly turbulent areas such as areas around stilling basins. This generally includes areas immediately downstream of water control structures. Therefore, a 50% increase in the standard minimum thickness is proposed in criterion 1. D_{100} can be determined when the gradation curves are constructed.

F. Comprehensive Design Procedure for a Riprap Apron Downstream of a Culvert

If the culvert barrel shown in Figure H5 was installed along the channel invert ($H' = -d_t$), the sizing criteria given by Equation H3 would not apply. A complete design procedure, however, for a riprap apron located downstream of a horizontal culvert installed along a channel invert was developed by the U.S. Army Corps of Engineers Waterways Experiment Station. An established riprap size criterion pertaining specifically to this situation is given in the USACE HDC 722-7 (1973). This requirement can be stated as

$$\frac{D_{50}}{D} = C \frac{D}{Tw} \left(\frac{Q}{D^{5/2}}\right)^{4/3} \tag{H8}$$

where

D_{50} = the median stone diameter
$C = 0.02$ for a horizontal apron
$Q =$ the discharge rate
$Tw =$ the tail water depth above the barrel invert
$D =$ the barrel diameter or width

Additionally, USACE HDC 722-5 (1973) provides accompanying criteria for determining the required length, thickness and width of the riprap apron. The length is given by

$$\frac{L_{sp}}{D} = 1.7\left(\frac{Q}{D^{5/2}}\right) + 8 \tag{H9}$$

where L_{sp} is the apron length. Equation H9 is largely empirical and should only be applied to the design conditions stated in this section. While the required apron thickness is specified by USACE HDC 722-5 (1973) as $2D_{50}$, the requirements discussed in the previous section are more recent and should be used. The apron width at the culvert outlet is 3D while it increases 1 foot for each foot of apron length. Hence, at a distance L_{sp} from the culvert outlet, the apron width will be $L_{sp} + 3D$. Both L_{sp} and D_{50} should be multiplied by an appropriate factor of safety.

G. Riprap Gradation

The stone gradation within a riprap apron can affect its resistance to erosion. In an apron comprised of well-graded riprap, the voids between the larger stones are generally filled with smaller stones, resulting in a more stable matrix. Thus, stone sizes from the minimum to the maximum should, in general, be well distributed. The distribution of stone size is specified in the form of a *gradation curve,* which is a plot of the stone diameter versus the percentage of stones whose diameter is less than or equal to that diameter. For example, the D_{50} value mentioned previously would be the diameter read from the gradation curve where 50% of the stone diameters are smaller than or equal to D_{50}. Moreover, *s*pecifications for stone gradation are usually comprised of two limiting gradation curves (i.e. a minimum and a maximum) in order to (i) provide more flexibility to the quarries in meeting specifications, and (ii) allow for reasonable changes in gradation that can occur due to breakage during transport and placement. The former is intended to help avoid the production costs that can be incurred in producing an order of stone that is of a stringent or specialized gradation. Example gradation curves are provided by Brown and Clyde (1989), and USACE (1991).

Gradation recommendations for riprap are provided by NRCS[3] (2007), Brown and Clyde (1989), Kilgore and Cotton (2005), AASHTO, and USACE (1991). The USACE recommendations are summarized as follows:

1. The upper limit of the D_{50} stone should not exceed five times its lower limit.

2. The lower limit of the D_{100} stone should be at least two times the lower limit of the D_{50} stone.

3. The upper limit of the D_{100} stone should not exceed five times the lower limit of the D_{50} stone.

4. The lower limit of the D_{15} stone should be at least one-sixteenth of the upper limit of the D_{100} stone.

5. The bulk volume of stone that is smaller than the D_{15} stone should not exceed the volume of voids that would exist within the apron if these smaller stones were not present.

6. Any gradation limit within the D_0 to D_{25} range can be used in place of D_{15} in the above specifications if it leads to better utilization of available stone sizes.

Table H1 contains the limiting gradation curves recommended by Brown and Clyde (1989).

Table H1. Gradation limits suggested by Brown and Clyde (1989)

Stone Size Range (ft.)	Stone Weight Range (lb)	Percent of Gradation Smaller
$1.5D_{50}$ to $1.7D_{50}$	$3.0W_{50}$ to $5.0W_{50}$	100
$1.2D_{50}$ to $1.4D_{50}$	$2.0W_{50}$ to $2.75W_{50}$	85
$1.0D_{50}$ to $1.15D_{50}$	$1.0W_{50}$ to $1.5W_{50}$	50
$0.4D_{50}$ to $0.6D_{50}$	$0.1W_{50}$ to $0.2W_{50}$	15

    H. Riprap Placement

While the purpose of these guidelines is limited to hydraulic design as opposed to construction practices, it should be emphasized that improper placement of the stone can result in segregation and breakage of the stones to the extent that its gradation is different than what was originally specified. This can compromise the design. Additionally, any oversized stones discovered during installation should be removed. These stones can lead to eventual failure of the apron since their presence can compromise supporting interactions between individual stones. This creates large voids that expose the underlying filter and bedding while also creating turbulence than can remove smaller stones. Practical guidelines for the placement of riprap stone are provided by NRCS[3] (2007) and USACE (1991).

    I. Riprap Filtration and Drainage

A riprap apron installed on a channel bottom or side slope must be underlain by a properly designed granular filter or geosynthetic material. This is essential for four primary reasons that are explained in detail by USDA-SCS (1991) and Holtz et al. (1998). First, the granular bed or geosynthetic must provide horizontal drainage beneath the riprap in order circumvent the development of pressures and exit velocities that can dislodge soil though the riprap. Koloseus (1985) provides an excellent discussion of this process. Second, this supporting layer is needed to prevent erosion of the underlying soil that can occur under normal seepage rates. Third, it helps to better distribute the loading imposed by the riprap on the underlying soil. Fourth, it prevents the mixing of the riprap with the underlying soil.

The use of a geosynthetic filter or geotextile is advantageous over a conventional gravel filter since it can be removed much more easily after the service life of the structure has ended. Moreover, it may be possible to refurbish and restore it for future use. According to NRCS[2] (2007), both nonwoven and woven geotextiles can be used for this function, except that a heat-bonded or resin-bonded nonwoven geotextile should not be used for this function due to its low permeability. USDA-SCS (1991) provides the properties required for geotextiles that will be used for riprap filtration and drainage. These requirements are too extensive to be reiterated here and the engineer should consult this reference when designing a filtration layer for a riprap apron. Additionally, the following guidelines and standards should be considered:

    1. AASHTO M-288 (Geotextile Specifications for Highway Applications)

    2. FHWA HI-95-038 (Geosynthetic Design and Construction Guidelines; Holtz et al., 1998)

Figure H6 summarizes the procedure for designing a riprap apron.

III. Gabion Mattress Design Procedures

The use of gabion mattresses for stabilizing a channel perimeter downstream of a water control structure may sometimes be the best alternative. A gabion mattress is comprised of stones contained within a wire mesh whose geometry resembles a mattress and is typically 5 – 12 inches high. The rock size requirements for a gabion mattress are less stringent than those of riprap since the wire mesh helps to keep the rock matrix intact. Such a feature could prove even more advantageous for channel side slopes where stones are subject to both gravitational and hydrodynamic forces. The NRCS[3] (2007) provides examples of situations where gabion mattresses are effective in stabilizing a channel cross section. Furthermore, gabion mattresses may be economically advantageous for a temporary water control structure project since they can potentially be recovered after the service period of the structure and either resold or stored for future use.

Design guidelines and procedures for gabion mattresses have been developed by Maynord (1995), Di Stefano and Ferro(1998), Freeman and Fischenich (2000), NRCS[3] (2007), Kilgore and Cotton (2005), Simons et al. (1984), and Clopper and Chen (1988). Unfortunately, these procedures and guidelines were developed for open-channel flow conditions or, in the case of Clopper and Chen (1988), embankment overtopping. No design guidance was found in the literature for using gabion mattresses to stabilize a channel under the highly turbulent conditions found immediately downstream of a structure. For the interim, the engineering departments of the various gabion mattress manufacturers should be contacted for technical assistance in specifying the gabion design features needed for a specific application. Useful information may also be found in ASTM 6711, ASTM D7014 and Section 02272 of the Technical Specifications contained within the District Engineering Standards. As experience is gained in this manner, guidelines can eventually be developed for designing the stable gabion mattress systems needed for channel stabilization downstream of District structures.

IV. Design Procedures for Turf Reinforcement Mats

Turf reinforcement mats (TRMs) fall within a family of stabilization measures known as rolled erosion control products (RECPs). They are composed of interwoven layers of geosynthetic materials such as polypropylene, nylon and polyvinyl chloride netting. These are stitched together to form a three-dimensional matrix that allows for soil filling and retention while providing scour protection for the underlying soil. Additional details on their construction are given by EPA (1999), Kilgore and Cotton (2005), and various manufacturers.

TRMs can be a viable alternative to stabilizing a canal perimeter where armored measures (riprap, gabions, etc.) are not feasible. They can be stapled to canal banks in a manner that will ensure both their stability and protection of the canal bank under harsh hydraulic conditions. TRMs can be a viable alternative to stabilizing a canal perimeter where armored measures (riprap, gabions, etc.) are not feasible. They can be stapled to canal banks in a manner that will ensure both their stability and protection of the canal bank under harsh hydraulic conditions.

```
                          ┌───────┐
                          │ Start │
                          └───────┘
                              │
                              ▼
                    ◇ Sharp-crested        yes    ┌─────────────────────────────┐
                      weir or culvert   ─────────▶ │ Compute D₉₀ with Eq. H3      │
                      discharging to            │ │                             │
                      a tail water? ◇           │ │ Compute apron length with   │
                              │                    │ Eqs. H4 & H7                │
                           no │                    └─────────────────────────────┘
                              ▼
                    ◇ Culvert              yes    ┌─────────────────────────────┐
                      installed on a   ─────────▶ │ Compute apron D₅₀ with Eq. H8│
                      channel                     │ Compute apron length with   │
                      invert? ◇                   │ Eq. H9                      │
                              │                    │ Compute width as indicated  │
                           no │                    └─────────────────────────────┘
```

Sharp-crested weir or culvert discharging to a tail water?

— **yes** → Compute D_{90} with Eq. H3

Compute apron length with Eqs. H4 & H7

— **no**

Culvert installed on a channel invert?

— **yes** → Compute apron D_{50} with Eq. H8

Compute apron length with Eq. H9

Compute width as indicated

— **no**

Compute D_{50} with maximum result of Eqs. H1 and H2

Compute apron length with Eq. H7

Compute stone size for side slopes with Eqs. H5, H6 and the equation used to determine stone size for the bottom.

Assign factor of safety (FS)
$1.1 \leq FS \leq 1.5$
Apply to stone size, apron length

Specify gradation

Determine apron thickness

Design underlying filter and drainage layer

End
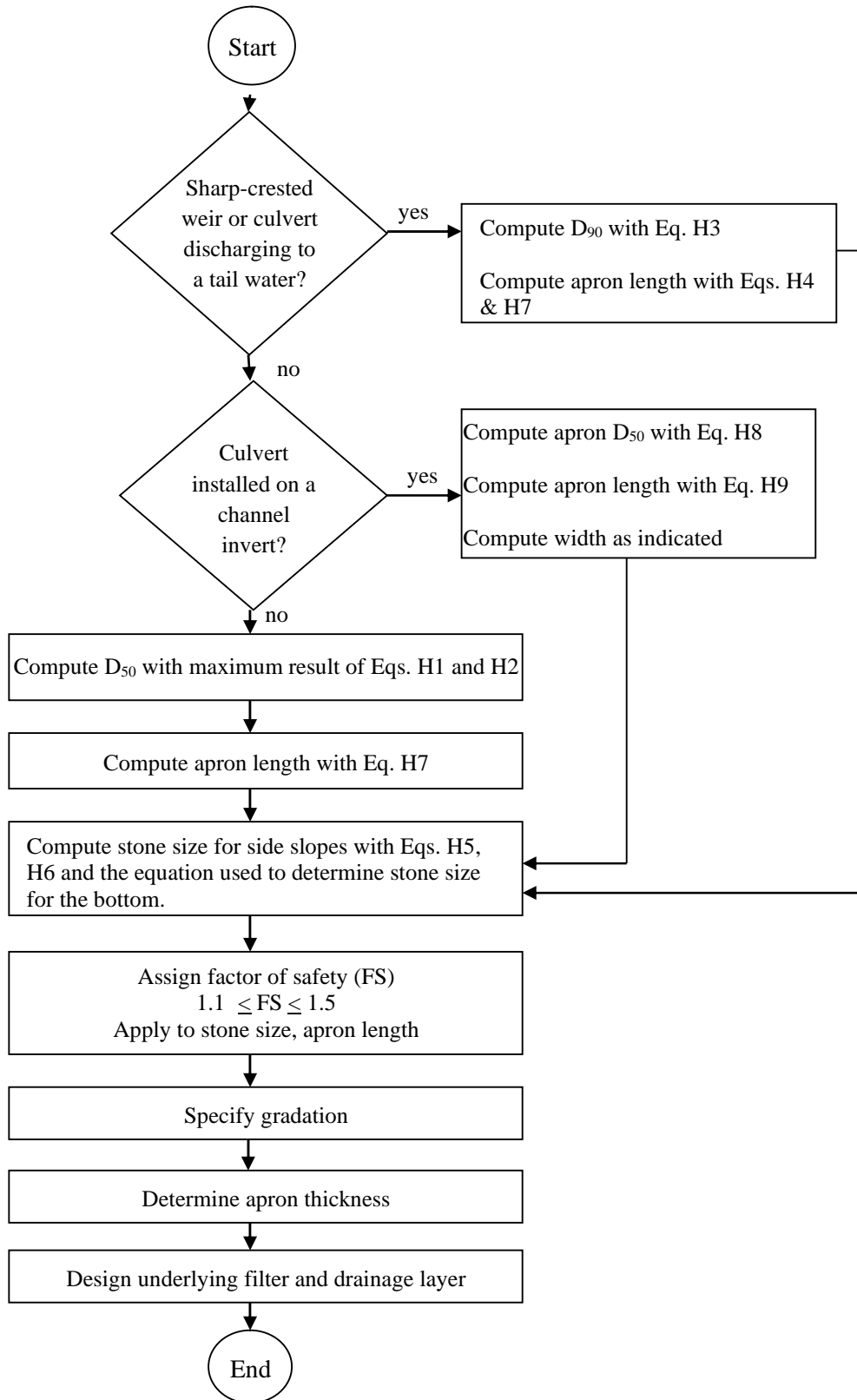
Figure H6. Hydraulic design procedure for riprap

Additionally, since they are constructed of non-degradable materials, it may be possible to remove them after the service period of the structure and store them for future use. The hydraulic conditions that a given TRM can be subjected to will vary with its construction features and manufacturer. According to EPA (1999), they generally cannot be used to stabilize a channel floor just downstream of a water control structure – armoring measures are generally most suitable for this.

Hydraulic design guidelines for TRMs are provided by Kilgore and Cotton (2005) for uniform open-channel flow conditions. There do not appear to be any general guidelines for designing or specifying a TRM that is needed to stabilize channel side slopes immediately downstream of a structure. For each application, it is best to consult the engineering staff of the various manufacturers in order to develop TRM designs, specifications and installation procedures.

Kilgore and Cotton (2005) indicate that there are no universally accepted testing protocol for assessing the quality of a TRM. Nonetheless, they provide a checklist based on ASTM D 6460 that can be used as a minimum standard for evaluating the testing procedures of TRM manufacturers. However, any requirements for vegetated linings used with TRMs should not be applicable here given the relatively short service life of a temporary structure. Kilgore and Cotton (2005) also indicate that the hydraulic properties or performance of a TRM cannot be inferred from any standard tests for TRM strength or reliability, nor can such tests be used to design a TRM-based channel lining. Rather, hydraulic properties should be determined through full-scale model tests. Since this will usually not be feasible or justifiable for a temporary structure, recommendations from the manufacturer's engineering staff should be followed. In any case, the design should consider the construction practices specified in Section 02278 of the Technical Specifications contained within the District Engineering Standards.

V. Design Procedures for Articulating Concrete Block Systems

Articulating concrete block systems (ACBs) can be a desirable alternative for channel stabilization downstream of a water control structure. They have been used throughout the country for bank stabilization and river training purposes as an alternative to traditional armoring techniques. An ACB system is comprised of a matrix of interconnected concrete blocks with specified hydraulic characteristics (Figure H4). They are usually underlain by geotextiles that serve as a filter layer. In some cases, the individual concrete blocks are interconnected by cables. Distinct advantages of ACB systems include their relative ease of installation and the fact that they can be readily removed and stored for future use after the service period of the structure has ended.

Manuals for the testing and design of ACB systems are provided by NRCS[4] (2007) and the Harris County Flood Control District (HCFCD, 2001). Additional design guidance can be found in Clopper (1991) while Melville et al. (2006) give additional insight into the failure mechanisms of cable-tied systems. The two design manuals can be obtained from

http://policy.nrcs.usda.gov/OpenNonWebContent.aspx?content=17822.wba

http://www.hcfcd.org/downloads/techinfo/ACB_designmanual.pdf

Both of these manuals contain comprehensive background information on the hydraulic properties of ACB systems and their failure mechanisms. Step-by step design instructions are provided along with a process to determine an appropriate factor of safety on a project-by-project basis. The reliance of the design procedure on a user-specified factor of safety to account for local hydraulic conditions makes it somewhat subjective. Since the shear stresses that the blocks will be subject to just downstream of a structure are highly uncertain, a large factor of safety is recommended. Additionally, the design requirements and construction practices specified in Section 02277 of the Technical Specifications contained within the District Engineering Standards should be adhered to, where appropriate.

VI.   Stabilization of Embankment Weirs

The downstream slope of a trapezoidal embankment normally experiences much higher velocities than those found in the channel downstream of the structure. Techniques for stabilizing and protecting the surface were evaluated through hydraulic models by Abt and Johnson (1991), Hartung and Scheuerlein (1970), Knauss (1979) and Olivier (1967). These studies addressed only the incipient movement and failure of riprap; other protective measured were not evaluated. Furthermore, only Hartung and Scheuerlein (1970) and Olivier (1967) evaluated slopes close to the 50% slope that characterizes the standard embankment weir design. Unfortunately, the results of Hartung and Scheuerlein (1970) cannot be conveniently used for design purposes since the mean flow depth along the downstream slope would have to be determined beforehand. Olivier (1967), however, found that the unit discharge q_{ot} at incipient stone movement can be expressed as

$$q_{ot} = 0.423 D_{50}^{3/2} [(\gamma_s - \gamma_w)/ \gamma_w]^{5/3} S_o^{-7/6} \qquad \text{(H10)}$$

where γ_s and γ_w are the unit weights of stone and water, respectively, and S_o is the embankment slope. q_{ot} can be determined from the embankment length and its design discharge while the remaining variables other than D_{50} are known. Equation H10 can therefore be used to determine the required D_{50} of the proposed riprap. An appropriate factor of safety would then be applied to this result.

Another alternative for sizing rip rap along the downstream face of an embankment would be to apply Equations H1 and H2 with the mean flow velocities determined using the techniques presented in Appendix F. The D_{50} values obtained in this manner could be compared to the value obtained with Equation H10. The most conservative of these results with an acceptable factor of safety should then be used for design.

An American Society of Civil Engineers (ASCE) task committee report by Powledge et al. (1989) summarized a number of case studies involving a variety of embankment protection methods. In addition to riprap, these included vegetation, geotextiles, cements, concrete blocks, gabions and roller-compacted concrete. Of these, only vegetation, geotextiles, concrete blocks, gabions and riprap would likely be economically feasible for a temporary weir. Vegetative measures, in particular, would require months to become established. Moreover, regular

inspections and maintenance would be required to ensure that the vegetative cover remained intact. Hence, this stabilization technique will seldom be practical. This implies that geotextiles, concrete blocks, gabions are the most promising alternatives. Furthermore, although a design procedure for riprap was presented above, this stabilization procedure should be used on embankments with discretion due to the unfavorable case studies cited by Powledge et al. (1989).

While Powledge et al. (1989) discuss a number of successful applications where the downstream slopes of earth embankments were successfully protected by concrete blocks, gabions and geotextiles, they do not provide any design guidance or procedures for these measures. It is probably best that design guidance be sought from the manufacturers of these products and their installation procedures followed.

VII.   Design Examples

A. Design Example 1

Determine the median stone size and blanket thickness required for the riprap needed to stabilize a channel located immediately downstream of a spillway where the flow velocity is 8 ft/s and the flow depth is 10 feet. The channel side slopes are 2:1 and its bottom width is 30 feet. Assume that the specific gravity of the stones is 2.65 and the riprap will have an angle of repose equal to 30^0.

Following the procedure outlined in Figure H6, the D_{50} stone size is computed with equations H1 and H2. From Equation H1, $D_{50} = 8^2/[2g(2.65-1)(0.86)^2] = 0.82$ ft $= 9.8$" ≈ 10".

The top width of the wetted perimeter is $30 + (2)(2)(10) = 70$ feet and the wetted area is $[30 + (2)(10)](10) = 500$ ft^2. The hydraulic depth is then $(8)(500)/(70) = 57.14$ ft. From Equation H2, $D_{50} = [1.65/g/(2.65-1)]^{3/2}/(57.14)^{1/2} (8)^3 = 0.37$' $= 4.5$". The greater result of $D_{50} = 10$" will be used. Applying a factor of safety equal to 1.2 yields $D_{50} = (1.2)(10) = 12$" $= 1$ ft. This applies to the channel bottom.

From Equation H5, $K_s = \{1-\sin^2[\arctan(0.5)]/\sin^2(30^0)\}^{1/2} = 0.45$. According to Equation H6, $V_{eff} = 8/(0.45)^{1/2} = 12$ ft/s. Substituting this velocity into Equation H1 yields $D_{50} = 144/[2g(1.65)(0.86)^2] = 1.83$' $= 22$" for the side slopes. Applying the same factor of safety results in $D_{50} = (1.2)(22) = 26.4 \approx 26$".

According to Section IIE, the blanket thickness on the bottom should be at least $(2.25)(1)(1.5) = 3.38 \approx 3.5$ feet while the side slopes should have a blanket thickness of at least $(2.25)(26/12)(1.5) = 7.3 \approx 7.5$ feet. These values should be compared to 1.5 times their respective D_{100} values once they are determined.

B. Design Example 2

Refer to the design example given in Appendix A. Design the riprap apron needed to stabilize the channel floor downstream from the structure comprised of 7 barrels, each 4 feet in diameter.

In this case, D = 4 feet and Q = 500/7 = 71.43 cfs. From the example description given in Appendix A, Tw = 9 – 0 = 9 feet. From Equation H8, $D_{50} = (4)(0.02)(4/9)(71.43/4^{5/2})^{4/3} = 0.1$ ft. With a factor of safety equal to 1.2, $D_{50} = 0.12$ ft = 1.44" ≈ 1.5".

The apron length given by Equation H9 is $L_{sp} = (4)[(1.7)(71.43/4^{5/2}) + 8] = 47.18 ≈ 47$ ft. With the factor of safety, $L_{sp} = (1.2)(47) = 56.4 ≈ 56$ ft. According to Section IIE, the required apron thickness is at least (2.25)(1.5)(1.5) = 5". This value should be compared to $1.5D_{100}$ after D_{100} has been determined through development of the gradation curves.

The apron width need not be determined in the manner discussed earlier since, for this design, the entire channel floor downstream of the structure will be blanketed with riprap. In this case, no riprap is proposed for the channel side slopes.

VIII.   References

Abt, S. R. and T. L. Johnson. 1991. Riprap Design for Overtopping Flow. *Journal of Hydraulic Engineering*, ASCE, 117(8), 519-522.

Anderson, A. G., A. S. Paintal and J. T. Davenport. 1970. Tentative Design Procedure for Riprap-Lined Channels. National Cooperative Highway Research Program Report 108, University of Minnesota, Minneapolis, MN.

Brown, S. A. and E. S. Clyde. 1989. Design of Riprap Revetment. Hydraulic Engineering Circular No. 11, FHWA Report No. FHWA-IP-016, McLean, VA.

Carter, A. C., E. J. Carlson and E. W. Lane. 1953. Critical Tractive Forces on Channel Side Slopes in Coarse, Non-Cohesive Material. Hydraulic Laboratory Report No. HYD-366, U. S. Bureau of Reclamation, Denver, Co.

Clopper, P. E. 1991. Protecting Embankment Dams with Concrete Block Systems. *Hydro Review*, X(2), April.

Clopper, P. E. and Y. H. Chen. 1988. Minimizing Embankment Damage During Overtopping Flow. Pub. No. FHWA-RD-88-181, U.S. Department of Transportation, Federal Highway Administration, Washington, D.C.

Di Stefano, C. and V. Ferro. 1998. Calculating Average Filling Rock Diameter for Gabion-Mattress Channel Design. *Journal of Hydraulic Engineering*, ASCE, 124(9), 975-978.

EPA. 1999. Storm Water Technology Fact Sheet: Turf Reinforcement Mats. Report No. EPA 832-F-99-002, U.S. Environmental Protection Agency, Office of Water, Washington, D.C.

Freeman, G. E. and J. C. Fischenich. 2000. Gabions for Streambank Erosion Control. Report No. TN-EMRRP SR-22, Engineer Research and Development Center, U. S. Army Corps of Engineers, Vicksburg, MS.

Hartung, F. and H. Scheuerlein. 1970. Design of Overflow Rockfill Dams. *Proc. Tenth Int. Congress of Large Dams,* 1, 587-598.

HCFCD. 2001. Design Manual for Articulating Concrete Block Systems. Harris County Flood Control District, Houston, TX.

Holtz, D. H., B. R. Christopher and R. E. Berg. 1995. Geosynthetic Design and Construction Guidelines. Publication No. FHWA-HI-95-038, U.S. Department of Transportation, Federal Highway Administration, Washington, D.C.

Isbash, S. V. 1936. Construction of Dams by Depositing Rock in Running Water. *2nd Congress on Large Dams, Communication No. 3*, International Congress on Cold Dams, 123-126.

Johns, D. D., S. R. Abt, C. C. Watson and P. G. Combs. 1993. Riprap Sizing for ARS-Type Low-Drop Stilling Basins. *Journal of Hydraulic Engineering*, ASCE, 119(7), 864-869.

Kilgore, R. T. and G. K. Cotton. 2005. Design of Roadside Channels with Flexible Linings. Report No. FHWA-NHI-05-114, U.S. Department of Transportation, Federal Highway Administration, Arlington, VA.

Knauss, J. 1979. Computation of Maximum Discharge at Overflow Rockfill Dams. *Proc. 13th Congress of Int. Commission of Large Dams,* 143-159.

Koloseus, H. J. 1984. Scour Due to Riprap and Improper Filters. *Journal of Hydraulic Engineering*, ASCE, 110(10), 1315-1324.

Maynord, S. T. 1988. Stable Riprap Size for Open-Channel Flows. Technical Report HL-88-4, Waterways Experiment Station, U. S. Army Corps of Engineers, Vicksburg, MS.

Maynord, S. T. 1995. Gabion-Mattress Channel-Protection Design. *Journal of Hydraulic Engineering*, ASCE, 121(7), 519-522.

Maynord, S. T. 2012. *Personal Communication*.

Maynord, S. T., J. F. Ruff and S. R. Abt. 1989. Riprap Design. *Journal of Hydraulic Engineering*, ASCE, 115(7), 937-949.

Melville, B., R. van Ballegooy and S. van Ballegooy. 2006. Flow-Induced Failure of Cable-Tied Blocks. *Journal of Hydraulic Engineering*, ASCE, 132(3), 324-327.

NRCS[1]. 2007. Stone Sizing Criteria. National Engineering Handbook, Part 654, Technical Supplement 14C, Natural Resources Conservation Service, U.S. Department of Agriculture, Washington, D.C.

NRCS[2]. 2007. Geosynthetics in Stream Restoration. National Engineering Handbook, Part 654, Technical Supplement 14D, Natural Resources Conservation Service, U.S. Department of Agriculture, Washington, D.C.

NRCS[3]. 2007. Streambank Armor Protection with Stone Structures. National Engineering Handbook, Part 654, Technical Supplement 14K, Natural Resources Conservation Service, U.S. Department of Agriculture, Washington, D.C.

NRCS[4]. 2007. Use of Articulating Concrete Block Revetment Systems for Stream Restoration and Stabilization Projects. National Engineering Handbook, Part 654, Technical Supplement 14L, Natural Resources Conservation Service, U.S. Department of Agriculture, Washington, D.C.

Olivier, H. 1967. Through and Overflow Rockfill Dams – New Design Techniques. *Proceedings, Institution of Civil Engineers*, March, 36, 433-471.

Peterka, A. J. 1958. Hydraulic Design of Stilling Basins and Energy Dissipators. Engineering Monograph No. 25, U.S. Bureau of Reclamation, Denver, Co.

Reese, A. J. 1988. Nomographic Riprap Design. Miscellaneous Paper HL-88-2, Waterways Experiment Station, U. S. Army Corps of Engineers, Vicksburg, MS.

Shafai-Bajestan, M. and M. L. Albertson. 1993. Riprap Criteria Below Pipe Outlet. *Journal of Hydraulic Engineering*, ASCE, 119(2), 181-200.

Simons, D. B., Y. H. Chen, and L. J. Swenson. 1984. Hydraulic Test to Develop Design Criteria for the Use of Reno Mattresses. Report prepared for Maccaferri Steel Wire Products, Ltd., Civil Engineering Dept., Colorado State University, Ft. Collins, Co.

Stevens, M. A., D. B. Simons and G. L. Lewis. 1976. Safety Factors for Riprap Protection. *Journal of the Hydraulics Division,* ASCE, 102(5), 637-657.

USACE. 1991. Report on Standardization of Riprap Gradations. Engineer Manual 1110-2-1601, U. S. Army Corps of Engineers, Lower Mississippi Valley Division, Vicksburg, MS.

USACE HDC 722-4. 1973. Storm Drain Outlets, Riprap Energy Dissipators. Hydraulic Design Chart 722-4, Waterways Experiment Station, U. S. Army Corps of Engineers, Vicksburg, MS.

USACE HDC 722-5. 1973. Storm Drain Outlets, Riprap Energy Dissipators. Hydraulic Design Chart 722-5, Waterways Experiment Station, U. S. Army Corps of Engineers, Vicksburg, MS.

USACE HDC 722-7. 1973. Storm Drain Outlets, Riprap Energy Dissipators. Hydraulic Design Chart 722-7, Waterways Experiment Station, U. S. Army Corps of Engineers, Vicksburg, MS.

USDA-SCS. 1991. Guide for the use of Geotextiles. Design Note No. 24, U.S. Department of Agriculture, Soil Conservation Service, Washington, D.C.

Appendix I. Hydraulic Design Procedures for Channel Transitions

I.   Introduction

Changes in the cross sectional dimensions of a by-pass channel will sometimes be necessary to accommodate the installation of a hydraulic structure, changes in subsurface conditions, or the occurrence of obstructions near the channel corridor. Under these circumstances, it is advisable that the channel reaches of different dimensions or geometry be connected through a transitional reach that is designed to minimize energy losses, destructive turbulence and flow separation processes. Procedures for the hydraulic design of such transitions are provided in this appendix for various changes in channel dimensions or geometry.

While channel transitions can take on various shapes and forms, only four common types of transitions will be addressed in these guidelines: (i) the contraction of a trapezoidal cross section to a smaller trapezoidal cross section; (ii) the expansion of a trapezoidal cross section to a larger trapezoidal cross section; (iii) the contraction of a trapezoidal cross section to a smaller rectangular cross section; and (iv) the expansion of a rectangular cross section to a larger trapezoidal cross section. The first two types of transitions could be used in instances where the by-pass channel needs to become wider or narrower to accommodate a linear weir whose design length is appreciably different than the channel design width at the weir crest elevation. Similarly, the latter two transition types could be used to provide rectangular approach and exit channel reaches for a labyrinth weir.

Three design procedures are presented below. The first is essentially a general methodology that has been used in practice for decades and can be used to design any of the transition types mentioned above, although it is proposed for only the first two. The second design procedure is an analytically based methodology that was developed by researchers specifically for the third transition type mentioned above. Likewise, the third design procedure discussed below was developed solely for the fourth transition type. Furthermore, unless stated otherwise, several assumptions are inherent to each of the design procedures. First, it is assumed that the by-pass channel has a horizontal bottom slope. Hence, the transition reach will have no bottom slope. Second, the design procedures are limited to subcritical flow only. The third assumption is that velocities are low, resulting in small velocity heads. Fourth, the minimization of head losses is considered to be a primary design objective. All of these assumptions are compatible with the low topographic relief typically encountered throughout most of southern Florida.

II.   General Procedure for Trapezoidal Channel Transitions

A.   Background

No design procedures developed specifically for trapezoidal channel transitions were found in the literature. The first published transition design methodology was formulated by Julian Hinds (1928) for connections between trapezoidal channels and rectangular flumes. Applications of this procedure are demonstrated by Chow (1959) and French (1985). A number of transition design procedures were also developed by the U.S. Bureau of Reclamation (USBR, 1964; USBR, 1974).

However, these are limited to transitions between small canals and specific structure designs. This also appears to be the case for the U.S. Department of Transportation (Thompson and Kilgore, 2006) procedures. Additionally, the U.S. Army Corps of Engineers (USACE, 1991) provides dimensions for several types of expansion transitions from rectangular to trapezoidal cross sections. The basis for these dimensions, however, is not clear.

The U.S. Soil Conservation Service (USDA-SCS, 1977) design procedure for contraction and expansion transitions appears to be based on the original approach by Hinds (1928) and is purportedly substantiated by experience. Additionally, USDA-SCS(1977) demonstrates the application of its procedure to both trapezoidal transitions and rectangular-trapezoidal transitions. Consequently, this approach with some appropriate refinements is proposed for use here.

B.   Design Procedure

The USDA-SCS(1977) design procedure is constrained by the following objectives:

1. The water surface should be smoothly transitioned to meet end conditions.

2. The water surface edges anywhere within the transition should not converge with the centerline at an angle greater than 28° nor diverge from it at an angle greater than 25°.

3. Designating the absolute difference between the pre-transition and post-transition velocity heads as Δh_v, the form (i.e. nonfrictional) head loss across a contracting transition should not exceed 0.1 Δh_v while the form head loss across an expanding transition should not exceed 0.2 Δh_v.

4. The bottom and side slopes of the transition should meet end conditions tangentially.

Conditions 1 and 4 can be met by dimensioning the transition so that the water surface conforms to a smooth curve that meets the upstream and downstream water surfaces tangentially. Hinds (1928) proposed that this be done by dimensioning the transition so that the water surface follows two reverse parabolas that meet at an inflection point located halfway through the transition. However, USDA-SCS (1977) indicates that any smooth curve can be used. Merkley (2004) demonstrates that a cubic function can be conveniently used, provided the boundary conditions are properly specified. Denoting the distance from the upstream end of a transition with a horizontal bottom as 'x', this implies that the water depth $y(x)$ within the transition is of the form

$$y(x) = Ax^3 + Bx^2 + Cx + D \qquad (I1)$$

where A,B,C and D are constants. Denoting $y(0)$ as y_o requires that $D = y_o$. The tangential boundary conditions required by condition 4 above are satisfied if $dy/dx(0) = dy/dx(L) = 0$, where L is the length of the transition. Applying this requirement to Equation (I1) yields $A = 2(y_o - y_L)/L^3$ and $B = -3(y_o - y_L)/L^2$, where $y_L = y(L)$. Equation (I1) then becomes

$$y(x) = 2(y_o - y_L)(x/L)^3 - 3(y_o - y_L)(x/L)^2 + y_o \tag{I2}$$

Conditions 1 and 4 will be satisfied if the water surface within the transition (including the ends) is given by Equation (I2).

Before Equation (I2) can be used, the length L of the transition must be known. For contractive transitions, Chow (1959) recommends that the value of L be determined so that a straight line connecting the water surface edges at the two ends of the transition makes the optimum angle of about 12.5^O with the centerline of the transition. For expansion transitions, Merkley (2004) indicates that the corresponding angle should be about 9.5^O. However, Alauddin and Basak (2006) claim that Mazumder (1967) determined this optimum angle to be approximately 8°. To be conservative, the latter value is proposed for use here. These transition angles are depicted in Figures I1 and I2. Specifying transition lengths based on these angles should satisfy condition 2.
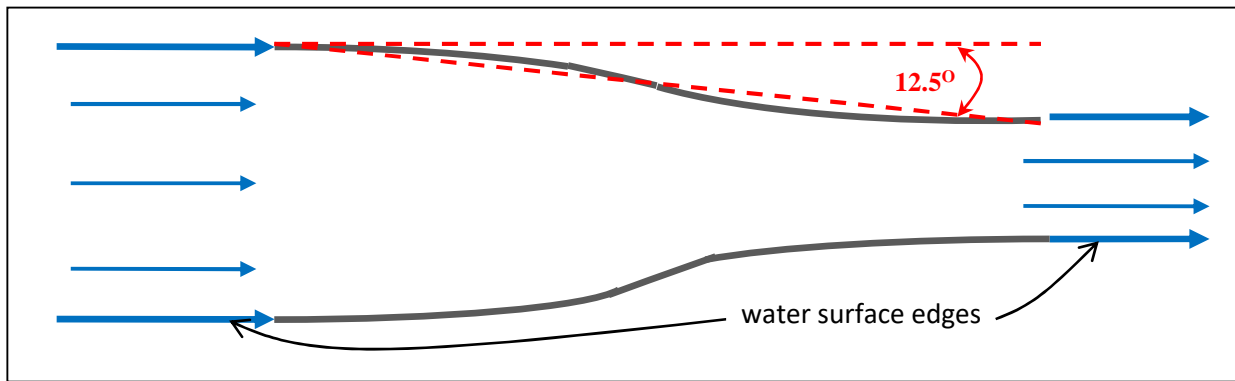

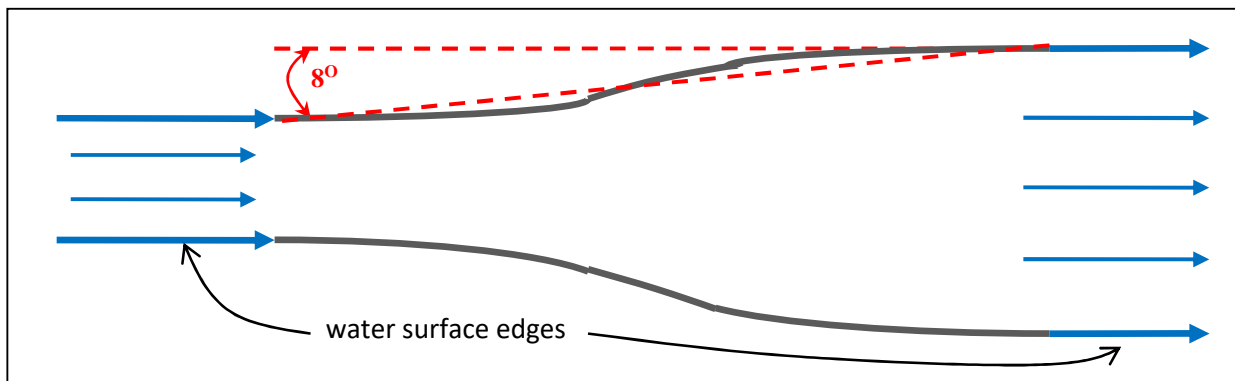**Figure I1. Optimum angle of a contraction transition**

Figure I2. Optimum angle of an expansion transition

Condition 3 above can be satisfied by dimensioning the transition so that the form head loss across it is equal to the value indicated. This is accomplished by performing the following steps in the order indicated:

1. *Determine the flow depth and velocity at the upstream and downstream ends of the transition.*

The flow depth and velocity at the downstream end of the transition, denoted y_L and V_L, respectively, must be determined through backwater computations between the downstream control structure and the transition. Procedures for performing backwater computations are discussed in Appendix B as well as in Chow (1959) and French (1985). Once y_L and V_L are known, y_o and V_o, the flow depth and velocity, respectively, at the upstream end of the transition are determined through a simple energy balance as follows:

$$z_o + y_o + V_o^2/2g \ = \ z_L + y_L + V_L^2/2g + h_f + h_m \qquad (I3)$$

where z denotes the bottom elevation, h_f is the friction head loss within the transition and h_m is the form head loss. As mentioned previously, friction energy losses are considered negligible for the range of velocities expected, so $h_f \approx 0$. Since the channel is assumed flat, $z_o = z_L$. Addition, the third design objective mentioned at the beginning of this section indicates that the transition must be dimensioned so that $h_m = c\Delta h_v$, where c = 0.1 for a contraction transition and c = 0.2 for an expansion transition. This reduces Equation I3 to

$$y_o + V_o^2/2g \ = \ y_L + V_L^2/2g + c|V_L^2/2g - V_o^2/2g \qquad (I4)$$

Equation (I4) can be written more conveniently as

$$y_o + eV_o^2/2g \ = \ y_L + eV_L^2/2g \qquad (I5)$$

where e = 1.1 for a contraction transition and e = 0.8 for an expansion transition. Considering the design discharge Q along with conservation of mass, it is common knowledge that

$$V_o \ = \ Q/A_o \qquad (I6)$$

while, for a trapezoidal channel,

$$A_o \ = \ (b_o + Zy_o)y_o \qquad (I7)$$

In Equation I7, Z is the channel side slope and b_o is the transition entrance width (i.e. the channel width upstream of the transition). The dimensions Z and b_o are determined previously from channel design considerations. Hence, the unknowns y_o, V_o and A_o can be determined from Equations I5 – I7. This allows the design water surface within the transition to be determined from Equation I2. At this point, the transition length L should be determined as discussed above.

2. *Discretize the water surface at a discrete number of stations.*

According to USDA-SCS (1977), the transition reach should be divided into 6 – 10 subreaches, beginning at the upstream end. Denoting the number of subreaches as n_r and the x coordinate of

the downstream end of the ith subreach as x_i, where $i = 0,1,..n_r$, $x_o = 0$ and $x_{nr} = L$, the water depth at each x_i can be computed using Equation I2.

3. *Determine the velocity at each station.*

Denoting the end locations of each subreach as x_i and x_{i+1}, Equation I5 implies that

$$y_i + eV_i^2/2g \ = \ y_{i+1} + eV_{i+1}^2/2g \tag{I8}$$

Since all y_i were determined in step 2 and V_o was computed in step 1, V_1 can be computed by applying Equation I8 to the first subreach. Likewise, V_2 - V_{nr} can then be computed for subreaches $2 – n_r$.

4. *Determine the wetted area at each station.*

At stations $i = 1 - n_r$, compute $A_i = Q/V_i$.

5. *Determine the transition width at each station.*

At the ith station, Equation I7 implies that the transition width b_i is given by

$$b_i = A_i / y_i – Zy_i \tag{I9}$$

The results of steps $1 – 5$ can be used to compute the transition width at each station. At this point, the dimensions of the transition satisfying design objectives $1 – 4$ are completely defined. The example below further illustrates this procedure.

Design Example

Design a transition that connects a trapezoidal channel with a bottom width of 30 feet and 2:1 side slopes to another trapezoidal channel with a bottom width of 10 feet and 2:1 side slopes. The design discharge is 900 cfs. Based on backwater computations, the flow depth at the location of the downstream transition end is 10 feet.

Step 1

The data specified in the problem statement along with an iterative solution to Equations I5 – I7 results in y_L = 10 ft, V_L = 3 ft/s, A_L = 300 ft^2, y_o = 10.1 ft, V_o = 1.78 ft/s and A_o = 507.02 ft^2.
As discussed previously, the transition length should allow a straight line connecting the water surface edges at the two ends of the transition to make an angle of about 12.5^O with the centerline. Based on the results just obtained, the top width of the wetted area at the upstream end of the transition is 70.4 feet while the downstream top width is 50 feet. Thus, L = ½ (70.4-50) / tan(12.5^O) = 46 feet.

Steps 2 – 5

After dividing the transition into 10 subreaches, the computations outlined in the preceding section for steps 2 – 5 were carried out at the endpoint of each subreach using e = 1.1 in Equation I8. The results are assembled in Table I1 and illustrated in Figure I2.

Table I1. Design computations for the contraction transition

i	x(i)	y(i)	V(i)²/2g	V(i)	A(i)	b(i)
0	0.00	10.10	0.05	1.78	507.02	30.00
1	4.60	10.10	0.05	1.82	494.34	28.76
2	9.20	10.09	0.06	1.94	464.19	25.83
3	13.80	10.08	0.07	2.10	428.36	22.35
4	18.40	10.06	0.08	2.28	394.31	19.05
5	23.00	10.05	0.09	2.46	365.13	16.23
6	27.61	10.04	0.11	2.63	341.61	13.97
7	32.21	10.02	0.12	2.78	323.57	12.24
8	36.81	10.01	0.13	2.90	310.68	11.02
9	41.41	10.00	0.14	2.97	302.77	10.26
10	46.01	10.00	0.14	3.00	300.00	10.00
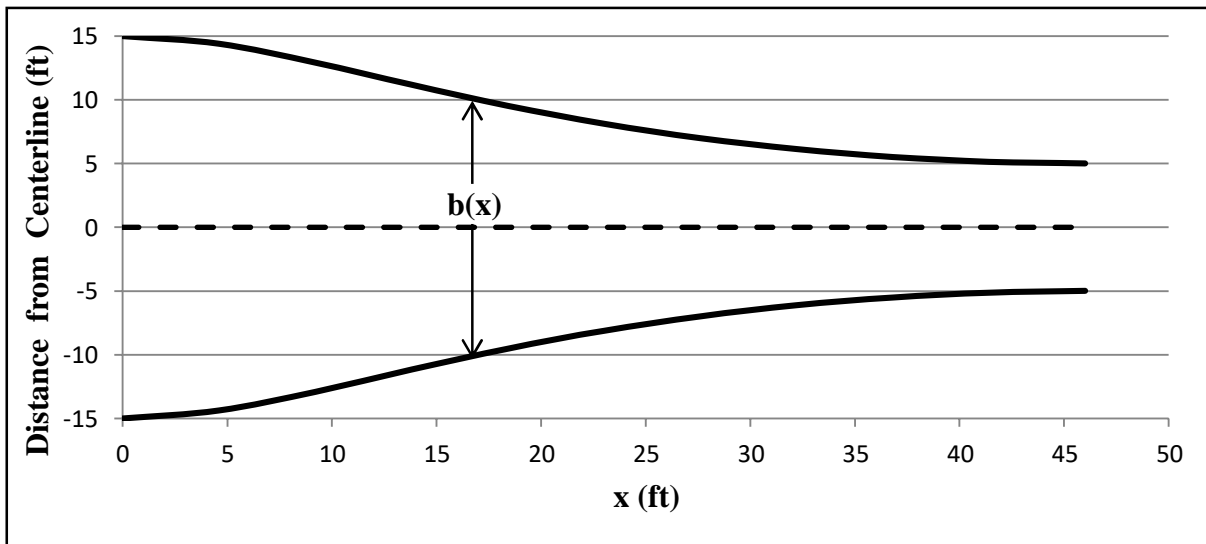
Figure I3. Plan view of the example transition

I6

III.   Specialized Procedure for Rectangular to Trapezoidal Transitions

One of the primary criticisms of the design procedure developed by Hinds (1928) is that it is based on the premise that the form head loss across the transition is a function of the upstream and downstream velocity heads only. To overcome this limitation, more advance procedures for designing optimal expansion transitions between rectangular flumes and trapezoidal channels were developed for subcritical flows in the 1980's and early 1990's. The first of these was by Vittal and Chiranjeevi (1983), where the optimal bed width profile was taken to be coincidental with the separation streamline near the bed in a sudden expansion flow from a rectangular to trapezoidal channel. In this study, an extensive laboratory investigation was carried out to determine the location of this streamline for different side slopes. Empirical expressions for the variation along the transition in bed width and side slope were proposed. French (1985) provides an example application of this design procedure.

Swamee and Basak (1992, 1993) later developed a more analytically based procedure for determining the optimum bed width and side slope profile along a rectangular to trapezoidal channel expansion. As before, the objective of their study was to minimize head losses, flow separation and eddy formation. Using conservation of mass, momentum and energy, Swamee and Basak (1993) derived a closed-form expression for the form head loss h_L across a transition with uniform inflow in terms of the centerline distance x downstream from the transition entrance, the transition length L, the entrance and exit channel bottom widths b_o and b_L, respectively, the water depth y, the bottom width b, the side slope m, and the design discharge Q. This expression is

$$h_L = \int_0^L \frac{Q^4}{g^2(b+my)^5 y^5} \left(\frac{db}{dx} + y\frac{dm}{dx} \right) dx \tag{I10}$$

Equation I10 is subject to the constraint that the water surface within the transition conforms to a gradually varied flow profile. Swamee and Basak (1993) express this profile as

$$\frac{dy}{dx} = \left\{ -\frac{dz}{dx} + \frac{Q^2}{g(b+my)^3 y^2}\left[1 - \frac{Q^2}{g(b+my)^2 y^3}\right]\frac{db}{dx} + \frac{Q^2}{g(b+my)^3 y}\left[1 - \frac{Q^2}{g(b+my)^2 y^3}\right]\frac{dm}{dx} \right\} / \left\{ 1 - \frac{Q^2(b+2my)}{g(b+my)^3 y^3} \right\} \tag{I11}$$

where z denotes the bottom elevation within the transition. Since the solution presented here is for the general case of open-channel flow through a transition, the assumption that $dz/dx = 0$ was not made. Furthermore, the investigators assumed uniform flow within the approach channel whose slope is S_{oo}, resulting in the following dimensionless expression for the discharge:

$$\frac{Q}{\sqrt{g b_o^5}} = -\frac{2.457 y_o}{b_o}\sqrt{\frac{S_{oo} y_o}{b_o + 2y_o}}\, ln\left[\frac{\varepsilon(b_o + 2y_o)}{12 b_o y_o}\right] \tag{I12}$$

where y_o is the depth at the transition entrance and ε is the channel roughness. Although the assumptions of uniform inflow to the transition and $dz/dx \neq 0$ are not consistent with a horizontal channel that is subject to backwater effects, Swamee and Basak (1993) demonstrated that the results of their study are applicable to channel slopes as small as 10^{-4}. Hence, it is reasonable to

assume that their design procedure will yield a reliable transition in situations where the channel bottom is flat and flow through the transition is gradually varied.

In addition to Equations I11 and I12, Swamee and Basak (1993) specified various boundary conditions that also serve as constraints to the optimization of Equation I10. These are

$$b(0) = b_o \tag{I13a}$$
$$m(0) = 0 \tag{I13b}$$
$$z(0) = 0 \tag{I13c}$$
$$b(L) = b_L \tag{I13d}$$
$$m(L) = m_L \tag{I13e}$$
$$db/dx(0) = 0 \tag{I13f}$$
$$db/dx(L) = 0 \tag{I13g}$$
$$dz/dx(0) = -S_{oo} \tag{I13h}$$
$$dz/dx(L) = -S_{oL} \tag{I13i}$$

In Equations I13, m_L and S_{oL} denote the downstream channel side slope and bottom slope, respectively.

After converting Equations I10 – I13 to a nondimensional form, the investigators used optimal control theory to minimize Equation I10 subject to the constraints specified in Equations I11 – I13. In fact, 5,184 optimizations were carried out for various combinations of design parameters in the following ranges:

$$0.1 < Q/(gb_o^5)^{1/2} \leq 2.0 \tag{I14a}$$
$$1.25 \leq b_L/b_o \leq 3.0 \tag{I14b}$$
$$2.0 \leq L/b_o \leq 8.0 \tag{I14c}$$
$$10^{-4} \leq S_{oo} \leq 10^{-2} \tag{I14d}$$
$$10^{-4} \leq S_{oL} \leq 10^{-2} \tag{I14e}$$
$$0.5 \leq m_L \leq 3.5 \tag{I14f}$$
$$10^{-6} \leq \varepsilon/b_o \leq 10^{-5} \tag{I14g}$$

After comparing all of the computed optimal bed width and side slope profiles Swamee and Basak (1993) found little variation between them and determined that the optimal bed width profile is given by

$$b = b_o + (b_L - b_o)\left[2.52\left(\frac{L}{x} - 1\right)^{1.35} + 1\right]^{-0.775} \tag{I15}$$

While the optimal side slope profile can be stated as

$$m = m_L\left(\frac{x}{L}\right)^{1.23} \tag{I16}$$

Equations I15 and I16 can be used to compute the bottom width and side slope at various values of x along the length of the transition. The length of the transition L, however, must be determined beforehand based on site conditions, the proposed channel corridor and project requirements. It is best that the transition length remain within the limits given by expression I14c, if possible.

It is worthwhile to note that, in most practical applications, it will be difficult to assign a value to the channel roughness parameter ε appearing in expression I14g. Under uniform flow conditions, Swamee and Basak (1992) show that the velocity is related to this parameter by the expression

$$V = -2.457\sqrt{gRS_o}\, ln\left(\frac{\varepsilon}{12R}\right) \tag{I17}$$

where S_o is the channel slope and R is the hydraulic radius. By equating this expression to Manning's equation, one can easily show that

$$\varepsilon = 12Re^{\left[\frac{-0.605R^{1/6}}{n\sqrt{g}}\right]} \tag{I18}$$

The preceding discussion does not imply that Equations I15 and I16 will yield an unacceptable transition design when minor deviations from the limits in expressions I14 occur. In fact, as mentioned previously, the limiting conditions given in expressions I14d and I14e will not be strictly met in most south Florida canals. Under these conditions, the limits for channel roughness indicated in expression I14g cannot be taken into account. Nonetheless, the reliability of Equations I15 and I16 will be enhanced if the rest of the constraints are satisfied. In situations where this is not practical or where large deviations occur, more frequent inspections and maintenance of the constructed transition may be needed.

The application of the design procedure discussed above is demonstrated in the example below.

Design Example

Design a transition that connects a rectangular channel with a bottom width of 10 feet to a trapezoidal channel with a bottom width of 30 feet and 2:1 side slopes. The design discharge is 900 cfs. Both channels are horizontal with a bottom that is 12 feet below land surface.

From the problem statement, Q = 900 cfs, b_o = 10 ft, b_L = 30 ft and m_L = 2. b_L/b_o = 30/10 = 3, and $Q/(gb_o^5)^{1/2}$ = 900/[(32.17)(10)^5]^{1/2} = 0.5. In the absence of any other requirements, L can be set to the value that allows L/b_o to fall within the middle of the range given in expression I14c. This results in L = (5)(10) = 50 feet.

Table I2 contains values of b and m computed with Equations I15 and I16 for various values of x. Included also at each location is the transition top width based on land surface. The bottom and top widths of the transition are shown graphically in Figure I3.

Table I2. Dimensions of the example expansion transition

x	b(x)	m(x)	T(x)
0	10.00	0.00	10.00
5	10.97	0.12	13.79
10	12.19	0.28	18.82
15	13.67	0.45	24.59
20	15.45	0.65	31.00
25	17.54	0.85	38.00
30	19.96	1.07	45.57
35	22.67	1.29	53.62
40	25.51	1.52	61.99
45	28.20	1.76	70.36
50	30.00	2.00	78.00
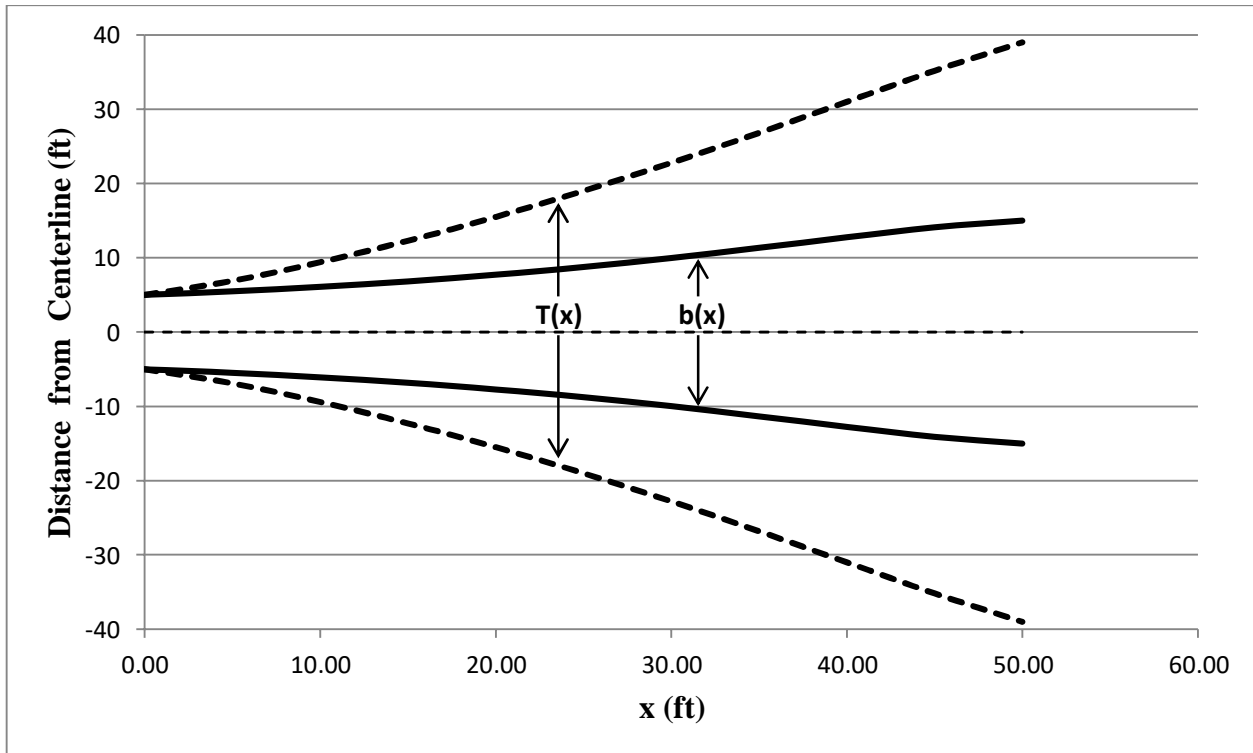
Figure I4. Bottom and top width profiles of the example transition

IV.   Specialized Procedure for Trapezoidal to Rectangular Transitions

The amount of research devoted to the hydraulic design of trapezoidal to rectangular channel contraction transitions appears to be limited compared to the number of studies that were carried out to improve the hydraulic design of expansion transitions between rectangular and trapezoidal channels. Form head losses across channel contractions were examined by Vittal (1978), although no transition design procedure was proposed. Swamee and Basak (1994) later developed an analytically based design procedure for trapezoidal to rectangular channel contraction transitions in a manner that was similar to the approach they previously used to develop a design procedure for the corresponding expansion transition (see section III above). However, in this effort the primary design objective was to minimize both form and friction head losses across the transition. They determined that the total head loss across the transition can be stated as

$$h_L = \int_0^L \left\{ \frac{Q^2[b+2y\sqrt{1+m^2}]}{6gy^3(b+my)^3} \left[ln\left(\frac{\varepsilon[b+2y\sqrt{1+m^2}]}{12y(b+my)} \right) \right]^{-2} - \frac{0.294Q^2}{gy^2(b+my)^3} \left(\frac{db}{dx} + y\frac{dm}{dx} \right) \right\} dx \quad \text{(I19)}$$

where all terms are as defined in the previous section. As in the previous case, Equation I19 is subject to the constraint that the water surface within the transition conform to a gradually varied profile. For the contraction transition under consideration here, Swamee and Basak (1994) found that the differential equation of gradually varied flow (see, for example, Chow, 1959) can be written

$$\frac{dy}{dx} = \frac{\left\{ -\frac{dz}{dx} - \frac{Q^2[b+2y\sqrt{1+m^2}]}{6gy^3(b+my)^3} \left[ln\left(\frac{\varepsilon[b+2y\sqrt{1+m^2}]}{12y(b+my)} \right) \right]^{-2} + \frac{0.294Q^2}{gy^2(b+my)^3}\left(\frac{db}{dx}+y\frac{dm}{dx} \right) \right\}}{\left[1 - \frac{Q^2(b+2my)}{gy^3(b+my)^3} \right]} \quad \text{(I20)}$$

Similar to the previous case, the following boundary conditions are also imposed as constraints on Equation I19:

$$b(0) = b_o \quad \text{(I21a)}$$
$$m(0) = m_o \quad \text{(I21b)}$$
$$z(0) = 0 \quad \text{(I21c)}$$
$$b(L) = b_L \quad \text{(I21d)}$$
$$m(L) = 0 \quad \text{(I21e)}$$
$$db/dx(0) = 0 \quad \text{(I21f)}$$
$$db/dx(L) = 0 \quad \text{(I21g)}$$
$$dz/dx(0) = -S_{oo} \quad \text{(I21h)}$$
$$dz/dx(L) = -S_{oL} \quad \text{(I21i)}$$

Assuming uniform flow conditions in the approach channel, the discharge was found to be

$$Q = -2.457y(0)[b + m_o y(0)] \sqrt{gS_{oo} \frac{y(0)[b+m_o y(0)]}{b+2y(0)\sqrt{1+m_o^2}}} \ ln\left\{\frac{\varepsilon}{12} \frac{b+2y(0)\sqrt{1+m_o^2}}{y(0)[b+m_o y(0)]}\right\} \quad (I22)$$

The formulations given above comprise an optimization problem where the objective is to minimize the head loss given by Equation I19 subject to the constraints stated in Equations I20 - I22. Swamee and Basak (1994) solved this problem using the same approach used by Swamee and Basak (1993) in optimizing the expansion transition between a rectangular and a trapezoidal channel. In this case the parameter ranges examined were

$$0.1 < Q/(gb_o^5)^{1/2} \leq 2.0 \quad (I23a)$$
$$0.3 \leq b_L/b_o \leq 0.8 \quad (I23b)$$
$$2.0 \leq L/b_o \leq 8.0 \quad (I23c)$$
$$S_{oo} \geq 10^{-4} \quad (I23d)$$
$$S_{oL} \leq 10^{-2} \quad (I23e)$$
$$0.5 \leq m_o \leq 3.5 \quad (I23f)$$
$$10^{-6} \leq \varepsilon/b_o \leq 10^{-5} \quad (I23g)$$

The optimal bottom width profile was determined by the investigators to be

$$b = b_o + (b_o - b_L)\left[1.41\left(\frac{1-\xi}{\xi}\right)^{1.23} + 1\right]^{-0.924} \quad (I24)$$

where $\xi = x/L$ is the dimensionless distance downstream from the transition entrance along its centerline. Similarly, the optimal side slope profile was found to be

$$m = m_o(1 - \xi^{1.52}) \quad (I25)$$

The application of these equations to a transition design is illustrated in the example below. The discussions given in the previous section regarding the parameter ranges (in this case, specified in expressions I23) apply here as well.

Design Example

Design a transition that connects a trapezoidal channel with a bottom width of 20 feet and 2:1 side slopes to a rectangular flume with a bottom width of 10 feet. The design discharge is 1200 cfs. Both channels are horizontal with a bottom that is 12 feet below land surface.

From the problem statement, Q = 1200 cfs, b_o = 20 ft, b_L = 10 ft and m_o = 2. b_L/b_o = 10/20 = 0.5, and $Q/(gb_o^5)^{1/2}$ = 1200/[(32.17)(20)^5]$^{1/2}$ = 0.12. In the absence of any other requirements, L can

be set to the value that allows L/b_o to fall within the middle of the range given in expression I14c. This results in $L = (5)(20) = 100$ feet.

Table I3 contains values of b and m computed with Equations I24 and I25 for various values of x. Included also at each location is the transition top width based on land surface. The bottom and top widths of the transition are shown graphically in Figure I4.

Table I3. Dimensions of the example contraction transition

x	b(x)	m(x)	T(x)
0	20.00	2.00	68.00
10	19.43	1.94	65.98
20	18.65	1.83	62.50
30	17.74	1.68	58.04
40	16.70	1.50	52.78
50	15.56	1.30	46.83
60	14.35	1.08	40.27
70	13.11	0.84	33.20
80	11.90	0.58	25.71
90	10.80	0.30	17.90
100	10.00	0.00	10.00
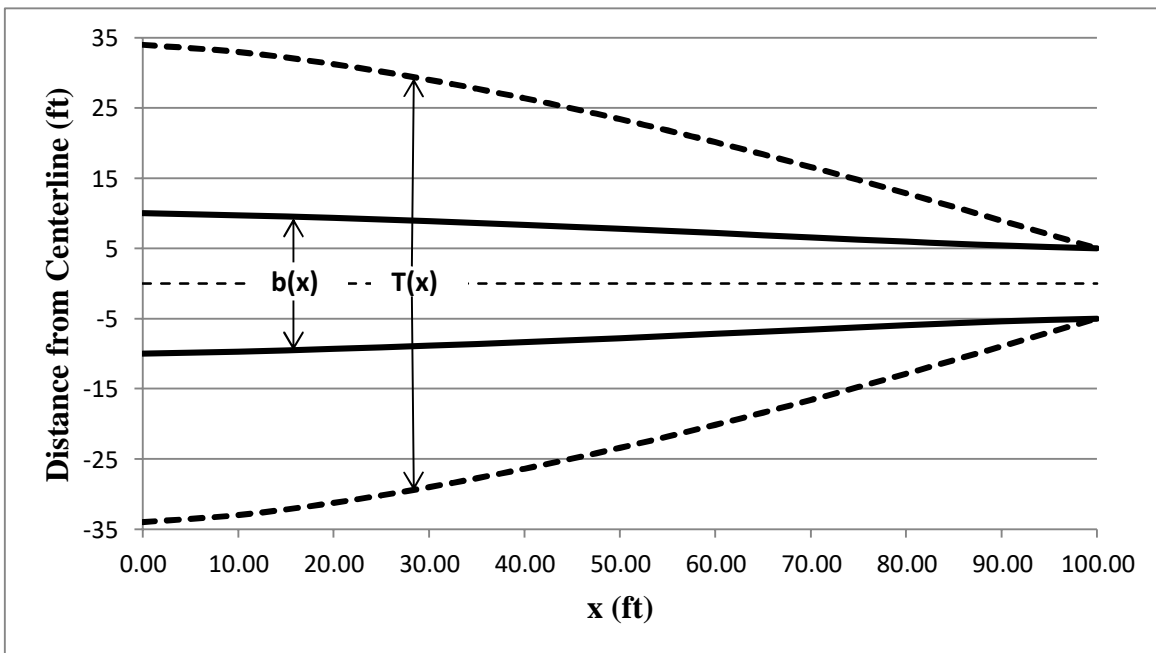
Figure I5. Bottom and top width profiles of the example transition

V.   Practical Considerations for Design and Construction

While the transition designs depicted in the preceding examples are hydraulically efficient, it will likely be difficult or economically infeasible to construct them as shown. Factors that should be considered are the project budget, subsurface conditions, the available excavation equipment and the skill of the contractor. In developing the construction drawings, the engineer should consider these factors and specify the transition dimensions that are as close as feasible to the dimensions determined through the design procedure. Significant deviations in the constructed transition dimensions from the design dimensions should be offset through more frequent inspections and maintenance.

VI.   References

Alauddin, M. and B. C. Basak. 2006. Development of an expansion transition in open channel sub critical flow. *Journal of Civil Engineering (IEB),* 34(2), 91-101.

Chow, V. T. 1959. *Open-Channel Hydraulics*, McGraw-Hill, New York, NY.

French, R. H. 1985. *Open-Channel Hydraulics*, McGraw-Hill, New York, NY.

Hinds, J. 1928. The hydraulic design of flume and siphon transitions. *Transactions of the ASCE,* vol. 92, 1423-1459.

Mazumder, S. K. 1967. Optimum length of transition in open channel expansive subcritical flow. *Journal of the Institute of Engineers,* India, 48(3), 463-478.

Merkley, Gary P., "BIE6300 - Irrigation & Conveyance Control Systems, Spring 2004" (2004). *Biological and Irrigation Engineering - OCW.* Course 2. http://digitalcommons.usu.edu/ocw_bie/2 (July 16, 2012).

USACE. 1994. Hydraulic Design of Flood Control Channels. EM 1110-2-1601, US Army Corps of Engineers, Washington, D.C.

USDA-SCS. 1977. Design of Open Channels. Technical Release No. 25, U.S. Department of Agriculture, Soil Conservation Service, Engineering Division, Washington, D. C.

U. S. Bureau of Reclamation. 1964. *Hydraulic Design of Transitions for Small Canals.* United States Government Printing Office, Washington, DC.

U. S. Bureau of Reclamation. 1978. *Design of Small Canal Structures.* United States Government Printing Office, Denver, CO.

Swamee, P. K. and B. C. Basak. 1992. Design of Trapezoidal Expansive Transitions. *Journal of Irrigation and Drainage Engineering,* ASCE, 118(1), 61-73.

Swamee, P. K. and B. C. Basak. 1993. Comprehensive Open-Channel Expansion Transition Design. *Journal of Irrigation and Drainage Engineering,* ASCE, 119(1), 1-17.

Swamee, P. K. and B. C. Basak. 1994. Design of Open-Channel Contraction Transitions. *Journal of Irrigation and Drainage Engineering,* ASCE, 120(3), 660-668.

Thompson, T. L. and R. T. Kilgore. 2006. Hydraulic Design of Energy Dissipators for Culverts and Channels. U.S. Department of Transportation Publication No. FHWA-NHI-06-086, Arlington, VA.

Vittal, N. 1978. Direct Solution to Problems of Open Channel Transitions. *Journal of the Hydraulics Division,* ASCE, 104(11), 1485-1494.

Vittal, N. and V. V. Chirenjeevi. 1983. Open Channel Transitions: Rational Method of Design. *Journal of Hydraulic Engineering,* ASCE, 109(1), 99-115.